WestVirginiaUniversity
THE RESEARCH REPOSITORY @ WVU

Graduate Theses, Dissertations, and Problem Reports

2001

Amiodarone-induced pulmonary toxicity in F344 rats

Michael Douglas Taylor
West Virginia University

Follow this and additional works at: https://researchrepository.wvu.edu/etd

Recommended Citation

Taylor, Michael Douglas, "Amiodarone-induced pulmonary toxicity in F344 rats" (2001). *Graduate Theses, Dissertations, and Problem Reports*. 1371.
https://researchrepository.wvu.edu/etd/1371

This Dissertation is protected by copyright and/or related rights. It has been brought to you by the The Research Repository @ WVU with permission from the rights-holder(s). You are free to use this Dissertation in any way that is permitted by the copyright and related rights legislation that applies to your use. For other uses you must obtain permission from the rights-holder(s) directly, unless additional rights are indicated by a Creative Commons license in the record and/ or on the work itself. This Dissertation has been accepted for inclusion in WVU Graduate Theses, Dissertations, and Problem Reports collection by an authorized administrator of The Research Repository @ WVU. For more information, please contact researchrepository@mail.wvu.edu.

Amiodarone-Induced Pulmonary Toxicity in F344 Rats.

Michael D. Taylor

Dissertation submitted to the
School of Medicine
at West Virginia University
in partial fulfillment of the requirements
for the degree of

Doctor of Philosophy
in
Pharmacology and Toxicology

Mark J. Reasor, Ph.D., Chair
Vincent Castranova, Ph.D.
Mary E. Davis, Ph.D.
Richard D. Dey, Ph.D.
Knox Van Dyke, Ph.D.

Department of Pharmacology and Toxicology

Morgantown, West Virginia

2001

Keywords: **Amiodarone, Amiodarone-Induced Pulmonary Toxicity, Oxidants, Free Radicals, Electronic Spin Resonance, Laser-Scanning Confocal Microscopy, Intratracheal Administration, Cytokine, Inflammation, Fibrosis, Acute Damage, SP-D, F344 Rats**

ABSTRACT

Amiodarone-Induced Pulmonary Toxicity in F344 Rats.

Michael D. Taylor

Amiodarone (AD) is gaining support as a first-line antiarrhythmic drug despite its potentially fatal pulmonary toxicity involving inflammation and fibrosis. The goals of this study were to develop and characterize a rat model of amiodarone-induced pulmonary toxicity (AIPT). A protocol was developed in which male F344 rats were instilled intratracheally (i.t.) with AD (6.25 mg/kg with a 3.125 mg/ml solution) in sterile water or the sterile water vehicle on days 0 and 2, a protocol that led to the development of pulmonary fibrosis on day 28 in the AD-treated animals. Bronchoalveolar lavage (BAL) resulted in the increased recovery of alveolar macrophages, neutrophils, and eosinophils from i.t. AD-treated rats. The BAL cells recovered from AD-treated rats at day 3 produced more integrated phorbol-myristate-acetate stimulated luminol-dependent chemiluminescence over 20 minutes than BAL cells from control rats. These findings indicate that this model exhibits a transient pulmonary inflammation, with the potential for elevated oxidant production in the lungs, and subsequent pulmonary fibrosis. Also, serum levels of surfactant protein-D, a protein normally found in the lungs, was elevated in the serum of i.t. AD-treated rats, and is proposed as a biomarker for the toxicity. However, attempts to elucidate the cytokine signaling behind the inflammatory events were unsuccessful. It was discovered that AD instillation produces a rapid and massive damage to the alveolar-capillary barrier, and cellular death or damage to lung airway and parenchymal cells. This pathology is not consistent with that found in human AIPT. AD in solution was found to be at least partly in the form of a free radical, and capable of generating hydroxyl radicals. An attempt to modulate the toxicity of i.t. AD by incorporating water-soluble antioxidants in the drug solution was unsuccessful, and might have exacerbated the condition. No consistent evidence for deiodination of AD in solution was found, leaving the mechanism and significance of free radical generation by AD undetermined.

Table of Contents

Abstract……. ii

Acknowledgements……... iv

List of Figures…… vii

Introduction…… 1

Objectives……... 17

Methods……. 19

Results…… 31

Discussion…….. 109

References…….. 134

Curriculum Vitae…… 143

Acknowledgements

I have been fortunate during my career as a student to have been guided in the classroom and out by a wonderful set of teachers, instructors, professors, advisors, and friends. First and foremost, my parents, Marlene and Roger Taylor, have guided and shaped me in every way imaginable, including nurturing my love for science practically since before I learned to read. By being teachers, friends, and mentors, they have always been the foundation of my success. They were assisted in this formidable task by four of the very best grandparents that have ever existed, Sue and Marlin King, and Clara and James Taylor, to whom I owe my very character. They will never know how much they have touched my life and how far their influence will reach through the lessons they have taught their grandchildren.

Although a great number of teachers have provided me with an excellent science education, several have played a very direct role in giving me the knowledge and the confidence to succeed in college and beyond. Drs. Ruth Davis, Gerald Wilcox, and Henry Falkowski, all of Potomac State College, forced me to realize my full potential by upholding rigorous academic standards, and thus they gave me the first real confidence that I ever felt in my own academic abilities. I owe special gratitude to Dr. Ruth Davis, my first advisor, for both an excellent science education as well as guidance of my personal growth during very formative times.

My interactions with excellent faculty members continued into graduate school. My advisor, Dr. Mark Reasor, has set the standard of excellence in science and in character that I will always strive to live up to. He has given me uncounted hours of his time and attention, and has provided me with the scientific foundation that I can build a future career on. There is no doubt that Dr. Reasor genuinely has the best interests of graduate students in mind, and because of that has fostered my independent thinking throughout my entire graduate career. My committee was one of the finest I could have assembled, and to each I owe a great debt of gratitude. Dr. Mary Davis has always had an open door, and numerous times I have taken advantage of it. She never hesitated to help me with any question that came up, and even directed and accompanied me to colleagues and various other resources. Dr. Richard Dey was graciously willing to join my committee when he was most needed, and even though he has considerable departmental and laboratory responsibilities, he has always made time to assist me in any way possible without a single complaint. Dr. Knox Van Dyke has been almost a co-advisor to me, spending countless hours with me in as well as outside of the laboratory, and has shaped both my knowledge base and my thought processes. He has proved to me that most science is actually done “in your head”, and shown me the importance of staying widely read, maintaining a broad perspective, and remaining truly versatile. I hope that I can bring his level of enthusiasm and satisfaction to my endeavors, because he clearly loves what he does. Although Dr. Phil Miles retired during the course of my project, my interaction with him both during and preceding my time in graduate school has profoundly influenced the way I approach both problems and their explanations. He engrained the mantra of keeping presentations and papers clear and concise, and I have relied on his advice many times during my graduate career, and will continue to do so. Of all of my committee members, I have had the longest relationship with Dr. Vincent

Castranova, and certainly own him a great amount of gratitude. He was willing to accept and begin the training of a very "green" undergraduate student when I was searching for direction, without any promise of benefit to himself or his lab. His willingness to serve as a committee member, mentor, and friend, despite his considerable obligations as a Branch Chief and faculty member, are gratefully acknowledged. It was through his laboratory that I was introduced to Dr. Linda Huffman, who spent considerable time teaching me basic laboratory techniques, many of which I used throughout my entire project. Her guidance gave me a head-start in graduate school, allowing me to begin lab work with confidence and experience, and I remain grateful for the time that she spent with me.

I met a number of other people at NIOSH that have assisted me greatly over the years. Mark Barger has always been willing to demonstrate many techniques, including catching more fish, and I continue to learn from him. Terry Meighan, Dr. Dale Porter, Vic Robinson, Dr. Jane Ma, and Joyce Blosser have always been willing to help, listen, and give suggestions at any time. Finally, Linda Bowman deserves more gratitude than I can put in this small section. She has been involved in every aspect of the project and my development since I met her, and has become a true friend. She has assisted me in more ways than I can probably even remember, and I am looking forward to continuing this relationship for years to come. Maybe I will even get the chance to start repaying her, although I will never be able to completely reimburse her for her time and effort.

A project such as this required an extensive amount of collaboration, and I have been fortunate to interact with excellent people in various fields. Lori Battelli, Patsy Willard, Dean Newcomer, and the entire histopathology laboratory at NIOSH have assisted me greatly. Dr. Ann Hubbs has always been willing to fit my slide reading into her busy schedule, and in addition she makes sure that I learn and benefit from our interactions. Dr. Xianglin Shi has been very generous with his expertise and ESR time. Steve Leonard has spent many hours with me and the ESR in the basement, which would send any normal person running, but Steve dutifully pretended to listen to my stories while we discovered many "interesting" properties of amiodarone solution. His assistance is gratefully acknowledged. I appreciate Dr. Jo Rae Wright, of Duke University, for assisting me with the surfactant protein work, and ultimately directing us to Dr. Robert Mason and Kathy Shannon, who actually ran the assays. Their work is greatly appreciated. Drs. Peter Gannett and Robert Griffith assisted considerably in my understanding of the physical chemistry of the drug, and gave considerable time to these discussions. Robert Smith donated his time and expertise, as well as time on the mass spectrometer, to the cause. Chris Van Dyke has went above and beyond the call of duty, helping with a myriad of problems, and offering advice on any topic which I brought to him. Chris is truly an asset to the department, and a friend.

One of the most productive and enjoyable collaborations I have had was with Dr. Jim Antonini and Jenny Roberts of NIOSH. They both went out of their way to assist me in numerous ways during my project, and I am looking forward to continuing a very satisfying and productive collaboration as part of their laboratory. I sincerely appreciate their time and effort.

As I write this, the Department of Pharmacology and Toxicology faces an uncertain future. Its likely dissolution saddens me, as it has been a great place to work and learn. I would like to express my sincere gratitude to Dr. William Fleming for

assembling such a fine collection of people, and allowing me to enjoy that interaction during my time here. The entire faculty and staff have always done everything within their power to make my time here enriching and rewarding, and for that I sincerely thank them. I hope that they can take this special feeling and spread it into the other departments that they eventually become part of, so that research and the atmosphere in the entire school can be enhanced.

I have had the support and assistance of an excellent group of friends, both in and out of this department. The students in Pharmacology and Toxicology, both past and present, have been special and have made my time here even more rewarding. Jim Culhane, Dave White, Lance Molnar, Janet Dowdy, Rich Johnston, and Fernando Suarez have all been great friends. Also, it has been a pleasure to know and work with Tripp Griffin, Erin Sikora, Stacey Brower, and Karen Rust. Although in other departments, Paul McConnell, Debbie Lenda, and Kevin Rowland have been great friends and co-conspirators. Finally, Scott Thomas has been a great friend, and even though our doctorates are slightly different, it has been a pleasure attaining this goal with him.

I have a small family that has unfortunately grown smaller, but closer, during my time here. In addition to my parents and grandmother Sue King, my brother Chris, uncle Jim, aunt Nancy, cousin Mike, and Rita Heavner have always been a great source of support. My wife Tami has been both supportive and understanding, and I owe her the utmost gratitude. Last, I would like to dedicate this work to the family members who did not get to see me reach this milestone; Clara Taylor and Marlin King, both of whom I lost too early, and Forrest Taylor, James Taylor, and Paul Horevay, all of whom I lost during my time in graduate school. I hope they know the influence they've had on me.

List of Figures

No.		Page
1	The structure of amiodarone……..	1
2	Amiodarone and desethylamiodarone accumulation in BAL cells following oral amiodarone treatment…….	45
3	Lipid phosphorous levels in BAL cells following one week of oral amiodarone or vehicle treatment……	46
4A	NOx production from BAL cells from rats given oral amiodarone or vehicle one week……	47
4B	NOx production from BAL cells recovered on day 5 from rats given intratracheal amiodarone or vehicle on day 0…….	48
5	Integral LDCL counts on Day 5 following intratracheal amiodarone administration in either sterile water or sterile saline or appropriate vehicle……..	49
6	Integral LDCL counts from BAL cells recovered from rats treated either with amiodarone or water orally for one week or treated intratracheally with amiodarone or water on day 0 and lavaged on day 5.	50
7	The effects of two intratracheal dosing protocols on right-lung hydroxyproline content…….	51
8	Right-lung hydroxyproline levels following either daily oral amiodarone treatment, i.t. amiodarone treatment, or combination treatments of both oral and i.t. amiodarone or vehicle treatments……	52
9	Right-lung hydroxyproline content at day 28……	53
10	Effect of AD on left lung histopathology……..	54
11	Representative fields of lung tissue obtained by laser-scanning confocal microscopy……	55
12	Effect of AD on average lung tissue area stained by lucifer yellow…….	56
13	Albumin in the first BAL fraction…….	57
14	Total cells recovered by BAL……	58

15	Alveolar macrophages recovered by BAL……	59
16	Polymorphonuclear leukocytes recovered by BAL……..	60
17	Eosinophilic leukocytes recovered by BAL…….	61
18	Total PMA-stimulated luminol-dependent chemiluminescence counts over 20 minutes from BAL cells……..	62
19	Potential oxidant production of total BAL cells……...	63
20	PMA-stimulated LDCL counts over 20 minutes from BAL cells on Day 3 with specific inhibitors……...	64
21	NOx (NO_2 and NO_3) production from BAL cells cultured at Day 3……	65
22	Effect of AD on surfactant protein-D levels in serum……..	66
23	Albumin in the first BAL fraction on day 3 following intratracheal amiodarone, vehicle, or acidic vehicle treatment on days 0 and 2……	67
24	Total BAL cells recovered on day 3 following intratracheal amiodarone, vehicle, or acidic vehicle treatment on days 0 and 2…….	68
25	Total alveolar macrophages recovered on day 3 following intratracheal amiodarone, vehicle, or acidic vehicle treatment on days 0 and 2……	69
26	Total neutrophils (PMNs) recovered on day 3 following intratracheal amiodarone, vehicle, or acidic vehicle treatment on days 0 and 2……	70
27	Total eosinophils recovered on day 3 following intratracheal amiodarone, vehicle, or acidic vehicle treatment on days 0 and 2…….	71
28A	Non-LPS-stimulated NOx production from cultured BAL cells lavaged at various time-points following intratracheal instillation of amiodarone or vehicle……	72
28B	LPS-stimulated NOx production from cultured BAL cells lavaged at various time-points following intratracheal instillation of amiodarone or vehicle……	73
29A	Non-LPS-stimulated TNF-α production from cultured BAL cells lavaged at various time-points following intratracheal instillation of amiodarone or vehicle……	74

29B LPS-stimulated TNF-α production from cultured BAL cells lavaged at various time-points following intratracheal instillation of amiodarone or vehicle…… 75

30 TNF-α levels in the first BAL fraction at various time-points following instillation of amiodarone or vehicle……. 76

31 IL-1β production from cultured BAL cells recovered by lavage 3 hours following intratracheal amiodarone or vehicle treatment……. 77

32A IL-6 production from BAL cells recovered by lavage 15 minutes following i.t. instillation of amiodarone or vehicle and cultured 24 hours. 78

32B IL-6 production from BAL cells recovered by lavage on day 3 following i.t. instillation of amiodarone or vehicle and cultured 24 hours……. 79

33A IL-10 production from BAL cells recovered by lavage 15 minutes following i.t. instillation of amiodarone or vehicle and cultured 24 hours. 80

33B IL-10 production from BAL cells recovered by lavage on day 3 following i.t. instillation of amiodarone or vehicle and cultured 24 hours…….. 81

34 Albumin in the first BAL fraction at various time-points following intratracheal amiodarone or vehicle treatment…… 82

35 LDH Activity in the first BAL fraction at two time-points following intratracheal amiodarone or vehicle treatment…… 83

36A Effect of AD, citrate buffer, or HCl on albumin in the first BAL fraction at 15 min……. 84

36B Effect of AD, citrate buffer, or HCl on LDH activity in the first BAL fraction at 15 min…… 85

37A Representative images obtained by LSCM of the effect of AD on cellular viability *in situ* at 15 min…… 86

37B Representative images obtained by LSCM of the effect of AD on cellular viability *in situ* at 3 hours…… 87

37C Representative images obtained by LSCM of the effect of AD on cellular viability *in situ* at day 3…… 88

38 Representative micrographs of thin sections obtained by LSCM for *in situ* quantification of the effect of AD on cellular viability at 15 min…… 89

39A Effect of AD on ethidium staining of airway and parenchymal cells at 15 min…… 90

39B Overall total cells, total airway cells, and total parenchymal cells per field at 15 min…… 91

40 Representative micrographs of thin sections obtained by LSCM for *in situ* quantification of the effect of AD on cellular viability at day 3……. 92

41A Effect of AD on ethidium staining of airway and parenchymal cells at day 3……... 93

41B Overall total cells, total airway cells, and total parenchymal cells per field at day 3……... 94

42 ESR spectra of AD solution without spin-trapping…… 95

43 ESR spectrum of AD powder…… 96

44 Time course of AD-induced DMPO peak formation in water; effects of inhibitors and exogenous chemicals…….. 97

45A Time course of AD-induced DMPO peak formation in water; effects of inhibitors and exogenous chemicals……... 98

45B Final spectra in the time course of AD-induced DMPO peak formation in PBS; effects of inhibitors and exogenous chemicals…….. 99

46 Time course of AD-induced DMPO peak formation in PBS; effect of heat-inactivation of inhibitor enzymes…… 100

47 Time course of AD-induced DMPO peak formation in PBS; effects of thiol antioxidants……. 101

48 ESR spectra of AD solution in chloroform with spin-trapping at 3 min…. 102

49 Effect of AD concentration on hydroxyl radical production at 30 min…… 103

50 ESR spectra of AD solution in water with spin-trapping at 30 min.; effects of UV irradiation and antioxidants…… 104

51A Effect of AD with and without antioxidants on albumin in the first BAL fraction at 15 min…….. 105

51B Effect of AD with and without antioxidants on LDH activity in the first BAL fraction at 15 min……. 106

52A Positive-ion electrospray mass spectra of AD in methanol and water……. 107

52B Negative-ion electrospray mass spectra of AD in methanol and water…… 108

53 Possible pathways for AD-induced hydroxyl radical formation; the effects of exogenous enzymes and chemicals…….. 123

Introduction

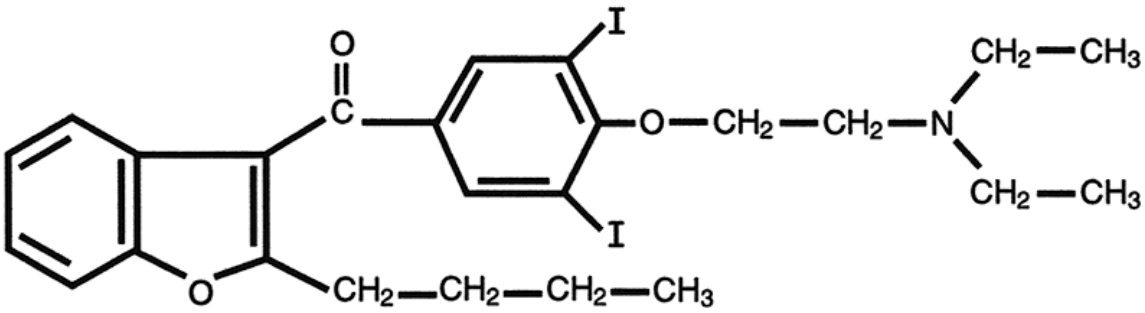

Figure 1: The structure of amiodarone.

Amiodarone (AD; 2-butyl-3-[3′,5′-diiodo-4′-α-diethylaminoethoxybenzoyl]-benzofuran), an iodinated benzofuran derivative (**Figure 1**), is a very effective class III antiarrhythmic drug. It prolongs myocardial refractory period without altering membrane potential. AD inhibits ventricular tachycardia and ventricular premature beats as well as ventricular fibrillation (Mason, 1987). AD is a synthetic derivative of khellin, a chemical extracted from a wild herbaceous Egyptian plant known as Umbelliferae. Extract of Umbelliferae had a reputation in folk medicine as a diuretic that could relieve renal colic, or spasmodic pains usually associated with a calculus blockage of the ureter or urethra. It was in Cairo in 1930 where a technician of Anrep, a professor of pharmacology, self-medicated his renal colic with khellin, and serendipitously found his angina disappeared (Sneader, 1996). AD was originally developed in the early 1960s in Belgium when analogs of khellin were first systematically produced and studied. AD was found to be a coronary vasodilator and used for the treatment of angina, but was withdrawn from the market in 1967 due to reports of corneal deposits, skin photosensitivity, and thyroid disorders (Sneader, 1996). Despite this, AD was soon found to have unique antiarrhythmic properties that, along with sotalol, formed the basis of the class III classification (Singh, 1971). Soon after this discovery, Argentinean cardiologist

Mauricio Rosenbaum began using AD to effectively treat patients with various types of arrhythmias and supraventricular tachycardias (Rosenbaum et al., 1974; Rosenbaum et al., 1976). AD was then introduced in the U.S. as an investigational antiarrhythmic drug in 1978 and as such was not subjected to large, controlled, multicenter clinical trials (Akoun et al., 1991). Soon after, the first reports of AD-induced pulmonary toxicity (AIPT), including pneumonitis and fibrosis, began to appear (Rotmensch et al., 1980). However, because of the numerous reports of its clinical effectiveness, and despite its known toxicity profile, AD was approved by the Food and Drug Administration in 1986 for use in the U.S. It has been noted that AD did not undergo the structured drug approval process and was actually approved on the basis of clinical experience rather than rigorous study (Winkle, 1985).

When first accepted, its use was primarily as a drug of last resort in situations where the severity of the arrhythmia outweighed the potential for side effects. Also, certain ventricular tachyarrhythmias are resistant to other treatments and respond only to AD (Singh et al., 1989; Gill et al., 1992). However, its effectiveness against various types of arrhythmias as well as an increasing trend in clinical acceptance (Bauman, 1997) has led to AD being the most frequently prescribed antiarrhythmic drug in 1998, with about 1.65 million total patients (Connolly, 1999). With arrhythmias accounting for approximately 20% of all deaths in the U.S., an estimated 4.3 million deaths in 1996 alone (American Heart Association), there is a potential for AD use to continue to grow. As the use of AD increases, the occurrence of its side effects will likely increase accordingly.

While AD produces several side effects, including corneal microdeposits, bradycardia, skin photosensitivity, and altered thyroid function, pulmonary toxicity is one of the most severe and potentially life-threatening (Mason, 1987; Martin and Rosenow, 1988a; Martin and Rosenow, 1988b). AIPT occurs in 10 to 17% of patients taking AD orally, and proves fatal in an estimated 5 to10% of affected patients (Pitcher, 1992). AIPT is manifested in humans in several ways, including phospholipidosis, pneumonitis, and fibrosis.

Phospholipidosis is an abnormal accumulation of phospholipid material in alveolar macrophages and lung parenchymal cells, and is caused by AD and some other cationic amphiphilic drugs (Akoun et al., 1986). The storage of this phospholipid material results in the formation of lysosomal lamellar inclusion bodies. In the lungs, the pulmonary macrophage is the cell type most affected (Akoun et al., 1986), but lung epithelial cells (Marchlinski et al., 1982) as well as extra-lung cell types such as Kupffer cells, skin macrophages, and peripheral neutrophils can be affected (Adams et al., 1985) as well as the cornea and conjunctiva (D'Amico and Kenyon, 1981). There is evidence that phospholipidosis is caused by an inhibition of lysosomal phospholipase A, an enzyme responsible for phospholipid degradation (Martin, 1990).

The more damaging aspects of AIPT are the pneumonitis, or inflammation, and pulmonary fibrosis, both of which can be fatal (Mason, 1987). The inflammatory response involves a thickening of the alveolar walls and the variable infiltration of inflammatory cells into the interstitial and alveolar spaces (Martin and Rosenow, 1988a) possibly associated with edema (Kennedy et al., 1987). AD-induced inflammation involves the recruitment of specific inflammatory cells, such as polymorphonuclear

leukocytes (PMNs or neutrophils), lymphocytes, plasma cells, eosinophilic leukocytes (eosinophils), and in some cases increased monocytes or macrophages (Akoun et al., 1986; Martin and Rosenow, 1988a; Martin and Rosenow, 1988b). Inflammatory cells are capable of releasing toxic species, such as reactive oxygen species (ROS) and damaging proteases, as well as inflammatory mediators such as cytokines and chemokines that can exacerbate the existing condition (Laskin and Pendino, 1995). ROS damage includes lipid peroxidation, protein polymerization, and DNA strand breakage (Nakazawa et al., 1996). Therefore, inflammation can lead to damage of the host lung cells and tissues.

Tumor necrosis factor (TNF)-α is widely believed to be the primary regulatory cytokine of many inflammatory processes. TNF-α production is regulated by a TATA box and promoted through a number of regulatory sites including NF-κB, CRE, AP-1, and AP-2 (Luster et al., 1999). TNF-α is also regulated via mRNA translation rates and stability; lipopolysaccharide (LPS) stimulation leads to a 100-fold accumulation of TNF-α message (Lindstein et al., 1989; Han et al., 1991). Following i.v. administration of LPS to humans and experimental animals, serum TNF-α levels peak within two hours before falling to baseline undetectable levels at four hours (Hesse et al., 1988). TNF-α in turn stimulates the production for other inflammatory mediators such as IL-1, IL-6, IL-8, macrophage inflammatory protein (MIP)-2, granulocyte macrophage-colony stimulating factor (GM-CSF), intracellular adhesion molecule (ICAM)-1, and endothelial leukocyte adhesion molecule (ECAM)-1 (Luster et al., 1999). These mediators can then act to enhance vascular permeability and recruit and activate leukocytes involved in the inflammatory response. IL-6 is produced by T-cells and macrophages and acts to stimulate B-cell proliferation and differentiation into antibody-forming cells (Kishimoto

and Hirano, 1988). Inflammation is usually resolved quickly, possibly involving the anti-inflammatory cytokine IL-10 and soluble cytokine receptors that act to bind pro-inflammatory cytokines away from cellular receptors (Suffredini et al., 1999). Chronic inflammation in the lungs may lead to the destruction or restructuring of parenchymal tissue, leading to a thickening of the alveolar walls and collagen deposition known as pulmonary fibrosis (Ward and Hunninghake, 1998). AD-induced fibrosis may be diffuse or focal, and also may be interstitial or intra-alveolar.

Pulmonary fibrosis is the accumulation of interstitial collagen fibers, which results in a thickening of the alveolar septa and a decrease in the ability of the lungs to expand to full capacity. Therefore, the fibrotic lung has less compliance and a reduced capacity to accomplish gas exchange than a normal lung (Poli and Parola, 1997). While the other pulmonary side effects of AD are potentially reversible, fibrosis is irreversible once it develops (Akoun et al., 1986; Mason, 1987; Martin and Rosenow, 1988a; Martin and Rosenow, 1988b). The development of fibrosis may be linked to the repair of lung damage, whether caused by a toxic insult or chronic inflammation. Following lung cell death or the recruitment of inflammatory cells, mediators are released that recruit and activate fibroblasts and smooth muscle cells to the alveolar septa and alveolar spaces (Poli and Parola, 1997; Ward and Hunninghake, 1998; Paine and Ward, 1999). Several signaling mechanisms have been implicated in the development of pulmonary fibrosis. TNF-α is important in various ways, including induction of inflammatory cell adhesion; initiation of the cytokine cascade; enhancement of a procoagulant environment; immunomodulation of lymphocytes; mitogenesis of mesenchymal cells; regulation of apoptosis; and regulation of collagen synthesis and reabsorption (Lasky and Brody,

2000). Also, TNF-α is key in the recruitment of various cell types to the lungs, including platelets and eosinophils, which themselves can release potent profibrotic mediators. These include Platelet-Derived Growth Factor (PDGF) and Transforming Growth Factor Beta (TGF-β). PDGF is one of the most potent mesenchymal cell mitogens, and has been seen in several models of pulmonary fibrosis with differing etiologies (Robledo and Mossman, 1999; Lasky and Brody, 2000). TGF-β is secreted by several pulmonary cells types, including macrophages, eosinophils, epithelial cells, endothelial cells, and fibroblasts, and acts to increase extracellular matrix synthesis while inhibiting matrix degradation (Lasky and Brody, 2000; Levi-Schaffer et al., 1999). Intracellular signaling cascades involved in these cellular responses include mitogen-activated protein kinases (MAPK) and NF-κB. Activation of transcription factors such as NF-κB and AP-1 have been linked to changes in early response genes such as *c-jun* and *c-fos*, which may govern proliferation and apoptosis in various cells (Robledo and Mossman, 1999). Thus, similar factors may be involved in both pulmonary inflammation and fibrosis. The role chronic inflammation plays in the development of AD-induced pulmonary fibrosis in not yet clear, but it may be a necessary factor in its development.

Current treatment for AIPT involves a reduction or elimination of the drug dosage, leaving the patient susceptible to the original arrhythmia, and sometimes corticosteriod therapy, which is accompanied by its own set of undesirable effects (Martin and Rosenow, 1988b). Furthermore, toxicity may recur when the steroid treatment is halted (Joelson et al., 1984).

While several potential mechanisms for the development of AIPT have been previously proposed and studied, the actual pathogenesis of AIPT is unknown (Massey et

al., 1995; Reasor and Kacew, 1996). Possible theories include the involvement of oxidative mechanisms (Kennedy et al., 1988; Vereckei, 1993), dependence on immunological mechanisms and the involvement of hypersensitivity (Akoun et al., 1984), the development of phospholipidosis (Martin, 1990), direct cytotoxicity (Martin and Howard, 1985), drug burden (Camus and Jeannin, 1984), and drug-induced alterations in membrane properties (Honegger et al., 1993).

While these theories are more easily studied in animal models of AIPT, there are some data from human patients that pertain to several. Phospholipidosis is generally present in all patients taking AD whether or not they present any other symptoms of the toxicity (Kennedy et al., 1987); therefore it is unclear what role the phospholipidosis plays, if any, in the development of the other aspects of the toxicity (Reasor and Kacew, 1996). While patients displaying other manifestations of AIPT also display phospholipidosis, the mere presence of phospholipidosis does not necessarily mean that other forms of the toxicity will develop.

There is evidence both for and against an immunological basis for human AIPT. Evidence for a hypersensitivity reaction in a patient with AD-induced pneumonitis was reported by Akoun et al. (1984) when bronchoalveolar lavage (BAL) revealed lymphocytosis with an inverted helper/suppressor T cell ratio. Another study found similar results in five patients, who subsequently responded well to corticosteriod therapy, also indicative of an allergic response (Venet et al., 1984). A humoral response to a lung-AD complex in a patient who had taken AD for approximately six months was also reported (Fan et al., 1987). Martin and Rosenow (1988b) examined the BAL fluid from 14 patients with AIPT and found five with normal BAL cell profiles, four with

lymphocytosis, three with a predominant neutrophilia, two with significant eosinophilia, one of which was also presenting with lymphocytosis. These differences in cell profiles may reflect different times in the development of the toxicity or differing mechanisms behind each case. Studies do exist that contain no evidence for immunological involvement (Adams et al., 1986; Liu et al., 1986; Kennedy et al., 1987). It is therefore possible that AIPT has various causes in different cases or is multi-factorial (Reasor and Kacew, 1996).

Attempts to elucidate the etiology of AIPT may be more direct when using animal models for the toxicity. The functional effects of phospholipidosis on lung cells have been studied in animal models (Wilson and Lippmann, 1993; Wilson et al., 1993; Reasor et al., 1996) with inconsistent results being reported, although the condition does not seem to be particularly deleterious alone.

Several labs have studied the possible role of oxidative mechanisms in the development of AIPT utilizing animal models. One animal study implicated oxidative processes occurring in the lung by showing decreased levels of the endogenous antioxidant glutathione, both reduced and oxidized, in the lungs of hamsters following a single intratracheal (i.t.) AD treatment (Leeder et al., 1996). Also, the ability of antioxidants to prevent AD-induced damage to isolated and perfused rabbit lungs was shown in another report (Kennedy et al., 1988). In contrast, Leeder et al. (1994) found that pretreatment of hamsters with antioxidants did not prevent the development of pulmonary toxicity following i.t. AD treatment. It is important to note, however, that animals were pretreated with antioxidants for only three days prior to AD administration, and no antioxidant treatment was given after AD treatment. Furthermore, Wang et al.

(1992) reported attenuation of AD-induced phospholipidosis and fibrosis in hamsters by the administration of taurine and/or niacin. The mechanisms of this protection are not clear, but taurine could be acting as an antioxidant. Blake and Reasor (1995a) reported that BAL cells recovered from hamsters following intratracheal AD administration produced more phorbol myristate acetate (PMA) stimulated luminol-dependent chemiluminescence (LDCL) than cells from control animals. These increases were diminished by superoxide dismutase and catalase addition, indicating the possible involvement of superoxide anion and hydrogen peroxide or their subsequent products in the response. It is not known what role these oxidants play in the development of AIPT.

Aromatic iodine derivatives are known to deiodinate via a free radical mechanism (Levy et al., 1973), and it has been shown that AD can generate free radicals under certain conditions. Much of the interest in AD free radical production stems from studies examining the mechanism of cutaneous photosensitivity, which occurs in 75-100% of patients receiving AD (Harris et al., 1983). Hasan et al. (1984) induced cytotoxicity to erythrocytes and lymphocytes after photoactivation of AD with ultraviolet (UV) irradiation. This damage was found to be both partially oxygen dependent and independent. Desethylamiodarone (dAD), the primary metabolite of AD *in vivo* (Brien et al., 1987), was more phototoxic than AD. The photolysis of AD was first studied spectroscopically by Li and Chignell (1987). Deiodination following UV exposure was shown in both AD and dAD, and aryl radical formation was demonstrated with spin trapping and electron spin resonance (ESR) spectroscopy in aerobic and anaerobic aqueous solutions. Paillous and Verrier (1988) confirmed this UV-induced deiodination and the structures of the products resulting from this photolysis. The resulting aryl

radical was shown to abstract a hydrogen atom from the solvent. They also demonstrated the production of singlet oxygen, formed by the reaction of AD and molecular oxygen, and the presence of hydroxyl radical. Therefore, oxygen-dependent (superoxide, hydrogen peroxide, and singlet oxygen) and oxygen-independent (direct hydrogen abstraction) mechanisms of free radical formation have been implicated following UV-induced deiodination of AD.

While these results have direct implications for studies of the phototoxicity of AD, the involvement of free radicals in AIPT remains unclear. Vereckei et al. (1993) speculated that aryl radical may be produced from AD during *in vivo* metabolism, but was unable to prevent pulmonary toxicity or liver microsomal lipid peroxidation induced by high-dose oral AD treatment to rats with dihydroquinoline-type antioxidants. The same group however did use vitamin E and silimarin separately to reduce AD-induced elevations in conjugated dienes in liver homogenates from AD-treated rats (Agoston et al., 2001), though the role of free radical generation in these changes was never actually established.

AD has also been postulated to act as a free-radical scavenger. Ide et al. (1999) protected cultured cardiac myocytes with AD from hydroxyl radicals produced by the Fenton reaction as well as used AD to quench hydroxyl radicals during ESR analysis. Ribeiro et al. (1997) has shown AD inhibited lipid peroxidation in rat liver mitochondrial membranes challenged by an iron-dependent oxygen radical generating system. Thus it seems that AD has both free radical producing and scavenging properties depending on the conditions in which it is examined.

Other studies using *in vitro* nonpulmonary cell culture systems have shown the cytotoxic effects of AD could not be prevented by antioxidants or free radical scavengers except for vitamin E, which was thought to exert membrane-stabilizing effects and not acting as an antioxidant (Kachel et al., 1990; Ruch et al., 1991). Honegger et al. (1995) utilized vitamin E to inhibit the development of phospholipidosis in cell culture by inhibiting the uptake of the drug into the cells. Also, when hamsters were supplemented with vitamin E in their diets (500 IU/kg chow) for 6 weeks prior to and 21 days following i.t. AD administration, AD-induced elevation of lung hydroxyproline, a biochemical indicator of fibrosis, and lung disease index were inhibited (Card et al., 1999). However, vitamin E supplementation also decreased hydroxyproline levels and disease index in control animals that received the AD vehicle as well. The effects of vitamin E supplementation of patients with AIPT have not been reported.

A review of animal evidence of an immunological cause of AIPT found inconsistent results as well (Reasor and Kacew, 1996). Findings of increased release of certain inflammatory cytokines by alveolar macrophages from animals given oral AD have been reported (Reasor and Kacew, 1996). Studies that find the elevation of lymphocytes in the bronchoalveolar lavage fluid of orally AD-treated rats (Wilson et al., 1989) and an influx of neutrophils and eosinophils into the lungs of hamsters treated with AD intratracheally (Cantor et al., 1984; Blake and Reasor, 1995b) implicate immune processes being active following AD administration. Lymphocytes and eosinophils are associated with hypersensitivity reactions, indicating a possible role of similar immune reactions in AIPT in some animal models. Eosinophils, once recruited, have the ability to release mediators such as platelet-activating factor, leukotrienes, prostaglandins,

histamine, cytokines, chemokines, and cationic proteins which have the potential to augment the inflammatory response and induce tissue damage and dysfunction (Hogan and Foster, 1997). The role of eosinophilic inflammation in the development of AIPT is not yet fully elucidated.

Blake and Reasor (1997) reported that treatment of hamsters with the corticosteriod dexamethasone prior to and following i.t. AD administration prevented the development of pulmonary fibrosis but did not block neutrophil influx or albumin leakage into the alveoli. The interdependence of immune reactions and fibrogenesis is not entirely clear, and the role of initial inflammation again warrants further study. However, dexamethasone may have a direct effect on fibroblasts to decrease collagen production (Ramalingam et al., 1997).

Amiodarone is usually administered to patients orally, although an intravenous preparation exists that can be used for cardiac emergencies in hospital settings. Attempts to reproduce the pulmonary toxicity seen in humans with animal models have met with limited success. Oral AD treatment of animals with moderate doses produces the characteristic phospholipidosis. However, animals seem resistant to the development of the other more damaging inflammatory and fibrogenic aspects of AIPT (Heath et al., 1985; Riva et al., 1987) except in a few studies when animals were given very high AD doses or treated for an inordinate amount of time (13 months) (Carvalho et al., 1996) and inflammatory cells (Wilson et al., 1991; Carvalho et al., 1996) or fibrosis (Vereckei, 1993; Carvalho et al., 1996) were found. Conversely, inflammation and fibrosis have been induced by the i.t. administration of AD to hamsters (Cantor et al., 1984; Daniels et al., 1989; Wang et al., 1992; Blake and Reasor, 1995a) and rats (Reinhart et al., 1996),

but this method lacks the phospholipidosis induced by chronic oral AD administration. However, since the role of phospholipidosis in the development of AIPT is in question, and inflammation and fibrosis are the more damaging and life-threatening aspects of the toxicity, the i.t. route of administration is currently favored in animals studies of AIPT (Reinhart et al., 1996; Reinhart and Gairola, 1997; Card et al., 1999).

The first report of i.t. AD administration to animals was from Cantor et al. (1984) in which hamsters were given a single i.t dose of AD and evaluated for pathological reactions. They found an initial inflammatory response to both AD and vehicle (normal saline with 2% Tween 80 and 1% benzyl alcohol) followed by resolution and a secondary inflammatory response in AD-treated animals involving eosinophilia and progressing to fibrosis. As this secondary response shared some common features with human AIPT, they concluded that i.t. AD administration may be useful in examining the mechanisms that underlie AIPT development. They chose the i.t. route of administration because it had been successfully employed to produce bleomycin-induced pulmonary fibrosis in hamsters (Snider et al., 1978). However, it has been subsequently noted that the pathology of bleomycin-induced fibrosis in mice differs depending on the route of administration employed, either i.t or i.v. (Lindenschmidt et al., 1986). Intratracheal bleomycin treatment leads to a rapid inflammatory response and relatively sooner fibrosis development in central lesions than does i.v. bleomycin treatment, which causes a less-pronounced inflammatory response and subpleural fibrotic lesions more similar to the distributions seen in humans. Thus the i.t. route of administration may change the localization and the onset of pulmonary toxicity. Intratracheal administration is more commonly employed as a surrogate for inhalation for airborne toxicants, especially

during screenings of multiple toxicants for multiple fractions of a complex toxicant, or when inhalation techniques are not feasible due to technical considerations (Driscoll et al., 2000). However, the development of the i.t. AD model was based on the perceived success of the i.t. model of bleomycin-induced pulmonary fibrosis, as i.t. AD produced similar results. The use of this route of administration has continued due to the subsequent findings of the lack of inflammation and fibrosis development from oral AD administration to animals. Thus, the i.t. route of administration has been the most widely employed animal model for the study of AD-induced inflammation and fibrosis in recent years.

Models of AIPT have been developed in hamsters (Cantor et al., 1984; Daniels et al., 1989; Wang et al., 1992; Rafeiro et al., 1994; Leeder et al., 1994; Blake and Reasor, 1995a) and rats (Reinhart et al., 1996; Reinhart and Gairola, 1997) in an attempt to elucidate the mechanisms by which this disorder develops. Intratracheal instillation of AD leads to an inflammatory reaction in hamsters (Blake and Reasor, 1995a) and a fibrotic reaction in hamsters (Cantor et al., 1984; Blake and Reasor, 1995b) and rats (Reinhart et al., 1996). Little information exists concerning the inflammatory reaction to i.t. AD in rats. While the hamster has been the animal of choice for many studies of AIPT, the rat model offers a greater potential for studies of the mechanisms that underlie AIPT due to the greater availability of certain molecular reagents and tools. A rat model for AIPT could allow research into the specific mediators, such and cytokines and cell-signaling molecules, of both the inflammatory and fibrotic responses. Furthermore, specific inhibitors could be used to ascertain the specific role of any single mediator.

Therefore the development of a rat model for AIPT is important in the attempt to elucidate mechanisms that may underlie the development of the toxicity.

Diagnosis of AIPT in patients taking amiodarone is difficult due to the lack of specific symptoms and often the presence of confounding factors (Martin and Rosenow, 1988a). AIPT is usually diagnosed based on the symptoms of dyspnea as well as radiological findings of diffuse pulmonary infiltrates (Nicholson and Hayward, 1989; Butler and Smathers, 1985; Delany et al., 1993). Patients with concurrent cardiac or respiratory disorders are more likely to go undiagnosed, and AIPT can be fatal in such cases (Pitcher, 1992). A specific marker for the pulmonary response to AD could aid in the early diagnosis of AIPT, possibly before overt toxicity develops. While several serum biomarkers have been proposed for the monitoring of lung diseases, at present none have been identified to detect the onset and progression of AIPT. Serum levels of mucin-1 were elevated in 8 out of 10 AD patients with AIPT, but mucin-1 levels were also increased in AD patients that exhibited non-pulmonary toxicities (Devine et al., 1998). Also, elevated serum lactate dehydrogenase (LDH) was found in a patient with AD-induced pneumonitis (Drent et al., 1998). However, LDH is not lung-specific and can be released into the blood in non-pulmonary toxicities.

Recently the serum levels of surfactant protein-D (SP-D) were found to be increased in patients with idiopathic pulmonary fibrosis, interstitial pneumonia with collagen disease, and pulmonary alveolar proteinosis (Honda et al., 1995). Since SP-D is produced in the lungs by alveolar type II cells and is found in the fluid lining the alveoli (Crouch, 1998), it may serve as a more specific marker for lung injury. No studies as of yet have examined the potential for SP-D to serve as a biomarker for AIPT.

Because of the current prescribing trends of using AD as more often as a first-line therapy to treat various types of arrhythmias, there is potential for a large patient population to become afflicted by AIPT. Research is needed to aid in the elucidation of the mechanisms behind the development of AIPT, so that inhibitors of the toxicity can be developed, and to identify a biomarker to aid in the early diagnosis AIPT, so that a potentially fatal condition can be averted.

Objectives

This study consists of three major objectives. The first was to select an animal model for AIPT that contained as many of the aspects of human AIPT as possible (i.e. phospholipidosis, inflammation, and fibrosis) or at least the most damaging aspects of human AIPT (inflammation and fibrosis). The second objective was to characterize the chosen model with regards to the development of initial damage, inflammation and subsequent fibrosis, including any cellular activation that may be occurring that could contribute to the damage observed. Also, the potential for serum SP-D to act as a biomarker for the toxicity was examined. The third objective was to identify the processes that occur soon after the AD dose is given, particularly focusing on the direct role of the drug versus the role of inflammatory cell recruitment to the lungs as factors in AD-induced damage.

Objective 1 was to determine the appropriate animal model to study AIPT. Two main routes of exposure exist for experimentally inducing AIPT in laboratory animals, either a daily oral dose of AD or an intratracheal bolus instillation of AD directly to the lungs. Each method develops different aspects of human AIPT and the appropriate model is chosen based on the endpoints being assessed. Oral AD treatment leads to lung drug accumulation and phospholipidosis while i.t. AD produces inflammation and fibrosis without drug and phospholipid accumulation. To assess the two dosing protocols in rats, a series of experiments was designed to examine several aspects of the pulmonary response. Rats were given AD or the sterile water vehicle either orally (150 mg/kg) daily for 7 or 14 days until lavage or a single dose intratracheally (6.25 mg/kg) on day 0 and lavaged on day 5.

Objective 2 was to characterize the chosen model with regards to early damage to the alveolar-capillary barrier, the number, type, and activation state of the inflammatory cells involved, and the development of pulmonary fibrosis. This was done by administering two i.t. doses of AD (6.25 mg/kg bw in a 3.125 mg/ml solution) or an equivalent volume of its vehicle on days 0 and 2 and subsequently examining the cells recovered by BAL or the level of collagen deposition in the lungs. Levels of SP-D in the serum were also measured.

Objective 3 was to examine the events immediately following the i.t. administration of AD or vehicle with regards to either cellular activation and potential inflammatory regulator release or direct action of the drug. The former was done by recovering the lung cells soon after the first or second instillation and placing them in culture 24 hours. The culture media could then assayed for these mediators. The role of direct AD cytotoxicity to the lungs was examined by analyzing biochemical indicators of damage as well as utilizing *ex vivo* microscopy of intact tissue and cellular viability determination. The ability of the drug to produce free radicals and the role of antioxidants in the toxicity were also examined.

Methods

Laboratory Animals: All studies were performed on adult male Fischer 344 rats (200-300g; Hilltop Laboratory Animals, Scottsdale PA). The animals were housed in the Robert C. Byrd Health Sciences Center's animal quarters and were allowed at least one week to acclimate after arrival from the supplier. Free access to food and water was allowed unless otherwise indicated.

Oral Treatment: Animals were given amiodarone (150 mg/kg) or the water vehicle 5 days per week with a syringe and ball-tipped feeding needle, which was introduced though the mouth and into the esophagus where the drug was administered. Rats were weighed regularly, and food was withheld from the water-treated control animals to maintain similar weights between the treatment groups. Animals given AD had free access to food, and all animals had free access to water.

Intratracheal Treatment: Animals were anesthetized with Brevital (sodium methohexital, 3 mg/kg), placed on a slanted board, and suspended from their maxillary incisors as well as held by an elastic strap across the abdomen. The tongue was held with gauze and a syringe with a ball-tipped 20-gauge feeding needle was inserted transorally into the trachea. Amiodarone (6.25 mg/kg in a 3.125 mg/mL solution; 4.5 mM; pH 3.7) or an equivalent volume of various control solutions (sterile water, HCl [4.5 mM], HCl [pH 3.7], citrate buffer [pH 3.7; Lillie, 1948], and antioxidant solution [45 mM Trolox and 22.5 mM ascorbate]) were then administered to the lungs. The rat was removed from the board and observed until consciousness is regained. If necessary, air from the in-house supply system was gently blown into the mouth or nose of animals experiencing difficulty breathing due to obstructed airways. Amiodarone or control solutions were

administered in several different protocols; some studies involved just one instillation, while others involved two separate instillations into the same animal at different time points. The first instillation occurred on what is designated day 0 and the second on either day 2, meaning the rats receive two instillations two full days apart, or day 7, where the rats receive two separate instillations one week apart. The single intratracheal dose protocol was reported by Reinhart et al. (1996), while the addition of a second instillation had not yet been reported in rats.

Combined Dosing Protocol: During one experiment the dosing protocols were combined so that the same animals were given amiodarone or vehicle both orally and intratracheally. Treatments started either concurrently, with animals receiving their first oral and i.t. doses on day 0, or staggered, with one group of animals being treated for one week orally before receiving the first of two i.t. doses. In both groups oral treatment continued for the duration of the experiment. Control animals were also weight-matched in this study by withholding food.

Bronchoalveolar Lavage: To harvest pulmonary cells for morphologic and functional analysis, BAL was performed by washing out the lungs with aliquots of calcium-free and magnesium-free phosphate-buffered saline (PBS). The first BAL volume was administered as 2mL per 100g body weight, and this volume was placed into the lungs for 30 seconds with light massaging, withdrawn, and again instilled into the lungs for 30 more seconds. Once withdrawn, this aliquot (designated the first BAL fraction) was kept separate from the rest of the lavage fluid that was recovered. BAL was continued with similar aliquots and pooled until 50 mL of BAL fluid, containing BAL cells, were recovered. The recovered fluid was then centrifuged, the supernatant decanted, and the

cells resuspended. The first BAL fraction was centrifuged separately and the supernatant was either assayed for lactate dehydrogenase activity and albumin content or aliquotted and frozen at -20^{o}C for subsequent albumin analysis (when LDH analysis was not done) and at -70 ^{o}C for cytokine content analysis. The cells from the first BAL fraction were then pooled with the rest of the cells recovered from that animal, and were washed two times. Total BAL cells were counted using a Coulter Counter equipped with a Channelizer (model Z_b, Coulter Electronics, Hialeah, FL). Aliquots of cells were then attached to microscope slides via a cytospin (Shandon Cytospin II, Shandon Inc, Pittsburgh, PA), dried, and stained with an automated slide stainer using Wright-Geimsa stain (Hema-Tec 2000, Bayer Corp., Elkhart, IN). Finally, the different cell types were identified and counted under a light microscope and the percentage of total cells as well as the total number of each cell type recovered from the lavage were obtained.

Serum Preparation: At the time of lavage, blood was drawn from each animal directly from the heart using a 21-gauge needle and syringe. The blood was allowed to clot and then was centrifuged. The serum supernatant was drawn off and frozen at -20^{o}C for subsequent surfactant protein analysis.

Analysis of Drug Accumulation: The accumulation of amiodarone and subsequent metabolites, such as desethylamiodarone, was measured in BAL cells. According to the method of Reasor et al. (1988), the AD and its metabolites were extracted from harvested BAL cells with acetonitrile, and the drug levels were measured using high-performance liquid chromatography (HPLC) and compared to a standard curve produced from known drug concentrations. L-8040 was used as an internal standard.

Analysis of Phospholipidosis: To index phospholipidosis in BAL cells, the cells were harvested by lavage as previously described and subjected to lipid extraction by chloroform/methanol (2:1, v/v) as described by Folch et al. (1957). Then total lipid phosphorus was measured by the method of Ames and Dubin (1960). Briefly, samples were ashed with 10% $MgNO_3$ in 70% ethanol to liberate inorganic phosphorus. The resulting phosphorus was measured colorimetrically.

Analysis of Albumin: The integrity of the alveolar-capillary barrier was evaluated by measuring the amount of albumin, a protein from the blood, in the first BAL fraction that was recovered from the lungs during lavage. BAL fluid albumin was determined according to a Sigma Diagnostics method utilizing the reaction of albumin with bromcresol green. The reaction product was then measured with a spectrophotometer at 628 nm and quantified against known concentrations of bovine serum albumin.

Analysis of LDH Activity: Lactate dehydrogenase activity in the first BAL fraction was used as an indicator of cellular death and injury. LDH leaks from dead or damaged cells when membrane integrity is lost. LDH activity was determined by the reduction of pyruvate coupled to the oxidation of NADH at 340 nm over time according to the method of Wroblewski and LaDue (1955). Measurements were performed with a Cobas Fara II analyzer (Roche Diagnostics Systems, Montclaire, NJ).

Performance of Luminol-Dependent Chemiluminescence (LDCL): To measure the release of oxidants from BAL cells, LDCL was performed as described by Antonini et al. (1994) on a Berthold LB9505C Luminometer. Rats treated with AD or water vehicle underwent BAL, and the BAL cells were counted as previously described. Luminol, used as a bystander to produce CL when oxidized, was dissolved in DMSO and then diluted in

PBS (pH 7.4). The final luminol concentration in the assay cuvette was 10^{-5} M. Phorbol myristate acetate was used to activate the oxidative burst at a final cuvette concentration of $2X10^{-6}$ M. An unstimulated baseline LDCL production was obtained by omitting PMA. To selectively inhibit oxidant species and determine the nature of the LDCL produced, the nitric oxide synthase inhibitor N^{ω}-nitro-L-arginine methyl ester (L-NAME; 1 mM final concentration) and superoxide dismutase (SOD; 0.2 mg/ml final concentration), a superoxide-scavenging enzyme, were added alone and combined to designated replicates. Samples containing inhibitors were pre-incubated five minutes prior to PMA addition and subsequent LDCL measurement. The final reaction volume for all samples was 500 µl and the reactions were measured at 37°C for 20 minutes. Integral CL counts were determined by KINB software for the Berthold 9505C Luminometer.

Analysis of Fibrosis: Pulmonary fibrosis was evaluated several ways in these experiments; biochemically, histopathologically, and with laser-scanning confocal microscopy (LSCM) at either 28 or 42 days after initial i.t. AD or vehicle treatment.

Biochemical Quantification of Hydroxyproline: Hydroxyproline is an amino acid that is relatively rare in most proteins, but is prominent in the left-handed helix of collagen fibers. An increase in lung hydroxyproline levels indicates an increase in lung collagen, which is characteristic and definitive of pulmonary fibrosis. Hydroxyproline was measured based on the assay developed by Witschi et al. (1985). The right-lung lobes of treated or control animals were hydrolyzed in strong acid at 100°C for 72 hours to release hydroxyproline. The hydroxyproline was then oxidized and converted to a colored

product that could be measured with a spectrophotometer at 560 nm, comparing the samples with standard solutions of trans-hydroxyproline.

Histopathological Evaluation of Fibrosis: Fibrosis was characterized histopathologically by inflating and fixing the left lung with 10% formalin solution, embedding the tissue in paraffin, and sectioning the tissue for the preparation of microscope slides. Sections of 5 μm were made and stained with either hematoxylin and eosin or trichrome, a stain specific for collagen fibers. A veterinary pathologist (Dr. Ann Hubbs, HELD/NIOSH, Morgantown, WV) then evaluated any pulmonary damage and fibrosis in these sections, and returned a detailed report of the findings.

Laser Scanning Confocal Microscopy (LSCM): Fibrosis was quantitated in the left lung lobes of AD- and water-treated animals at day 28 based on the method of Antonini et al. (1999). The left lung was inflated and fixed with 10% formalin, sectioned into blocks, dehydrated in a graded series of ethanol washes, stained with Lucifer Yellow (0.1 mg/mL) for 24 hr, and embedded in Spurr's epoxy for LSCM analysis (Rogers et al., 1992). Images were recorded using a Sarastro 2000 (Molecular Dynamics, Inc., Sunnyvale, CA) laser scanning confocal microscope (Optishot-2, Nikon, Inc., Melville, PA) fitted with an argon-ion laser. Emission spectra >510 nm were diverted to a separate photodetector and used to image lung tissue and cells. Using a 20X objective, the tissue areas (excluding large airways and blood vessels) of 25 random scans per block (3-4 blocks per animal; 75-100 scans per animal) were randomly scanned by Jenny Roberts (HELD/NIOSH, Morgantown, WV). An image field of 1024 μm x 1024 μm (1.05×10^6 μm^2) was defined over a region of parenchyma entirely filling the field. Using ImageSpace software (Molecular Dynamics), threshold pixel intensity levels were

established that defined lucifer yellow-positive and lucifer yellow-negative sites, thus identifying the presumed connective tissue matrix material. Fluorescent signals below a pixel intensity value of 38 were thresholded out, which eliminated the measurement of cells and debris within the air spaces. The area of tissue stained above the intensity threshold was obtained for each image. All random scans of the lung tissue for each treatment group were recorded ~3-5 μm from the top of the tissue block at a photomultipier tube (PMT) setting of 450, pinhole aperture setting of 50 μm, and the same laser voltage setting of 20 mW. This analysis resulted in a data set expressed as connective tissue (lucifer yellow-positive) area in μm^2 per image field. For statistical analysis of difference between groups, all measurements per each animal were averaged, and the mean tissue area/field of each animal was obtained (N=3 per treatment).

Surfactant Protein-D Levels: Levels of SP-D were assayed in the sera of naïve and AD- and vehicle-treated rats at various time points by Kathy Shannon in the laboratory of Dr. Robert Mason (National Jewish Medical and Research Center, Denver, CO.). Serum SP-D levels were assayed with a sandwich enzyme-linked immunosorbent assay (ELISA) technique. Rat SP-D, which was purified from lavage fluid from rats 28 days after silica instillation according to the method of Shimizu et al. (1992), was used as a standard for the assay. Polyclonal anti-rat SP-D rabbit IgG (10 μg/ml in 0.1 M sodium bicarbonate) was prepared by the method of Shimizu et al. (1992) and bound to wells in microtiter plates (Immulon I plates; Dynatech Laboratories, Alexandria, VA) at room temperature overnight. The wells were then incubated with a 5% (wt/vol) solution of non-fat dry milk in PBS (blocking buffer) to block non-specific binding. After washing, 100 μl containing purified rat SP-D (0-20 ng) for standards or appropriately diluted serum samples were

added to each well. Plates were then incubated for 90 minutes at 37^{o} C and then washed with 20% blocking buffer, 1% Triton X-100 (vol/vol) in PBS (antibody buffer). After washing, 200 µl of anti-SP-D antibody-conjugated horseradish peroxidase (30 µg/ml in antibody buffer) were added to the wells and the plates incubated for 90 min at 37^{o} C. After further washing with 1% Triton X-100 in PBS, 200 µl of the color-developing agent (0.1% *o*-phenylenediamine, 0.015% hydrogen peroxide in 0.1 M citrate buffer, pH 4.6) were added. The reaction was carried out for 5 min at room temperature in a darkened room and was stopped by the addition of 100 µl of 1 M sulfuric acid. The absorbance at OD 490 nm was recorded with a Microplate Autoreader EL-311s (BIO-TEC Instruments Inc., Winooski, VT).

Cell Culture: To assess certain products of BAL cells over time, cells were harvested by lavage, counted, and cultured in EMEM 24 hours. The culture media consisted of Eagle's minimum essential medium (MEM; BioWhittaker, Walkersville, MD) supplemented with 1 mM glutamine (GIBCO, Grand Island, NY), 10 mM HEPES, 100U/mL of penicillin-streptomycin (GIBCO), 100 µg/mL of kanamycin (GIBCO), and 10% (vol/vol) fetal bovine serum (BioWhittaker), with a final pH of 7.4. The medium was made using endotoxin-free water (BioWhittaker) and sterile-filtered at 0.2 µm. Cells were cultured in 24-well plates at a density of 2 x 10^{6} cells/mL/well in duplicate in a 37^{o}C incubator with 5% CO_2. Cells were cultured in duplicate either with or without 10 µg/mL LPS. LPS was added as a stimulant of the inflammatory response as a positive control and to obtain maximal response.

NOx Assay: After culture, the NO oxidation products nitrate (NO_3) and nitrite (NO_2), collectively referred to as NOx, were assayed in the media. Samples were first incubated

with *Escherichia coli* nitrate reductase to convert NO_3 to NO_2. Then NO_2 was measured colorimetrically with the Greiss reaction (Green et al., 1982). NOx levels were determined by comparing to sodium nitrite standards. Conversion of NO_3 to NO_2 was checked in every assay by measuring the formation of NO_2 from NO_3 standards.

Cytokine Levels: Levels of the pro- and anti-inflammatory cytokines TNF-α, IL-1β, IL-6, and IL-10 were assayed in the media after the 24-hour culture period. Cytokine protein concentrations were determined with an enzyme-linked immunosorbent assay (ELISA) immunoassay kit from Biosource International (Camarillo, CA). This technique is a sandwich ELISA that utilizes an antibody specific for each rat cytokine (depending on the kit) coating the wells of a microtiter plate. Samples, including standards of known cytokine concentrations, were added to the wells along with a biotinylated second antibody in the solution phase. This mixture was allowed to incubate while the rat cytokines bind simultaneously to the capture antibody on the plate as well as the secondary biotinylated antibody at a second site. After washing with an automated plate washer to remove excess secondary antibody, a streptavidin-labeled peroxidase enzyme was added. This bound to the biotinylated antibody to complete a four-membered sandwich. After a second washing removed the excess (unbound) enzyme, a substrate for the peroxidase enzyme was added. The bound enzyme acted upon this substrate to produce a colored product. Once this reaction was stopped and the color stabilized, the intensity of the color produced was directly proportional to the concentration of cytokine present in the original sample. This color was read with a plate spectrophotometer and concentrations of unknowns were compared to known cytokine standards using Softmax Pro software.

***In Situ* Viability Determination Using LSCM:** At 15 minutes, 1 hour, and 3 hours after the first intratracheal AD administration, and on day 3 after installations on day 0 and 2, rats were anesthetized and their lungs inflated with ethidium homodimer solution (4 μM; Molecular Probes, Eugene, OR) to a pressure of 30 cm of water for 15 min.

Cryosections for Quantification: The lungs were then cryopreserved with Tissue-Tek O.C.T. compound (Sakura Finetek, Inc., Torrence, CA) and frozen in liquid nitrogen. Cryosections were made (10 μm thick), vapor-fixed with 2% paraformaldehyde, and counter-stained with YO-PRO-1 (2μM; Molecular Probes, Eugene OR). For each treatment at each time point, 150-250 fields of fluorescently labeled lung tissue were randomly scanned using a Sarastro 2000 (Molecular Dynamics, Inc., Sunnyvale, CA) laser scanning confocal microscope (Optishot-2, Nikon, Inc., Melville, PA) fitted with an argon-ion laser. Micrographs were recorded by Jenny Roberts (HELD/NIOSH, Morgantown, WV) through a 40X objective using a 488-nm laser line. All random scans of lung tissue for each group were recorded at the same PMT setting of 490, pinhole aperture setting of 50 μm, and the same laser voltage setting of 20 mW. Total cells (green) and ethidium homodimer-positive cells (red) were counted using ImageSpace software (Molecular Dynamics, Sunnyvale, CA). Cells with both stains appear yellow and are also counted as ethidium homodimer-positive. For statistical analysis, all fields from each treatment and time were pooled, and comparisons were made between each time and treatment.

Fixation for Intact Tissue Analysis: The lungs were inflated with 2% paraformaldehyde solution to a pressure of 30 cm of water for 6-8 hours. The lungs were then removed, grossly sectioned, and counter-stained with YO-PRO-1 (2μM). Tissues were then imaged

with LSCM using a 20X water-immersion objective at the same settings as above. Three-dimensional images were generated from the reconstruction of serial optical sections of tissue using Voxel View Ultra software (Vital Images, Inc., Fairfield, IA).

Free Radical Measurements: Electron spin resonance with and without spin trapping was used to examine free radical generation with the assistance of Stephen Leonard (HELD/NIOSH, Morgantown, WV). While direct radical measurement was used to detect longer-lived species, spin trapping was necessary to examine highly reactive radicals. Spin trapping involves the addition reaction of a short-lived radical with a diamagnetic compound (i.e. spin trap) to form a relatively long-lived free radical product, termed the spin adduct, which can be studied with conventional ESR. The intensity of the spin adduct signal corresponds to the amount of short-lived radical trapped, and the pattern of hyperfine splittings of the spin adduct are generally characteristic of the original, short-lived, trapped radical. To determine the presence of aryl and hydroxyl radicals, 5, 5-dimethyl-1-pyrroline *N*-oxide (DMPO) was used as a spin trap in these studies. Measurements were made with a Bruker Instruments Inc. ESP 300E spectrometer and a flat cell assembly (Billeria, MA). Spex 300 software (Clarksville, MD) was used for data collection and analysis. The Fenton Reaction ($FeSO_4 + H_2O_2$) was used to generate hydroxyl radicals as a positive control. Hydroxyl signals were quantified and compared by measuring and averaging the height of the two center (doublet) peaks (in mm). Reactants were initially mixed in test tubes and transferred to quartz flat cells for analysis. Final concentrations for reactants are listed in figure legends. Enzymes indicated as heat-inactivated were placed in a boiling water bath for at

least 10 min. Oxygen consumption of AD solution (25 mg/mL) was performed on a Gilson oxygraph over 20 minutes.

Statistics: All data are presented as means ± SEM. Comparisons between two means were analyzed using a student "t" test between mean values; all other data were analyzed using the appropriate ANOVA (one-way for multiple comparisons at a single time-point; two-way for multiple comparisons and time-points) followed by Tukey's protected "t" post-hoc test. Statistical significance was established when $p<0.05$.

Results

The first objective of the project was to identify an appropriate rat model for the study of AIPT. The presentations of oral AD versus i.t. AD were compared. Rats were given AD or the sterile water vehicle either orally (150 mg/kg) daily for 7 or 14 days until lavage or a single dose intratracheally (6.25 mg/kg) on day 0 and lavaged on day 5. **Figure 2** shows the accumulation of AD or its primary metabolite desethylamiodarone in BAL cells after 7 and 14 days of oral treatment as determined by HPLC analysis. Drug levels were not detected in any cells from control animals. Drug levels were detected in macrophages from i.t.-treated rats at day 5, but the levels were below the quantifiable range of this technique. **Figure 3** shows the lipid phosphorous levels in BAL cells from rats receiving either oral AD or the water vehicle for 7 days. Oral AD treatment resulted in a significant increase in lipid phosphorous, indicating an increase in cellular phospholipid content.

In order to assess any differences in cellular activation following oral or i.t. AD treatment, an experiment was conducted in which rats were treated either orally with AD or water for 7 days or rats were given a single i.t. dose of AD or water on day 0. Rats were lavaged either on day 7 for the orally treated group or day 5 for the i.t.-treated group. The BAL cells were then cultured for 24 hours in the presence or absence of LPS. After culture, levels of NO_2 or NO_3, stable products of NO and oxygen reactions collectively referred to as NOx, were assayed. **Figure 4A** shows that NOx production from BAL cells from rats treated orally with AD was not different than from cells from rats treated with water. Conversely, **Figure 4B** shows that non-LPS-stimulated BAL

cells taken from rats treated intratracheally with AD produced significantly more NOx than those treated with i.t. water.

Another and perhaps more direct method to assay oxidant production is to use luminol-dependent chemiluminescence. To determine the appropriate vehicle for subsequent studies with i.t. AD, an experiment was performed to compare the effects of the vehicle used to deliver the AD on BAL cell LDCL. AD was given to rats i.t. on day 0 either suspended in sterile normal saline or dissolved in sterile water at the same concentration (6.25 mg/mL). **Figure 5** shows that, while there are no statistically significant differences, there is a trend for AD in water to increase LDCL when rats are lavaged at day 5. To maximize the potential response, AD dissolved in sterile water would be used for subsequent instillations.

To further compare cellular activation between the two dosing routes, LDCL was compared between BAL cells taken from rats either treated orally with AD or vehicle for 7 days or treated once with i.t. AD or vehicle on day 0 and lavaged on day 5. **Figure 6** shows that there is a trend for BAL cells from rats treated with i.t. AD to produce more LDCL than cells treated with i.t. water or oral AD or vehicle, although statistical significance was not attained. Also, more inflammatory cells were recovered by BAL from i.t. AD-treated rats than the i.t. water vehicle or than the oral AD or vehicle treatments (results not shown). The i.t. route of administration with AD dissolved in sterile water tended to be the most inflammatory and activating route of administration for the short-term endpoints of inflammation, LDCL activation, and NOx production.

This protocol of a single i.t. dose of AD did not lead to significantly elevated hydroxyproline levels at day 28 as had been reported in the rat with this technique

(Reinhart et al., 1996). In attempt to produce a more consistent and significant fibrosis, a second i.t. dose of AD or vehicle was added to the dosing regimen. To determine when to administer the second dose, an experiment was performed that compared either giving the doses of AD or vehicle on days 0 and 2 or giving the doses on days 0 and 7, the latter a protocol used in the hamster to induce fibrosis (Blake and Reasor, 1995b). **Figure 7** shows that the day 0 and 2 protocol produces a significantly elevated right-lung hydroxyproline response in the AD-treated animals at day 28 where the day 0 and 7 protocol does not. Dosing on days 0 and 2 was determined to be the more effective protocol and was used for subsequent experiments involving fibrosis and the events prior to fibrosis development. To determine the appropriate time to analyze fibrosis, right-lung hydroxyproline levels were assayed at both day 28 (4 weeks) and day 42 (six weeks) following i.t. AD or vehicle treatment at days 0 and 2. No differences were found between the two time-points (results not shown), implying that by 4 weeks maximal fibrosis is reached.

In an attempt to elevate right-lung hydroxyproline levels even further and develop a more physiologically relevant model containing phospholipidosis, inflammation and fibrosis, a study was performed that combined both the day 0 and 2 i.t. dose with a daily oral dose (150 mg/kg) of AD or vehicle. Two combined dosing protocols were used; rats were either started concurrently with the day 0 i.t. of AD or water and the first oral AD or water dose, or they were pretreated orally with AD to establish the characteristic lung drug accumulation and phospholipidosis for 7 days before being given the first of two i.t. AD or vehicle doses. For comparison, two other treatment groups were included in the experiment; first, a group that only received daily oral AD for 28 days, and second,

a group that only received i.t. AD on days 0 and 2 with no oral treatment. The control group was given both daily water orally and a water i.t. on days 0 and 2. Food was withheld from the controls to match the weight loss experienced by the three orally AD-treated groups. Other controls were excluded as this was a preliminary experiment to determine the future dosing regimen. **Figure 8** shows the results of this experiment. Oral AD treatment failed to elevate right-lung hydroxyproline levels, and in fact may have been protective against fibrosis in the orally pretreated group. Since additional drug treatment did not elevate fibrosis above the levels found in the i.t.-only group, the i.t.-only protocol was chosen for the subsequent characterization studies.

The second objective of the study was to characterize the chosen model of AIPT, with i.t. AD doses (6.25 mg/kg) at days 0 and 2. The potential use of serum SP-D as a biomarker for AIPT in the model was also examined. The fibrotic reaction was characterized biochemically, histopathologically, and by using LSCM with Lucifer Yellow staining. Increases were found in right-lung hydroxyproline levels at day 28 in AD-treated rats (**Figure 9**), and at day 28, minimal to mild, multifocal, interstitial pulmonary fibrosis was found in all rats treated with AD on days 0 and 2 (**Figure 10**). An increase in lung tissue area similar in magnitude to the hydroxyproline increase was found with LSCM, indicating septal thickening (**Figures 11 and 12**). To examine the early events involved in the toxicity, rats were treated on day 0 and 2 with intratracheal AD (6.25 mg/kg in a 3.125 mg/mL solution) and were subjected to BAL at various time points following dosing. To analyze the integrity of the alveolar-capillary barrier, albumin, a protein from the blood, was assayed in the first BAL fraction from AD- or vehicle-treated rats (**Figure 13**). Albumin was elevated at day 3 following AD treatment

on days 0 and 2, showing initial damage and leakage from the blood to the airways after AD administration. **Figure 14** shows total cell number recovered in the lavage fluid of AD- or vehicle-treated rats. Total cells recovered were elevated on both days 3 and 5 follow AD i.t. on days 0 and 2. **Figure 15** shows that most of the cells recovered are alveolar macrophages, which are also significantly increased on days 3 and 5 following AD treatment. **Figure 16** shows an increase in the number of PMNs recovered by lavage on day 3. **Figure 17** shows an increase in eosinophilic leukocytes at days 3 and 5.

To assess the level of oxidant production and thus infer their level of activation, PMA-stimulated LDCL was performed on the cells recovered by BAL. **Figure 18** indicates that the cells at day 3 are capable of producing more oxidants when stimulated. Since the cells are activated on a per/cell basis, and significantly more cells are present following AD treatment, potential oxidant production was calculated by multiplying the LDCL by the total number of BAL cells recovered. This is illustrated in **Figure 19**, which shows the much greater potential for oxidant production due to the increased number of activated cells at days 3 and 5 in the lungs of AD-treated rats.

To determine the oxidant species possibly involved in the LDCL response at day 3, specific inhibitors to various oxidants where utilized**.** L-NAME is an inhibitor of nitric oxide synthase, leading to reduced NO levels, while SOD in an enzymatic scavenger of superoxide. **Figure 20** shows that SOD treatment inhibits a large portion of the light production, indicating involvement of superoxide radicals, and while L-NAME also inhibits significantly alone, combined with SOD it inhibits light production down to the levels of non-PMA stimulated cells. To determine if the incomplete inhibition of L-NAME was due to its inability to penetrate the cells, L-NAME was pre-incubated for 10

minutes with cells prior to LDCL rather than the standard 5, but inhibition was not significantly increased (results not shown). In another attempt to show increased levels of NO production following AD treatment, rats treated with AD or vehicle on days 0 and 2 were lavaged on day 3, and the BAL cells were subsequently cultured 24 hours. NOx levels in the spent media were than assayed and displayed in **Figure 21**. NOx levels were elevated from non-LPS-stimulated cells from AD treated rats.

To assess the value of serum SP-D, a protein from the fluid lining of the lungs, as a biomarker for AIPT in this model, the levels of SP-D were assayed in the serum of naïve, vehicle-, and AD-treated rats. SP-D levels were elevated in rat serum following AD treatment from day 3 through day 7, during the time of the initial damage and inflammatory reaction (**Figure 22**).

To determine if any of the inflammatory response seen after AD treatment could be attributable to the low pH of the AD solution (pH 3.7), rats were treated intratracheally with either sterile water, AD in sterile water, or sterile water adjusted with HCl to match the pH of the AD solution. Rats were treated on days 0 and 2, and lavaged on day 3, where cell counts and differentials were performed. **Figure 23** shows acidic water did not alter alveolar albumin levels above normal water controls while AD solution does. **Figure 24** shows the acidic water did not induce the increase in total BAL cells recovered during lavage as seen following AD treatment. **Figure 25** displays the macrophage number recovered, where only rats treated with AD showed a significant increase over the sterile water control. **Figure 26** is the number of PMNs recovered, again with the only increase coming after AD treatment. **Figure 27** shows that eosinophils were recruited only after AD treatment and not after acidic water treatment.

Objective 3 was to characterize the events occurring soon after i.t. AD or control instillations to determine the direct role of the drug vs. the role of inflammation in the toxicity. To assess the ability of the initial i.t. to activate the BAL cells, rats were lavaged 15 minutes, 1 hour, and 3 hours after i.t. treatment and cultured with and without LPS. NOx levels were then assayed in the culture media following a 24-hour culture. **Figure 28A** shows that cells are not activated above control levels when not cultured with LPS. **Figure 28B** shows the same time points with cells stimulated with LPS, and again AD treatment does not significantly alter NOx production.

To examine the possibility that the inflammatory cytokine TNF-α was involved during the early time points, rats were treated with a single i.t. dose of AD (6.25 mg/kg) or sterile water and lavaged 1 or 3 hours later, or treated at days 0 and 2 and lavaged on day 3. BAL cells were then cultured 24 hours with and without LPS addition. The conditioned media was then assayed for TNF-α. **Figure 29A** displays the TNF-α produced by non-LPS-stimulated cells in culture. No differences were seen between TNF-α production from BAL cells from control and AD-treated animals. However, when these cells were stimulated with LPS, TNF-α production from cells from AD-treated rats was inhibited at the 3-hour and 3-day time points (**Figure 29B**). Finally, TNF-α levels were assayed directly in the first BAL fraction, which represents the most accurate sampling of the actual *in vivo* situation in the lung. **Figure 30** also shows a significant inhibition of TNF-α at the 3-hour time point, with a trend of less TNF-α at all time points in the lavage fluid of AD-treated animals.

In an attempt to identify other inflammatory cytokines that may be involved it the inflammatory response, IL-1β was also assayed in the media from cultured BAL cells

lavaged from rats 3 hours after i.t. administration of AD or vehicle. **Figure 31** indicates that IL-1β production is also significantly inhibited in LPS-stimulated cells from animals treated with AD vs. control. While not significant, basal (non-LPS-stimulated) levels of IL-1β tended to be decreased as well. Other cytokines examined were the immunomodulatory cytokine IL-6 and the anti-inflammatory cytokine IL-10. Animals were treated with i.t. AD or vehicle and lavaged 15 minutes later, the BAL cells were cultured 24 hours with and without LPS, and IL-6 was measured in the conditioned media. No significant differences in IL-6 production were found (**Figure 32A**). When rats treated with i.t. AD or vehicle were lavaged at day 3 following instillations on days 0 and 2 and their BAL cells cultured, IL-6 production again was not significantly altered from control (**Figure 32B**). To examine the possible involvement of IL-10, levels were also examined in the conditioned media from BAL cells. However, no significant differences were found in IL-10 production from cultured BAL cells, both basal and LPS-stimulated, when BAL was 15 minutes after the instillation (**Figure 33A**) or on day 3 following instillations on days 0 and 2 (**Figure 33B**).

To examine the direct role of the drug vs. the effect of inflammatory cells in any early damage that may be occurring after the i.t. administrations, albumin was measured in the first BAL fraction obtained by lavage at 15 min, 1 hour, and 3 hours following the initial i.t. AD or vehicle treatment or at day 3 following i.t. doses on days 0 and 2. **Figure 34** shows a massive damage to the alveolar-capillary barrier soon after AD was administered. LDH activity in the first BAL fraction was also significantly increased at 15 min post-AD i.t, but was not different from control at day 3 (**Figure 35**). An experiment was designed to determine the effects of the acid instilled with AD in this

early damage, since AD is a hydrochloride and also may act to buffer the pH of its solution. Citrate buffer (pH 3.7), HCl (equimolar to the AD solution; pH 2.5), AD (3.125 mg/mL; pH 3.7), or an equivalent volume of sterile water was intratracheally instilled to rats and albumin (**Figure 36A**) and LDH activity (**Figure 36B**) in the first BAL fraction was examined at 15 min. Neither acid control significantly increased either damage indicator above the levels found after i.t. sterile water treatment.

Exact cellular differentials of the BAL cells from AD-treated rats were not possible at these early time-points due to the presence of unidentifiable amorphous cells, possibly epithelial cells. Cellular yield was very low from AD-treated animals, and cellular viability of the BAL cells at 15 min was 29.8% (meaning a 70.2% mortality rate) as determined by trypan blue exclusion. Experiments utilizing various concentrations of trypsin in the BAL fluid in an attempt to release macrophages that may have became activated and attached to the lung parenchyma were unsuccessful in increasing cell yield (data not shown).

LSCM was then used to examine the *in situ* viability of airway and parenchymal cells after i.t. AD or water treatment. Microscopic examination of grossly sectioned tissue was performed at 15 min (**Figure 37A**) and 3 hours (**Figure 37B**) following the initial i.t. treatment, and on day 3 (**Figure 37C**) following i.t. instillations of AD or water on days 0 and 2. Foci of massive cellular death or damage were found in the lung tissue of animals receiving i.t. AD at 15 min and 3 hours. To quantitate the effect of AD on lung cell viability, thin sections were made from animals at 15 min after the initial i.t. of AD or water (**Figure 38**). The number of ethidium-positive and total cells in random fields of lung tissue was determined, and the tissue was further categorized as either

airway or parenchyma. **Figure 39A** shows a significant increase in the number of ethidium-positive cells in all areas 15 min after i.t. AD. **Figure 39B** shows that the average number of cells in each field was not different, indicating an adequate "N" value for comparison. **Figure 40** shows representative fields on day 3 from animals that received either i.t. AD or water on days 0 and 2. The only difference in ethidium staining that was found was in the parenchyma, with more ethidium-positive cells found in animals that received AD (**Figure 41A**). However, ethidium staining in general was minimal compared to the levels found 15 min post-i.t. AD administration. Again there were no differences in the average number of cells per field at day 3 (**Figure 41B**).

To examine the possibility of free radical production in AD solution, a series of ESR experiments was performed. **Figure 42** shows a carbon-based radical in the AD solution, presumably the AD molecule itself. The radical signal can be reduced by increasing the concentration of the drug in the solution, possibly by autoquenching. No O_2 consumption was detectable over 20 min in a solution of AD (25 mg/mL). **Figure 43** shows that at least some of the carbon-based radical is present in the AD powder before it is placed into solution. By using DMPO as a spin trap, the production of hydroxyl radicals can be examined. **Figure 44** is a time-course of hydroxyl radical production from AD in water with various affectors. The inhibitions by catalase and deferoxamine indicate possible oxygen dependence (inhibitable portion) and independence (non-inhibitable portion). Formate competes with any hydroxyl in solution for the DMPO, but in this case it raised the pH of the AD solution, increasing its apparent signal by increasing the efficiency of DMPO to trap hydroxyl at the higher pH. While formate was the only chemical to change the pH of the AD solution measurably, another experiment

was performed in PBS to maintain the pH of the solutions (**Figure 45A**), even though the solutions became partly cloudy as some of the AD precipitated. The inhibitor profile remained the same, with reductions of hydroxyl signal following catalase and deferoxamine indicating both possible oxygen dependence and independence. Also the effect of H_2O_2 was examined in this study by its exogenous addition. The increase in hydroxyl signal after H_2O_2 addition indicated the presence of something in the AD solution that acted as a transition element. Since chelation of metals by deferoxamine did not completely inhibit hydroxyl production, several mechanisms of hydroxyl production may have been occurring. Attempts to add exogenous iron to infer the presence of H_2O_2 in the AD solution were unsuccessful as the charged iron forced AD out of solution. This was the case even after chelation of the iron with EDTA. The last spectrum from each sample for the time course of hydroxyl production in PBS is presented in **Figure 45B**. Note the partial splitting of the hydroxyl-DMPO signal by formate, indicating trapped hydroxyl radicals were free in solution.

In an attempt to determine if the effects of SOD and Cat were specific for their actions or simply effects of exogenous protein, SOD and Cat were heat-inactivated. **Figure 46** shows that normal SOD and Cat did not follow their previous inhibitory patterns in this experiment, but instead had no effect (SOD) or possibly enhanced (Cat) hydroxyl production from AD. However, heat-inactivated SOD showed the typical inhibition pattern, indicating its effects in the earlier studies maybe simply due to the protein in solution. However, the heat inactivation of Cat completely changed its inhibitory profile, possibly by denaturing the protein and releasing the active-site moiety into solution, making it more available to interact with constituents of the solution.

Thiol-containing antioxidants are known to adduct and quench aryl radicals, so *N*-acetyl cysteine (NAC) and reduced glutathione (GSH) were separately added to AD solution in PBS and hydroxyl production was examined by ESR (**Figure 47**). However, hydroxyl production was increased when either thiol antioxidant was present. Neither compound had an effect on the pH of the AD solution. To examine the nature of the parent-compound radical, DMPO spin-trapping was performed in chloroform. **Figure 48** shows a radical signal trapped by DMPO, and is presumably the AD parent compound. When NAC was added, the presence of an *N*-acetyl cystyl radical was detected. Thus AD oxidized the antioxidant instead of adducting with it, and more hydroxyl radicals were produced in solution when NAC is present. Thus the *N*-acetyl cystyl radical may interact with components of the solution to produce hydroxyl radical. A preliminary experiment attempting to use NAC to block i.t. AD-induced damage resulted in massive lung hemorrhaging and death of the animal.

As Figure 42 indicated that the carbon-based radical signal decreased with increasing AD concentration, **Figure 49** shows a similar effect of AD concentration on hydroxyl radical production at the highest concentration tested. Higher concentrations of AD could not be examined because the AD solution "solidified" as if it cross-linked. These findings support the hypothesis that AD can be both a free-radical generator and scavenger, depending on the conditions and concentration.

Attempts to examine free radical production *in vivo* were unsuccessful. DMPO was instilled with AD into rats, and then withdrawn, but even the expected baseline hydroxyl-DMPO signal was absent. Protocols involving the treatment of excised lungs,

lung homogenates, and varying concentrations of BAL cells failed to yield any radical signals (data not shown).

Figure 50 shows that UV light can induce aryl radical formation in AD solution (3.125 mg/mL; 4.5 mM) in water (B), possibly by the deiodination of AD, but aryl radical formation seems minimal under normal conditions (A). The aryl peaks (B) split with the hydroxyl peaks, producing a radical signal with more, but less substantial, peaks. Also, the hydroxyl radical signal (without UV exposure) can be completely eliminated by the simultaneous addition of Trolox (45 mM) and ascorbate (22.5 mM). Because the radical signal was eliminated, this solution was given i.t. to animals in an attempt to modulate the toxicity and gain insight into the role of free radicals in the damage seen after i.t. AD administration. **Figure 51A** shows that having the antioxidant solution together with AD increased the amount of albumin in the first BAL fraction at 15 min post-i.t. This indicates an even more severe damage to the alveolar-capillary barrier occurs when the antioxidants are instilled in the same solution as AD. The antioxidants alone had no effect on the level of albumin in the first BAL fraction as compared to sterile water. **Figure 51B** shows no difference in LDH activity at 15 min in the first BAL fraction between animals receiving i.t. AD with and without antioxidants in the solution. Again the antioxidants alone had no effect on the LDH activity in the first BAL fraction as compared to sterile water control.

To examine any structural changes that might have occurred when AD was heated and dissolved in water vs. being readily dissolved in methanol, the two solutions were compared using electrospray mass-spectroscopy. **Figure 52A** shows the positive-ion spectra of AD in both methanol (A) and water (B). While several variations of the parent

compound were found in each solution, differing only by a hydrogen, no evidence of a mono- or di-deiodinated AD compound was found in the methanol solution. There were more peaks, however, in the AD-water solution, and one could possibly represent a di-deiodinated AD (~393 Da). However no evidence for mono-deiodinated AD was found, which would have been expected if AD was undergoing deiodination. **Figure 52B** shows the negative-ion spectra of AD in both methanol (A) and water (B), and no evidence of free iodine was found in either solution. Free iodine would have been expected in solution if AD were undergoing deiodination. The ~393 Da peak could represent another breakdown or recombination product of AD. ^{1}H Nuclear Magnetic Resonance (NMR) analysis of the AD powder confirmed that it is in its expected structure as drawn in Figure 1 (data not shown). Therefore, significant deiodination of AD in water under normal laboratory conditions does not seem likely.

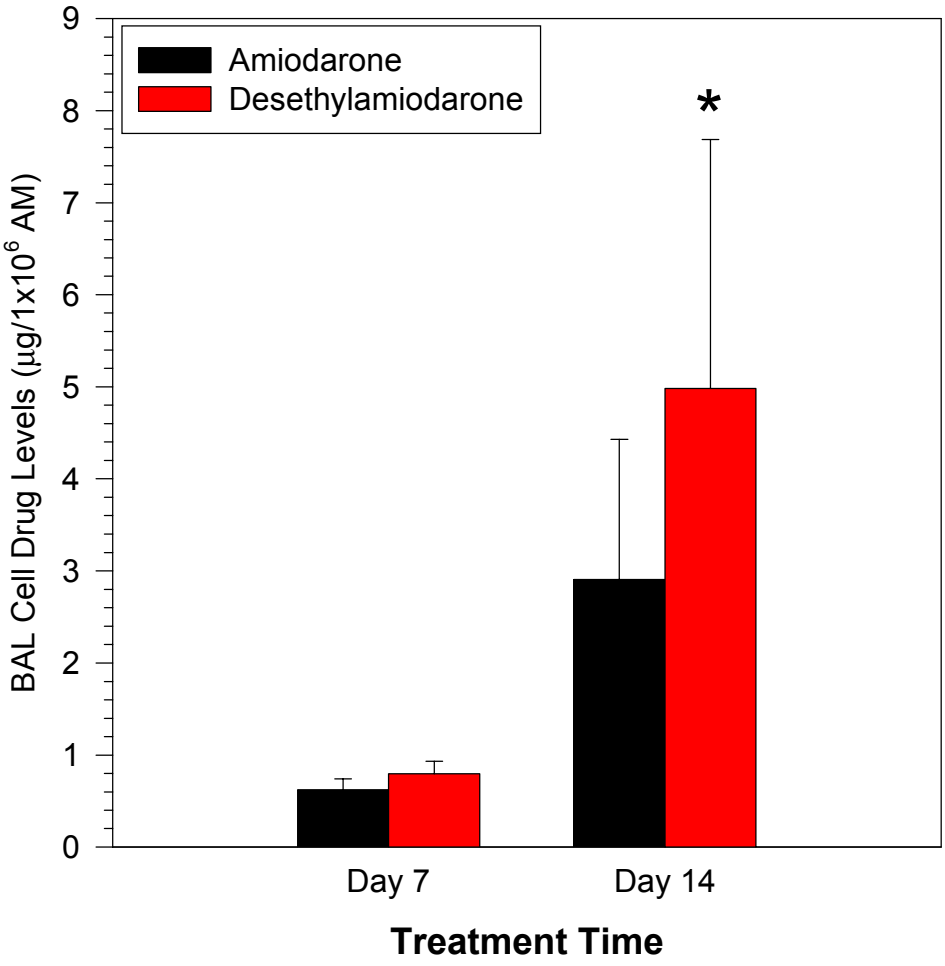

Figure 2: Amiodarone and desethylamiodarone accumulation in BAL cells following oral amiodarone treatment. Rats were treated daily (5 days/ week with AD [150 mg/kg]) until days 7 or 14 and were then subjected to BAL. Cellular drug levels were measured by HPLC analysis. Values are means ± SEM. N=2-6. *Significantly different from day 7 value ($p<0.05$).

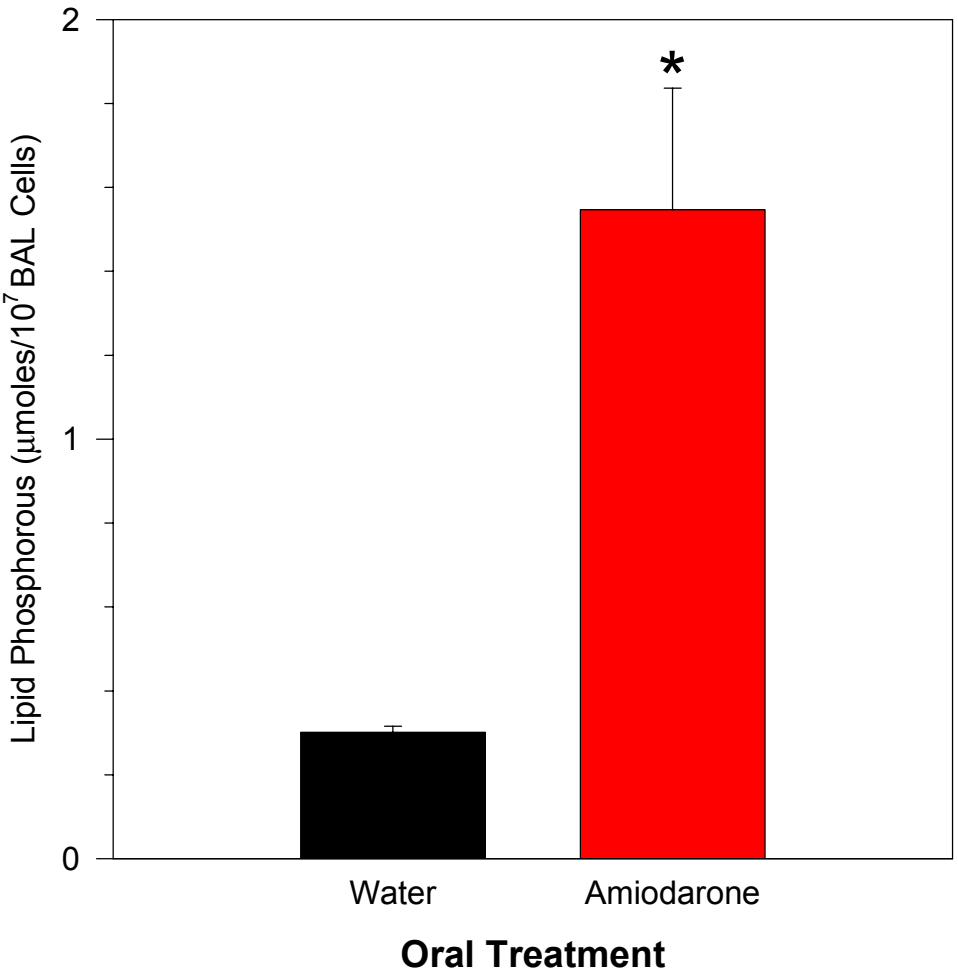

Figure 3: Lipid phosphorous levels in BAL cells following one week of oral amiodarone or vehicle treatment. Rats were treated orally with AD (150 mg/kg) for one week (5 days/week) and then subjected to BAL. Lipid phosphorous levels were then measured in the BAL cells. Values are means ± SEM. N=6. *Significantly different from water control ($p<0.05$).

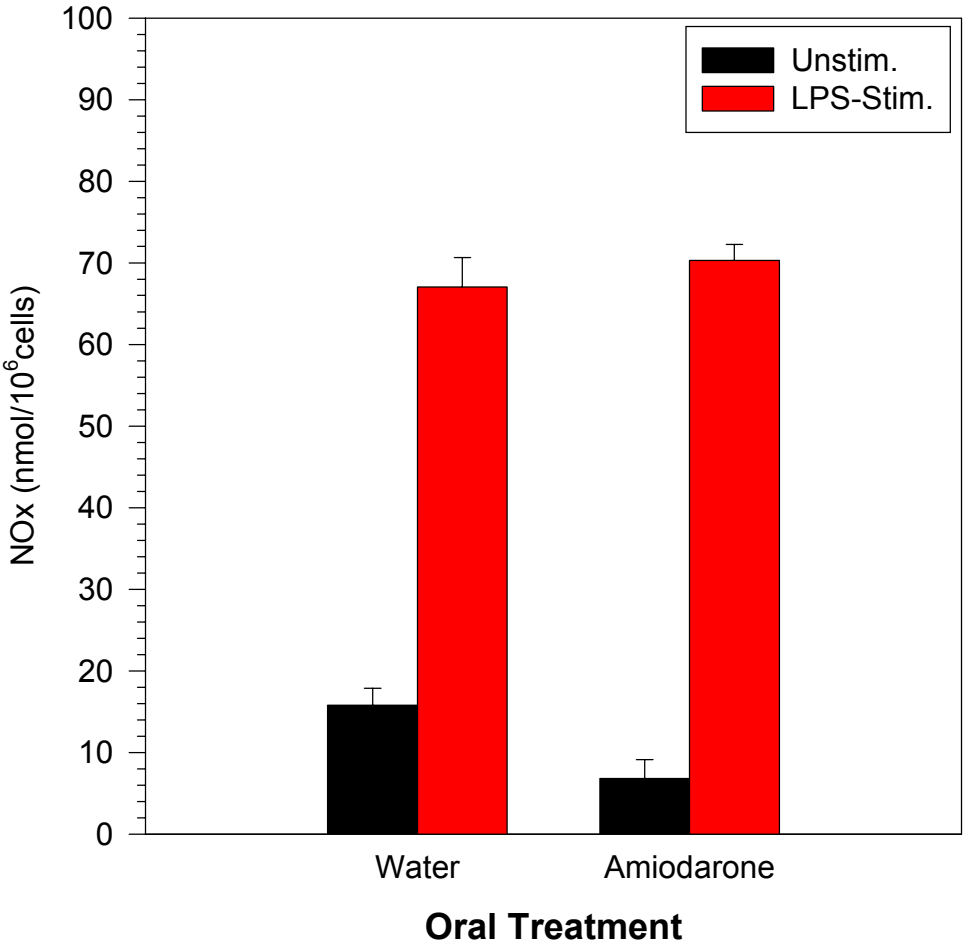

Figure 4A: NOx production from BAL cells from rats given oral amiodarone or vehicle one week. Rats were given AD (150 mg/kg) or vehicle one week (5 days/week) and subjected to BAL. BAL cells were then cultured 24 hours with and without LPS and NOx was measured in the spent media. Values are means ± SEM. N=5-6. No significant differences were found from water control ($p<0.05$).

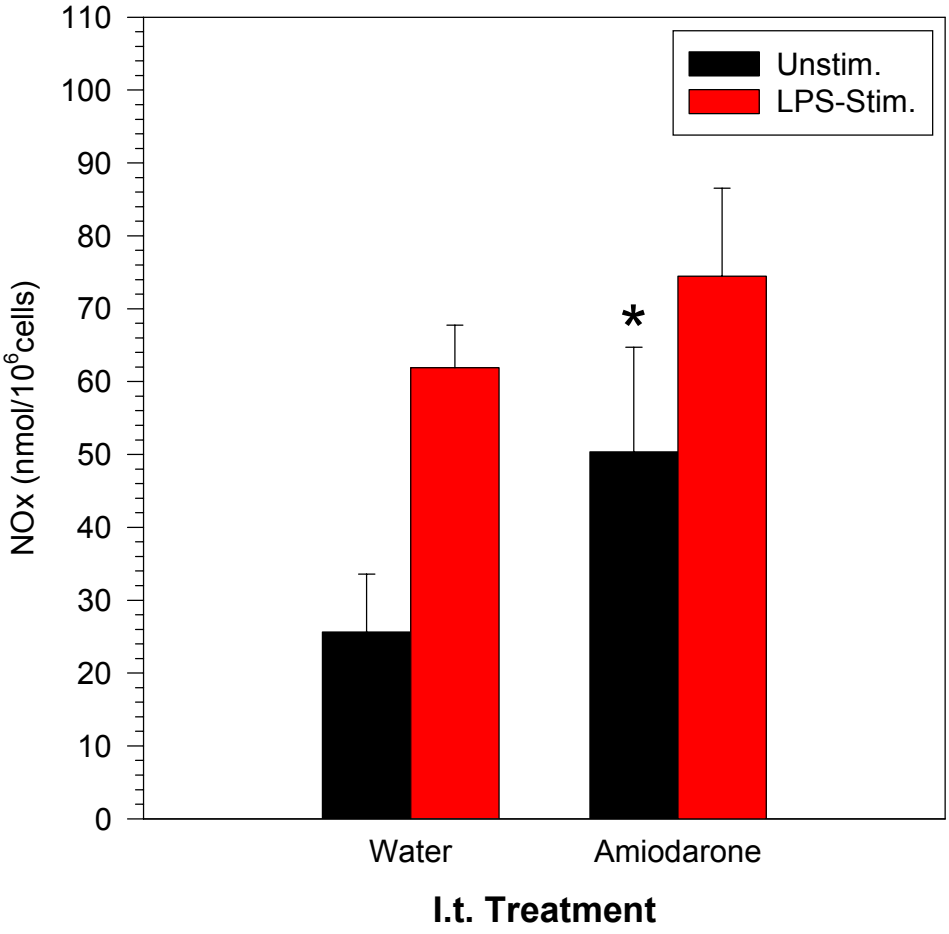

Figure 4B: NOx production from BAL cells recovered on day 5 from rats given intratracheal amiodarone or vehicle on day 0. Rats were given i.t. AD (6.25 mg/kg) or water on day 0 and subjected to BAL on day 5. BAL cells were then cultured 24 hours with and without LPS and NOx was measured in the spent media. Values are means ± SEM. N=7-8. *Significantly different from non-LPS-stimulated water control ($p<0.05$).

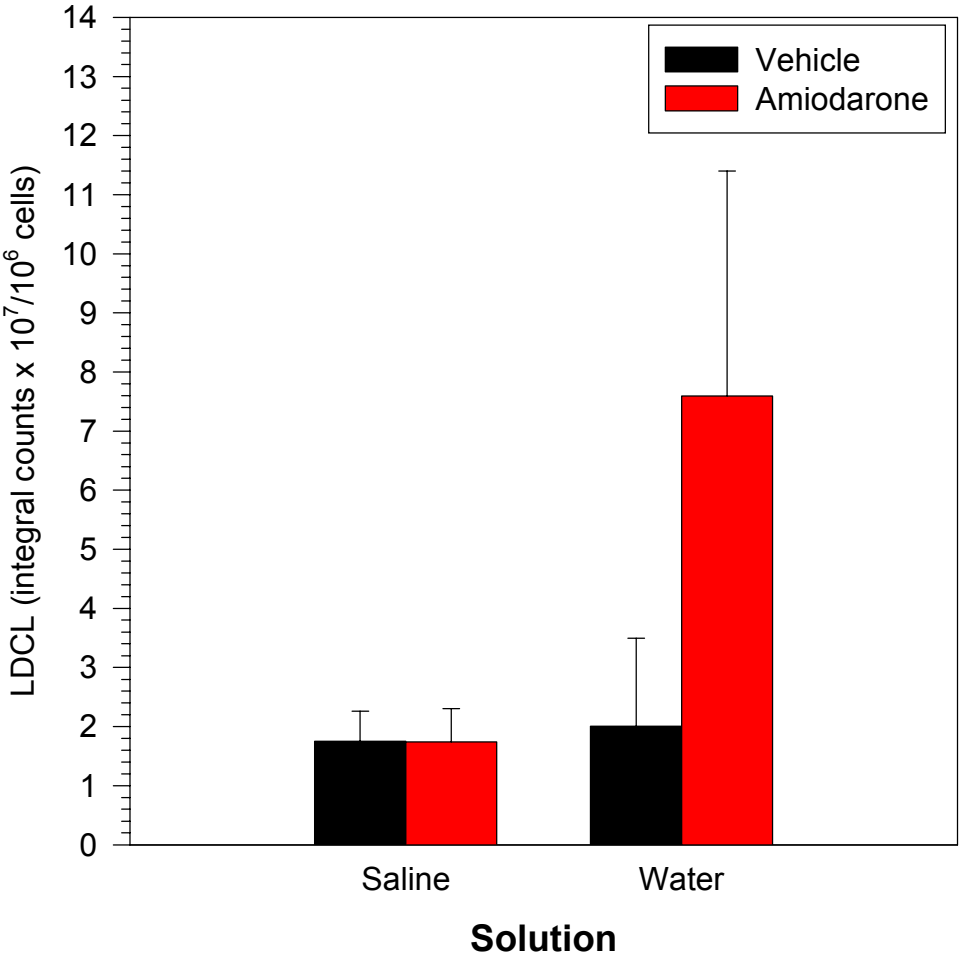

Figure 5: Integral LDCL counts on Day 5 following intratracheal amiodarone administration in either sterile water or sterile saline or appropriate vehicle. Rats were given i.t. AD (6.25 mg/kg) in saline or water on day 0 and subjected to BAL on day 5. BAL cells were then subjected to LDCL. Values are means ± SEM. N=3. No significant differences were found ($p<0.05$).

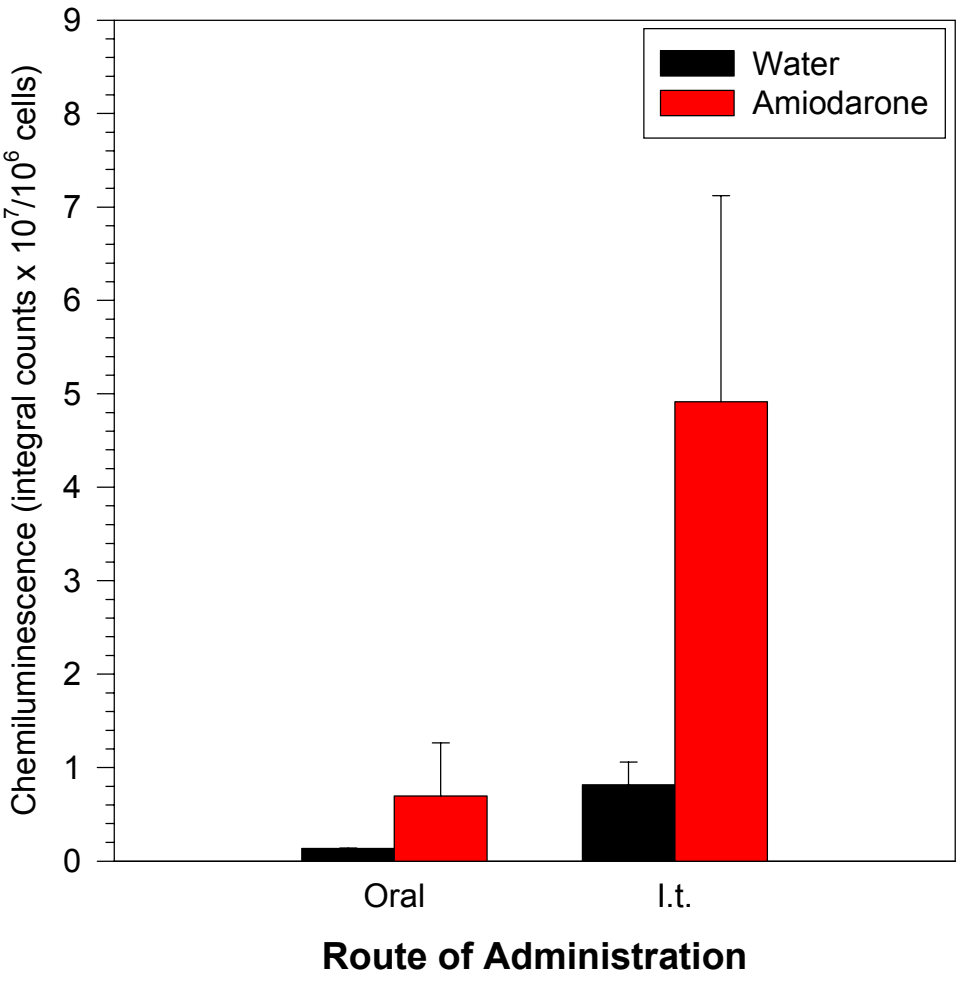

Figure 6: Integral LDCL counts from BAL cells recovered from rats treated either with amiodarone or water orally for one week or treated intratracheally with amiodarone or water on day 0 and lavaged on day 5. Rats were treated either orally with AD (150 mg/kg) or water for one week (5 days/week) or intratracheally with AD (6.25 mg/kg) or water on day 0 and subjected to BAL on day 5. BAL cells were then subjected to LDCL. Values are means ± SEM. N=2-6. No significant differences were found ($p<0.05$).

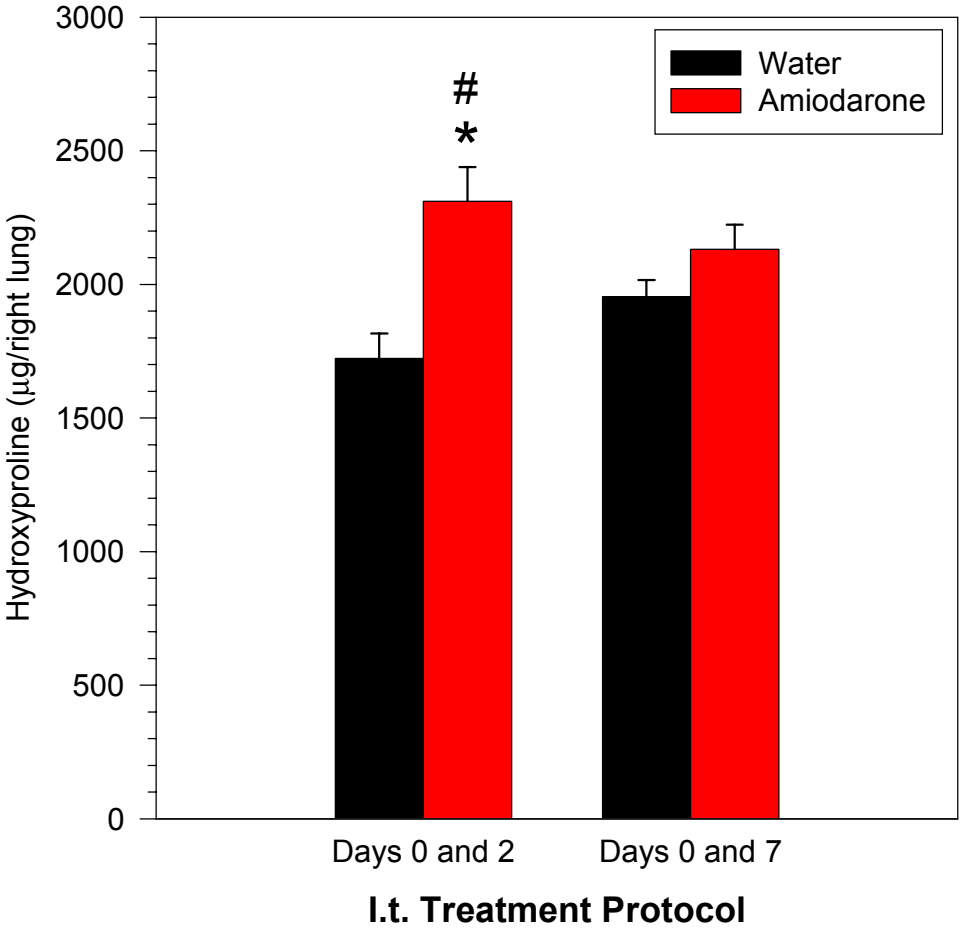

Figure 7: The effects of two intratracheal dosing protocols on right-lung hydroxyproline content. Rats were given i.t. AD (6.25 mg/kg) or water on either days 0 and 2 or days 0 and 7. At day 28 the right lung was removed and subjected to hydroxyproline measurement. Values are means ± SEM. N=4. *Significantly different from corresponding water control ($p<0.05$). #Significantly different from day 0 and 7 water control ($p<0.05$).

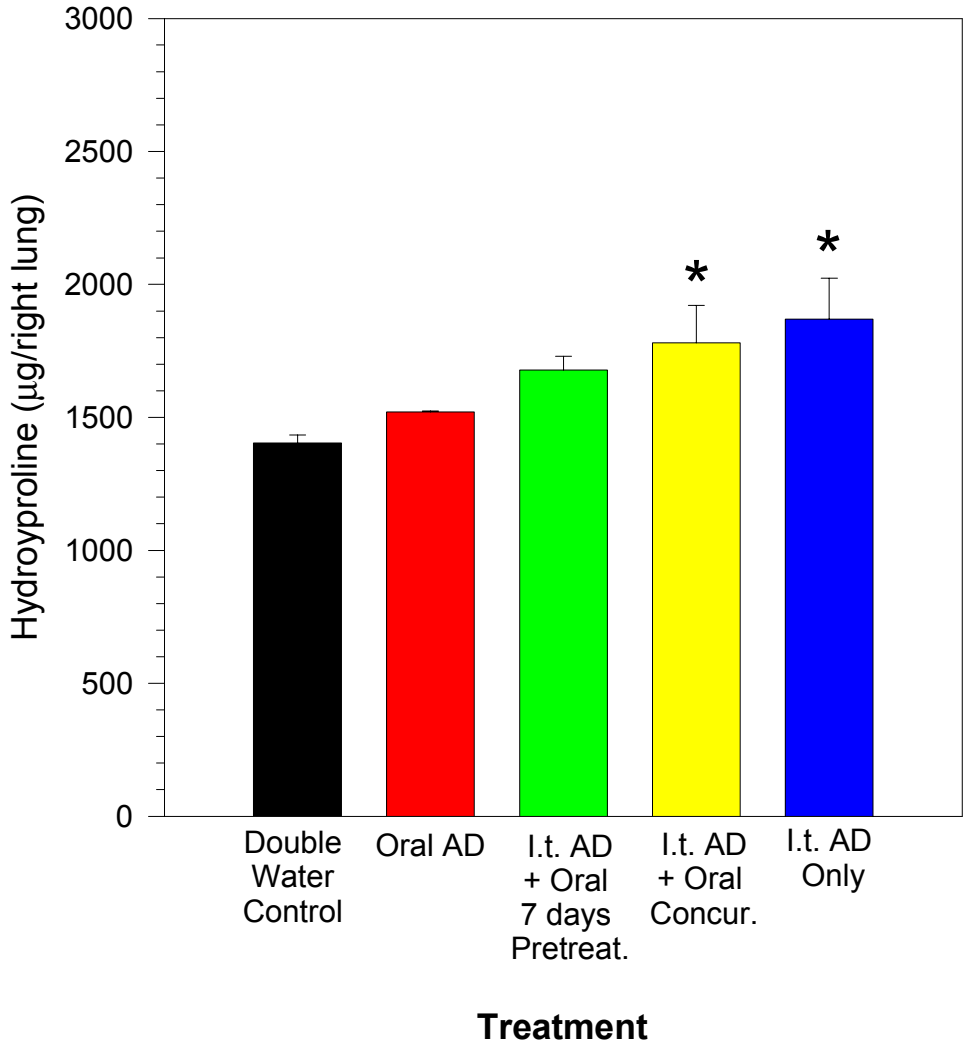

Figure 8: Right-lung hydroxyproline levels following either daily oral amiodarone treatment, i.t. amiodarone treatment, or combination treatments of both oral and i.t. amiodarone or vehicle treatments. Rats were either given daily oral AD (150 mg/kg 5 days/wk), i.t. AD (6.25 mg/kg) on days 0 and 2, daily oral AD and i.t. AD on days 0 and 2 or vehicle started concurrently, or oral AD for 7 days followed by two i.t. AD doses. Right lungs were removed 28 days after the initial i.t. treatment (or after the initial oral treatment in the oral-only treatment group) and subjected to hydroxyproline measurement. Values are means ± SEM. N=4-6. *Significantly different from double water weight-matched control ($p<0.05$).

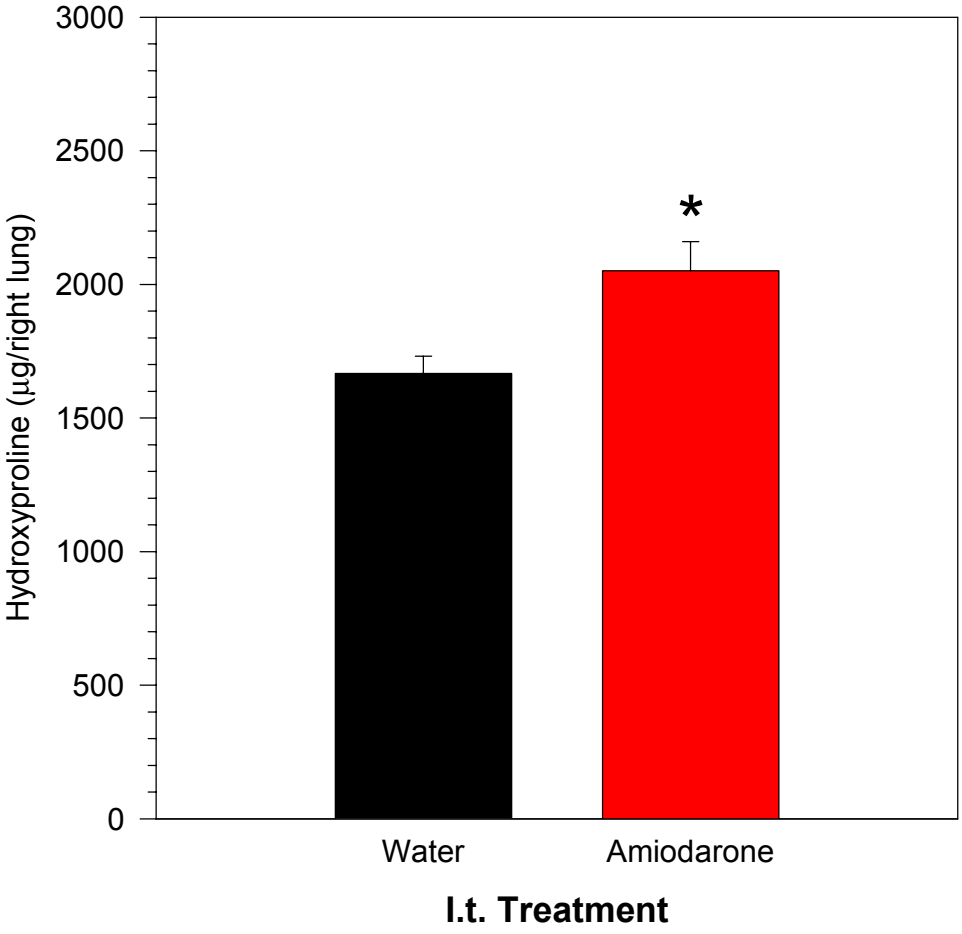

Figure 9: Right-lung hydroxyproline content at day 28. Rats were instilled intratracheally with sterile water or AD (6.25 mg/kg) on days 0 and 2. Right-lung lobes were removed at day 28 and subjected to hydroxyproline analysis. Values are means ± SEM. N=8-9. *Significantly different from control ($p<0.05$).

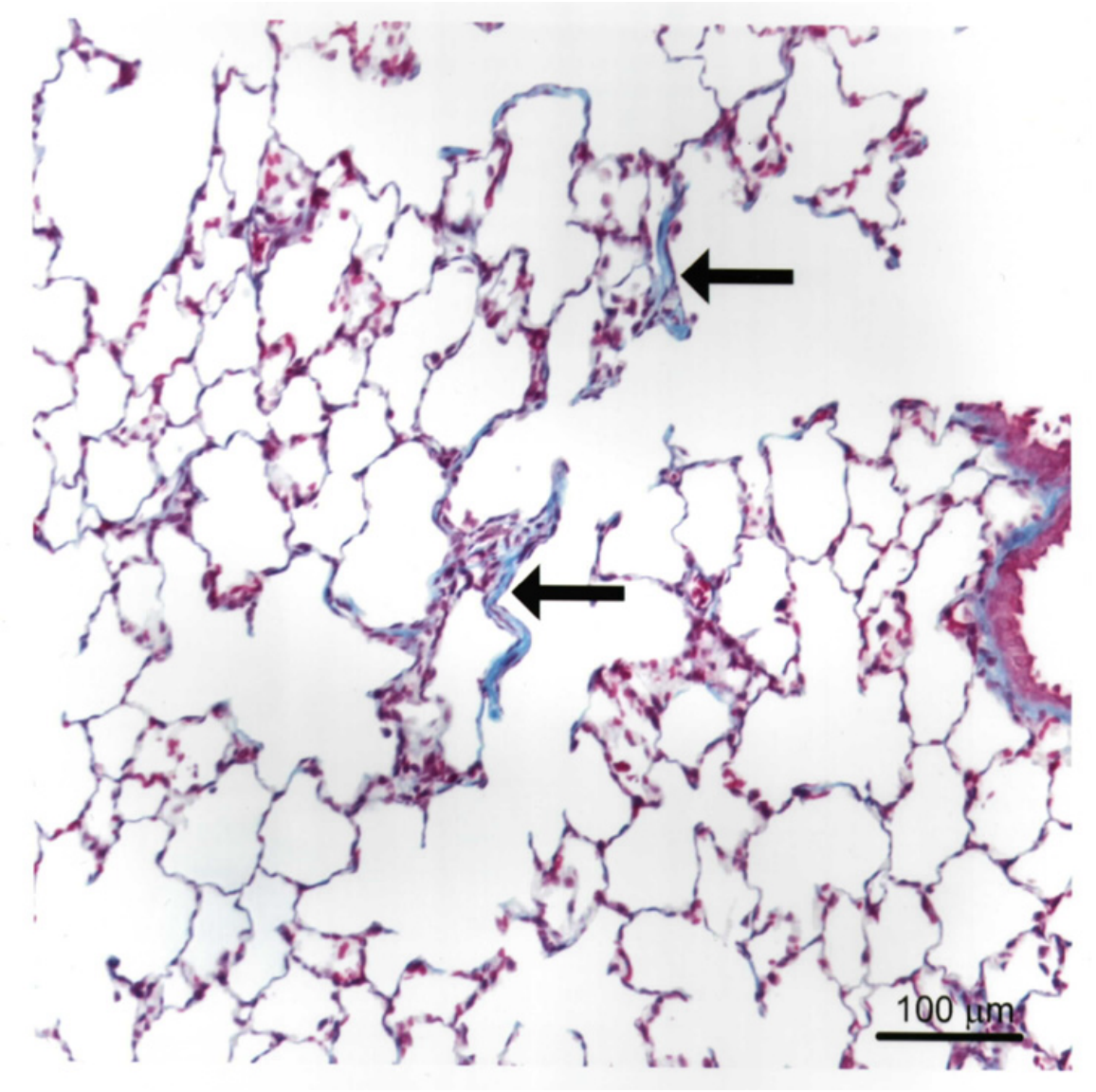

Figure 10: Effect of AD on left lung histopathology. Rats were instilled intratracheally with sterile water or AD (6.25 mg/kg) on days 0 and 2. Left lungs were obtained at day 28, inflated, and fixed, and slides were prepared. All tissues from control animals exhibited normal lung architecture (N=5, data not shown). Lungs from all AD-treated rats displayed minimal to mild, multifocal, interstitial pulmonary fibrosis (N=5). Fibrosis was most frequently observed near alveolar duct regions. A representative field is shown from an AD-treated animal. Arrows indicate areas of septal thickening and collagen deposition evidenced by trichrome staining. Bar indicates 100 µm.

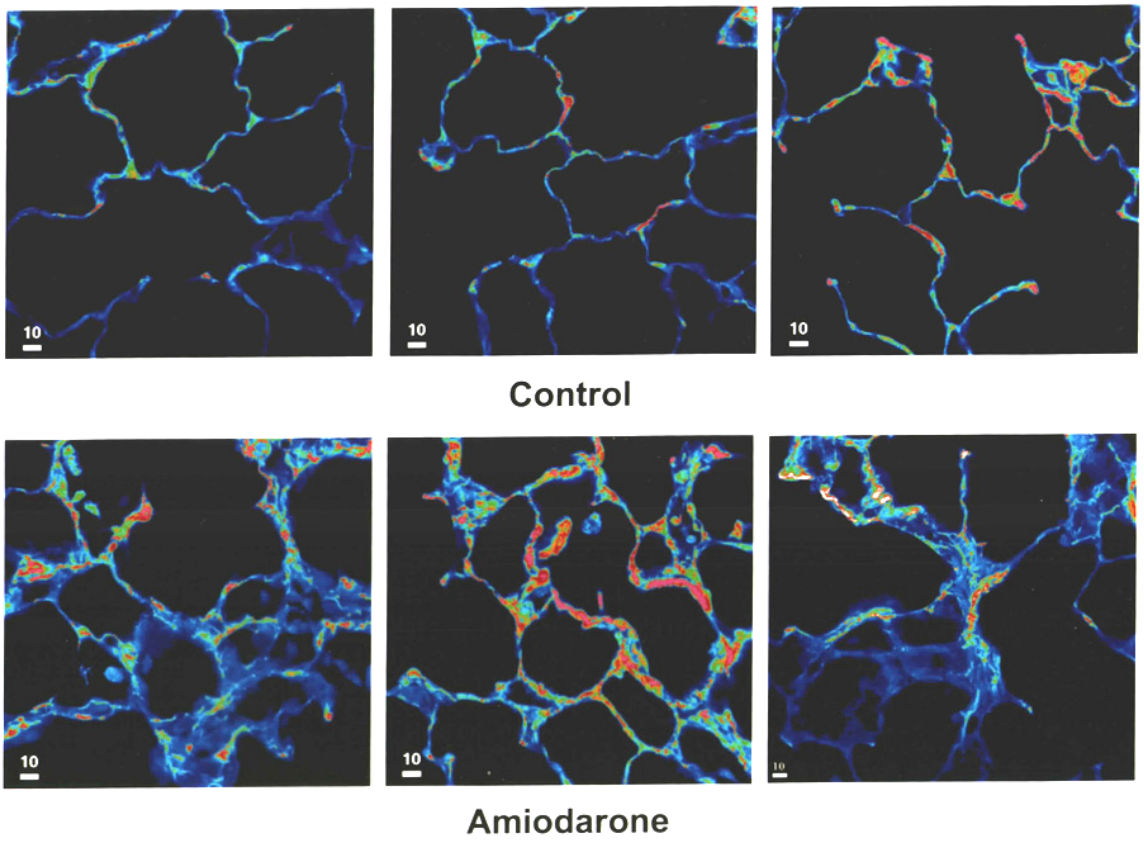

Figure 11: Representative fields of lung tissue obtained by laser-scanning confocal microscopy. Rats were instilled intratracheally with amiodarone (6.25 mg/kg) or an equivalent volume of sterile water on days 0 and 2. Left lungs were inflated and fixed at day 28, sectioned into blocks, stained with Lucifer Yellow, and analyzed by LSCM. This technique measures the entire stained area of the alveolar septa, with alveolar cells and debris removed from analysis by incorporating a threshold value. Colors indicate staining intensity, from blue, green, yellow, red, to white, respectively, as the intensity increases. Scale bars indicate 10 μm.

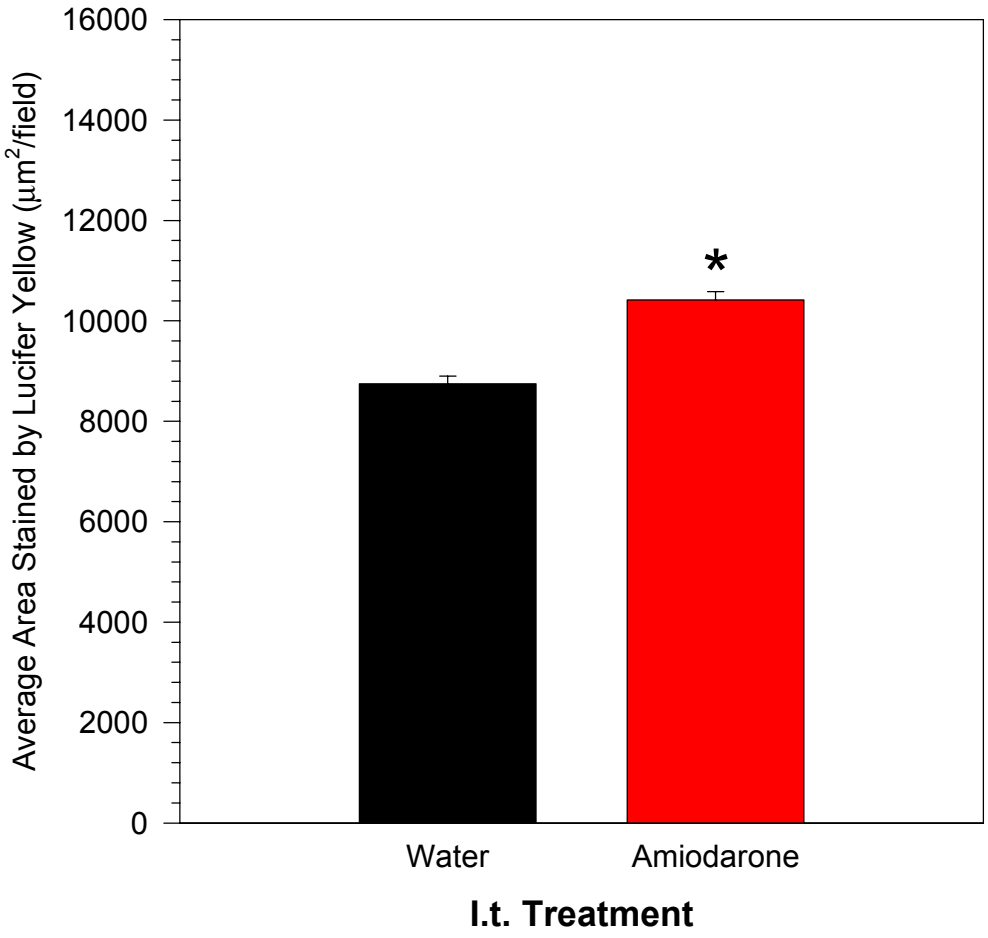

Figure 12: Effect of AD on average lung tissue area stained by lucifer yellow. Rats were instilled intratracheally with amiodarone (6.25 mg/kg) or an equivalent volume of sterile water on days 0 and 2. Left lungs were inflated and fixed at day 28, sectioned into blocks, stained with Lucifer Yellow, and analyzed by LSCM. Values are means ± SEM. N=3. *Significantly different from control ($p<0.05$).

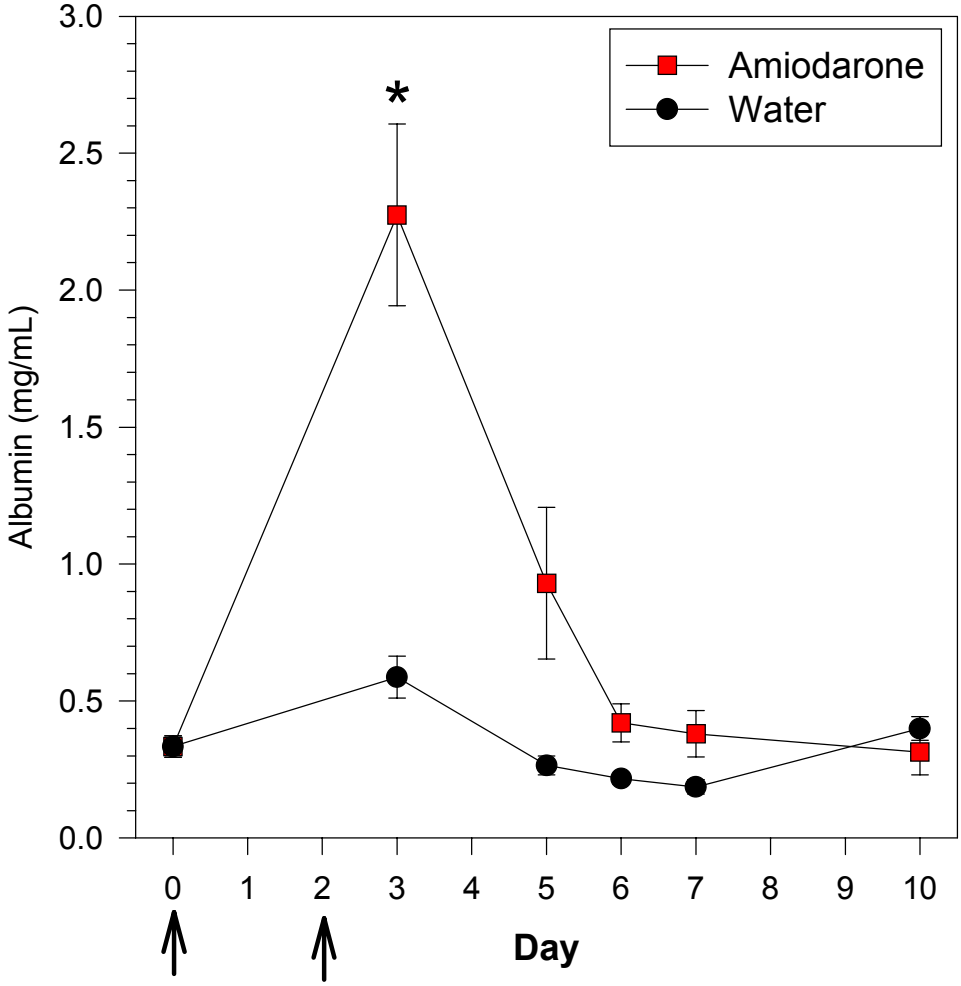

Figure 13: Albumin in the first BAL fraction. Albumin in the first BAL fraction was assayed at various time points following intratracheal instillations of sterile water or amiodarone solution (6.25 mg/kg) on days 0 and 2. Naïve values are represented at day 0 and arrows indicate intratracheal treatments. Values are mean ± SEM. N=5-9. *Significantly different from control ($p<0.05$).

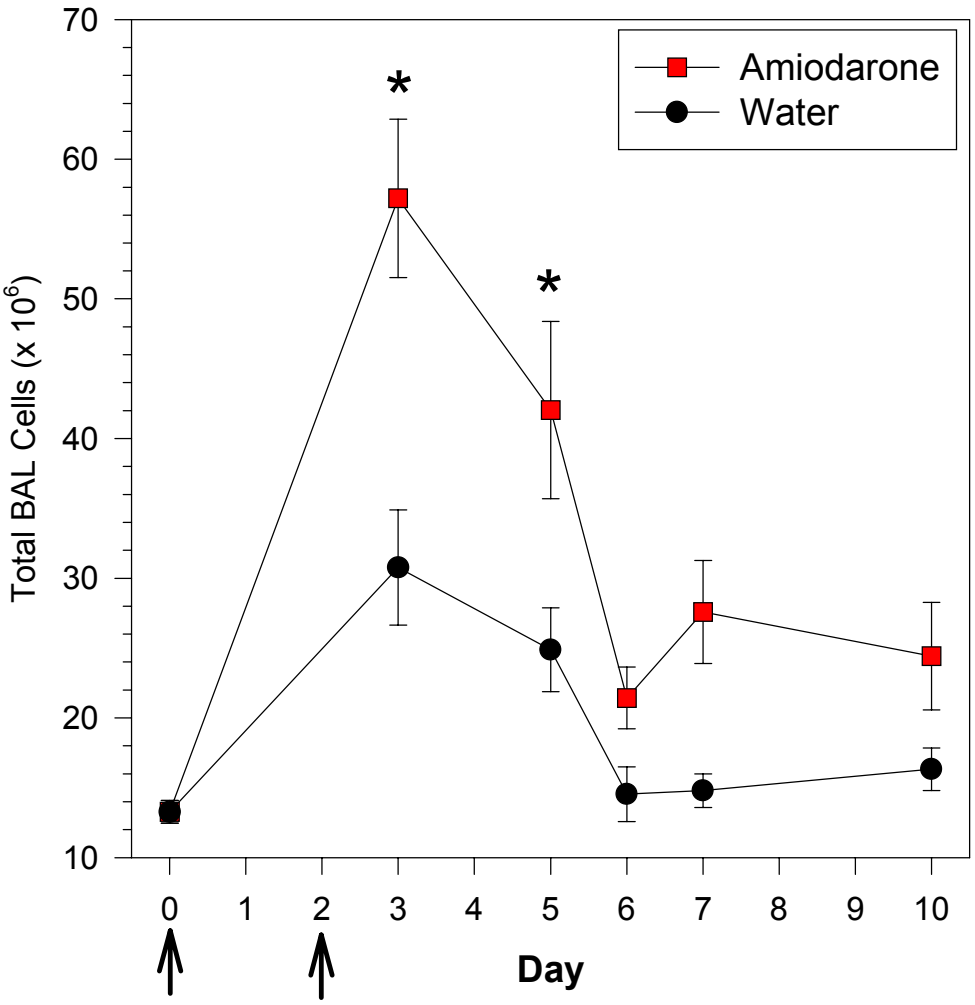

Figure 14: Total cells recovered by BAL. Rats were given intratracheal instillations of sterile water or amiodarone (6.25 mg/kg) on days 0 and 2 and lavaged at various time points following treatment. Total cell number recovered in the BAL fluid was determined. Naïve values are represented at day 0 and arrows indicate intratracheal treatments. Values are means ± SEM. N=5-9. *Significantly different from control ($p<0.05$).

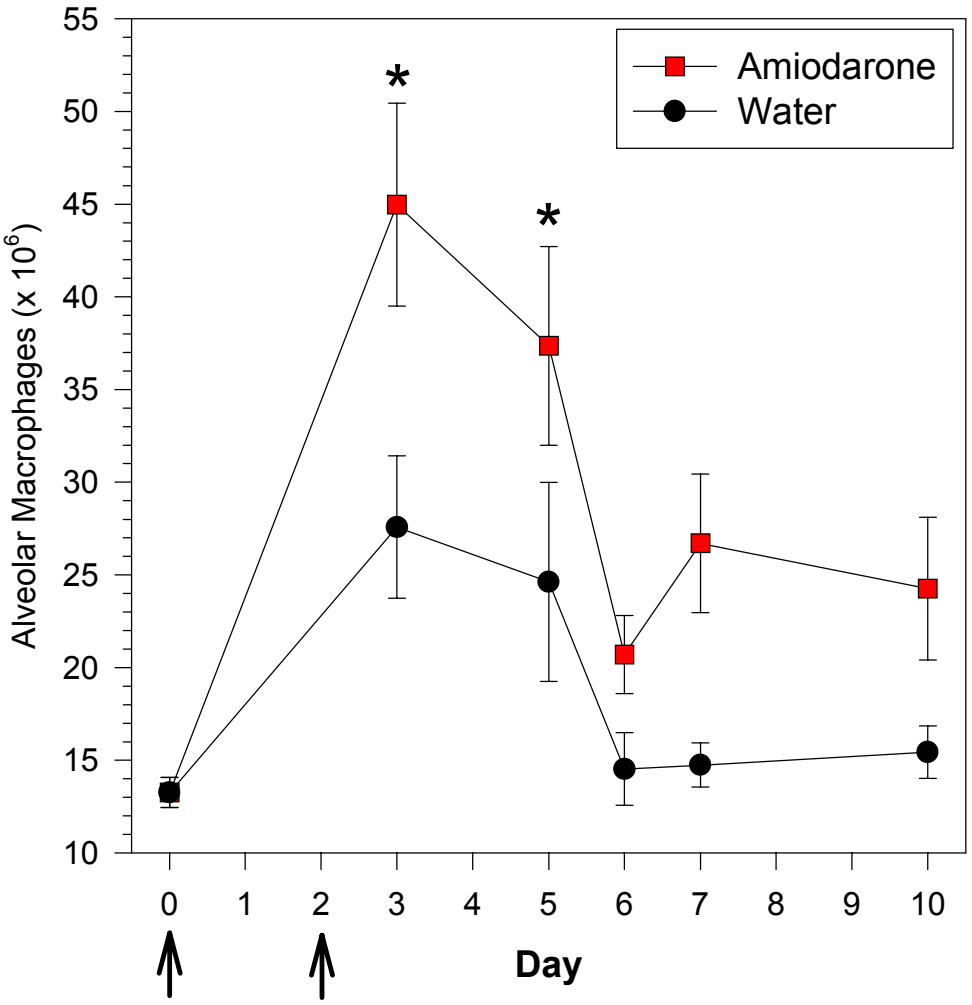

Figure 15: Alveolar macrophages recovered by BAL. Rats were given intratracheal instillations of sterile water or amiodarone (6.25 mg/kg) on days 0 and 2 and lavaged at various time points following treatment. The number of alveolar macrophages recovered in the BAL fluid was determined. Naïve values are represented at day 0 and arrows indicate intratracheal treatments. Values are means ± SEM. N=5-9. *Significantly different from control ($p<0.05$).

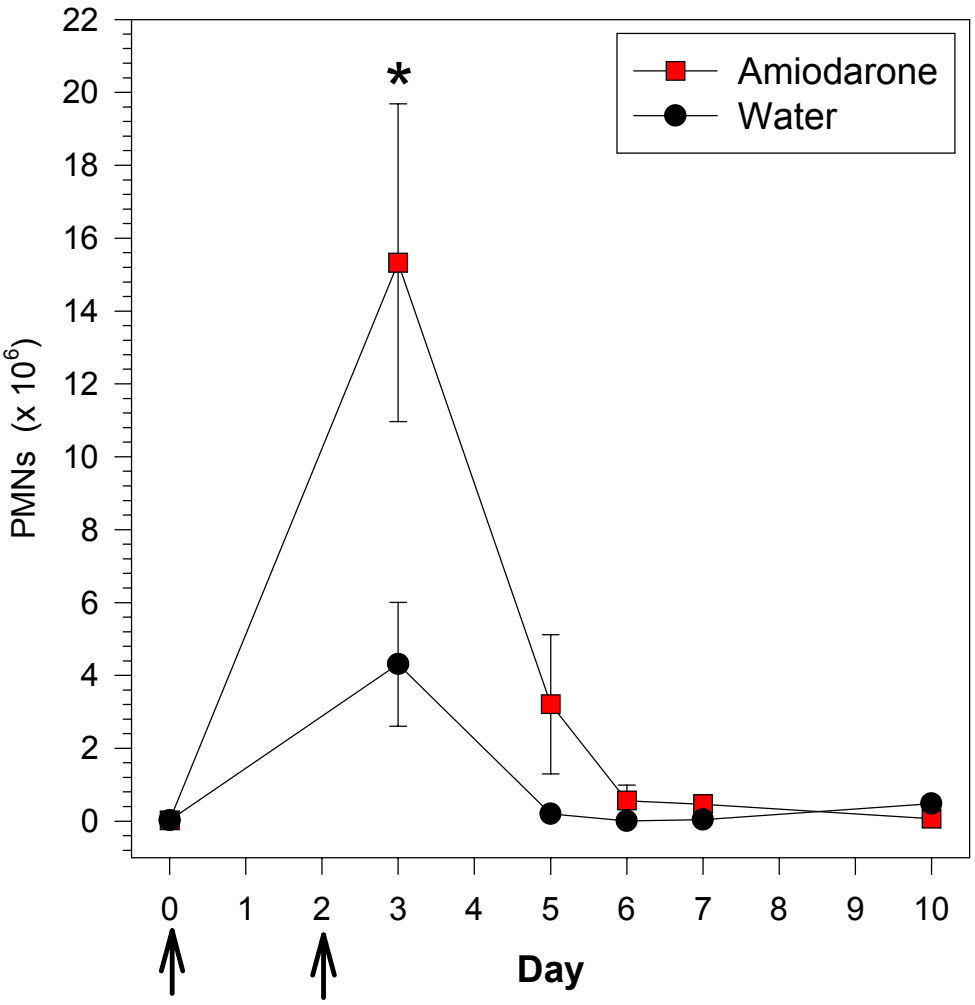

Figure 16: Polymorphonuclear leukocytes recovered by BAL. Rats were given intratracheal instillations of sterile water or amiodarone (6.25 mg/kg) on days 0 and 2 and lavaged at various time points following treatment. The number of PMNs recovered in the BAL fluid was determined. Naïve values are represented at day 0 and arrows indicate intratracheal treatments. Values are means ± SEM. N=5-9. *Significantly different from control ($p<0.05$).

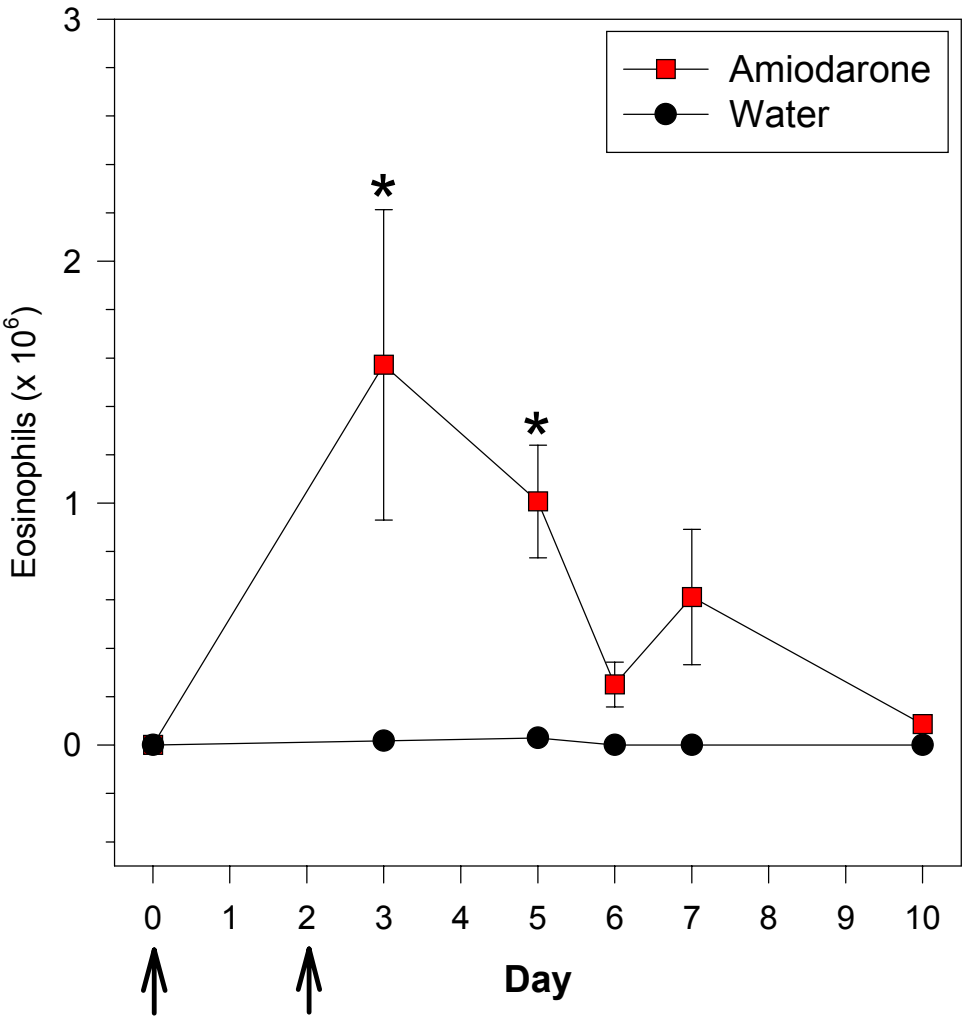

Figure 17: Eosinophilic leukocytes recovered by BAL. Rats were given intratracheal instillations of sterile water or amiodarone (6.25 mg/kg) on days 0 and 2, lavaged at various time points following treatment, and the number of eosinophils recovered in the BAL fluid was determined. Naïve values are represented at day 0 and arrows indicate intratracheal treatments. Values are means ± SEM. N=5-9. *Significantly different from control ($p<0.05$).

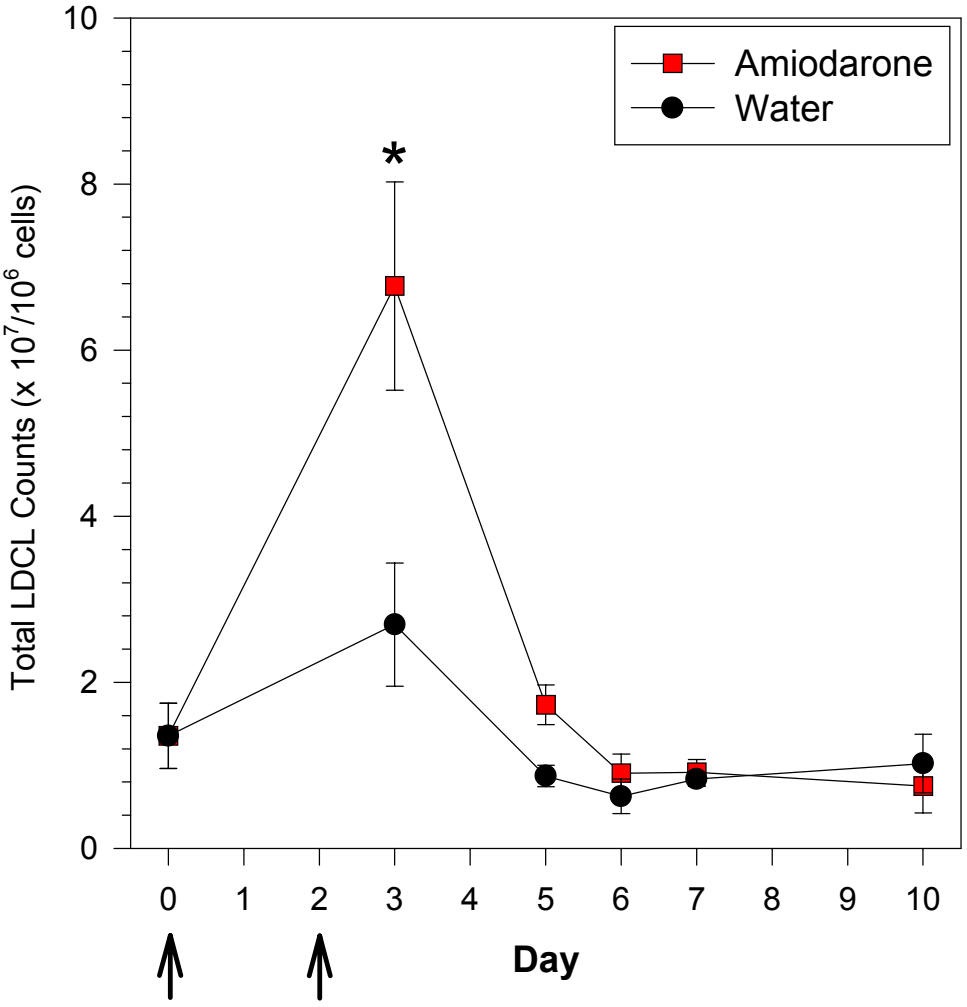

Figure 18: Total PMA-stimulated luminol-dependent chemiluminescence counts over 20 minutes from BAL cells. Rats were given intratracheal instillations of sterile water or amiodarone (6.25 mg/kg) on days 0 and 2 and lavaged at various time points following treatment. The recovered cells were subjected to LDCL with PMA stimulation. Naïve values are represented at day 0 and arrows indicate intratracheal treatments. Values are means ± SEM. N=5-9. *Significantly different from control ($p<0.05$).

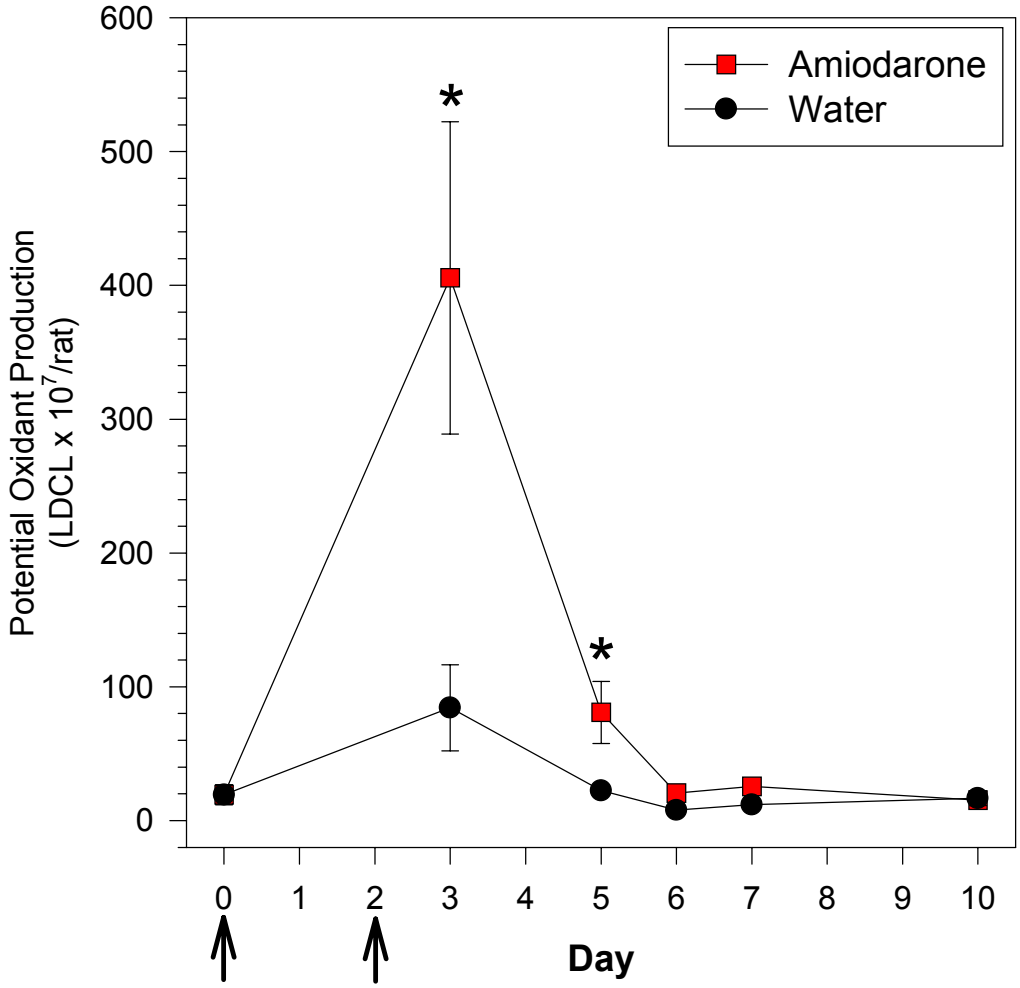

Figure 19: Potential oxidant production of total BAL cells. Rats were given intratracheal instillations of sterile water or amiodarone (6.25 mg/kg) on days 0 and 2 and lavaged at various time points following treatment. The number of cells recovered from each animal was multiplied by the per-cell LDCL value. Naïve values are represented at day 0 and arrows indicate intratracheal treatments. Values are means ± SEM. N=5-9. *Significantly different from control ($p<0.05$).

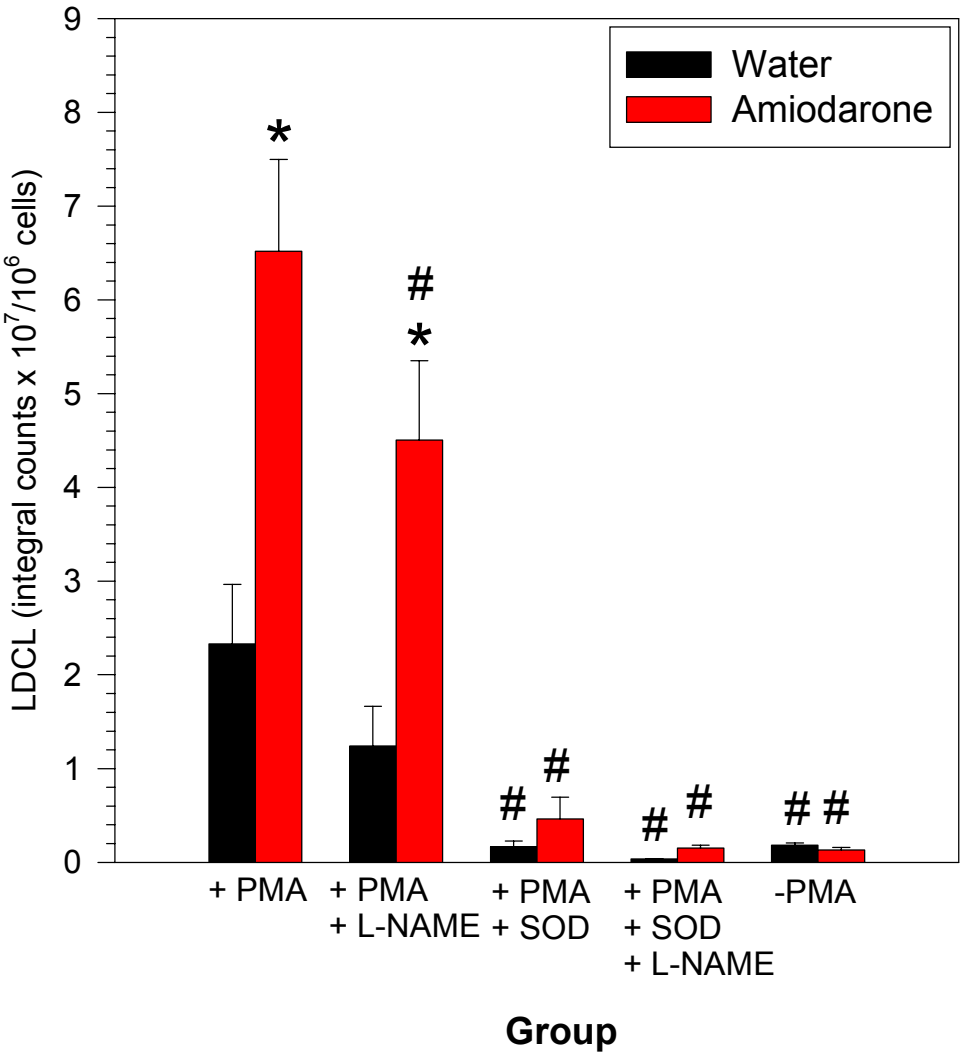

Figure 20: PMA-stimulated LDCL counts over 20 minutes from BAL cells on Day 3 with specific inhibitors. Cells recovered in the BAL fluid of rats at day 3 following i.t. instillations of sterile water or AD (6.25 mg/kg) on days 0 and 2 subjected to LDCL with and without PMA. Group assignments: PMA alone=only PMA; L-NAME= N^{ω}-nitro-L-arginine methyl ester and PMA; SOD=Superoxide Dismutase and PMA; SOD + L-NAME=both inhibitors and PMA. Values are ± SEM. N=5-9. *Significantly different from control ($p<0.05$). #Significantly different than corresponding PMA alone value ($p<0.05$).

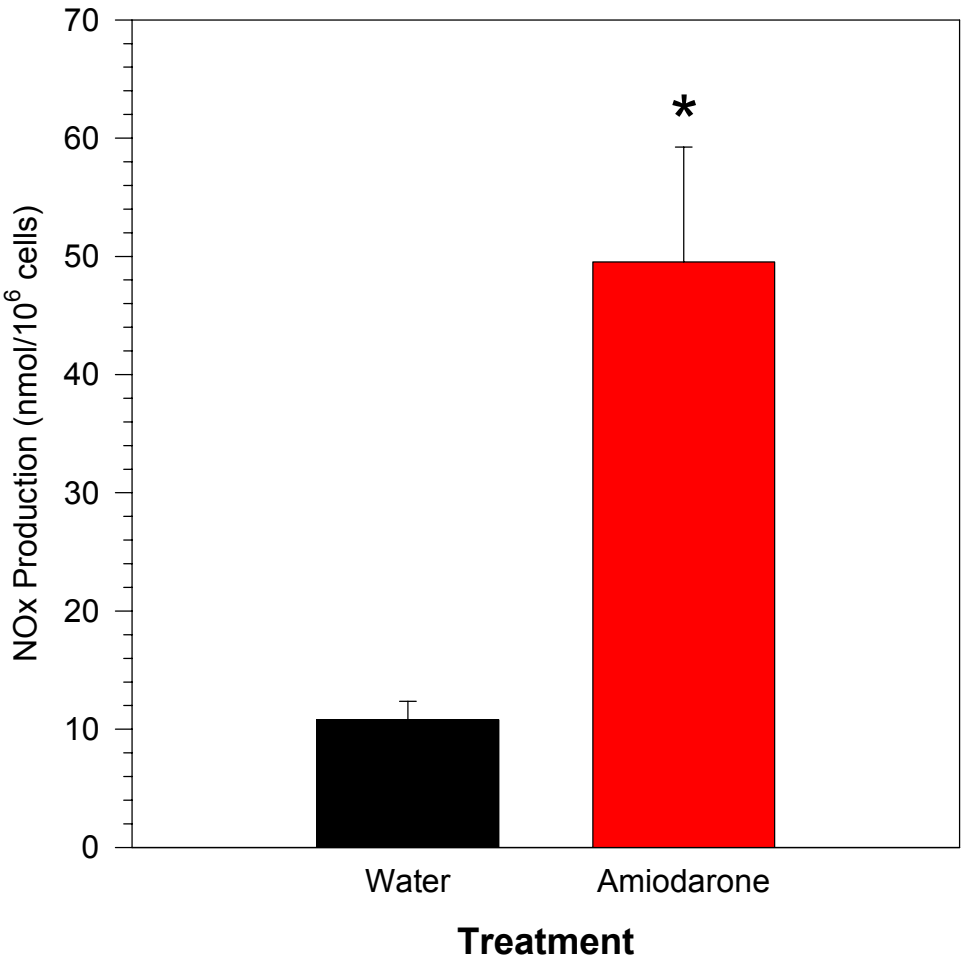

Figure 21: NOx (NO_2 and NO_3) production from BAL cells cultured at Day 3. Rats were given i.t. AD (6.25 mg/kg) or sterile water on days 0 and 2 and lavaged on day 3. The BAL cells were then cultured 24 hours, after which the media was assayed for nitrate (NO_3) and nitrite (NO_2), collectively referred to as NOx, which are the stable products of NO in solution. Values are means ± SEM. N=3. *Significantly different from control ($p<0.05$).

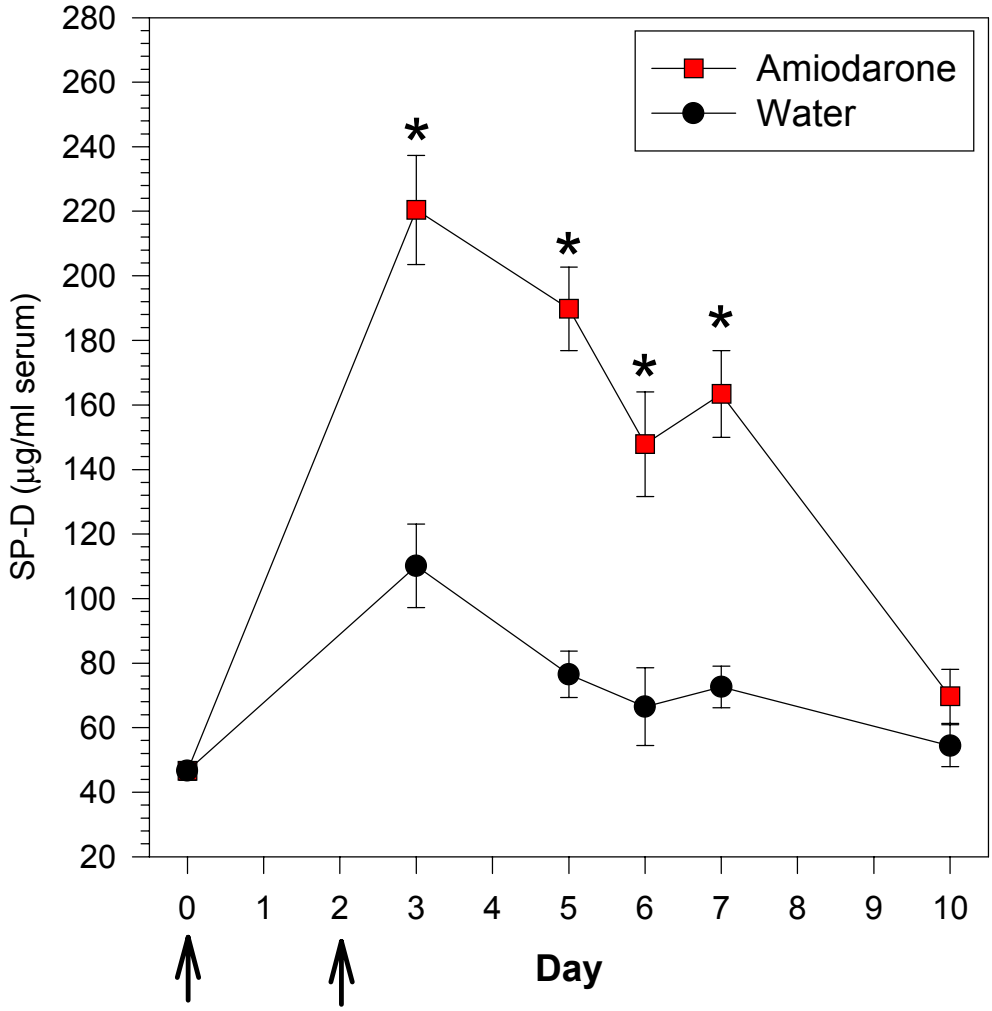

Figure 22: Effect of AD on surfactant protein-D levels in serum. Rats were given i.t. AD (6.25 mg/kg) or an equivalent volume of sterile water on days 0 and 2. Serum was collected as various time points and assayed for SP-D. Naïve values are represented at day 0 and arrows indicate intratracheal treatments. Values are means ± SEM. N=5-9. *Significantly different from control ($p<0.05$).

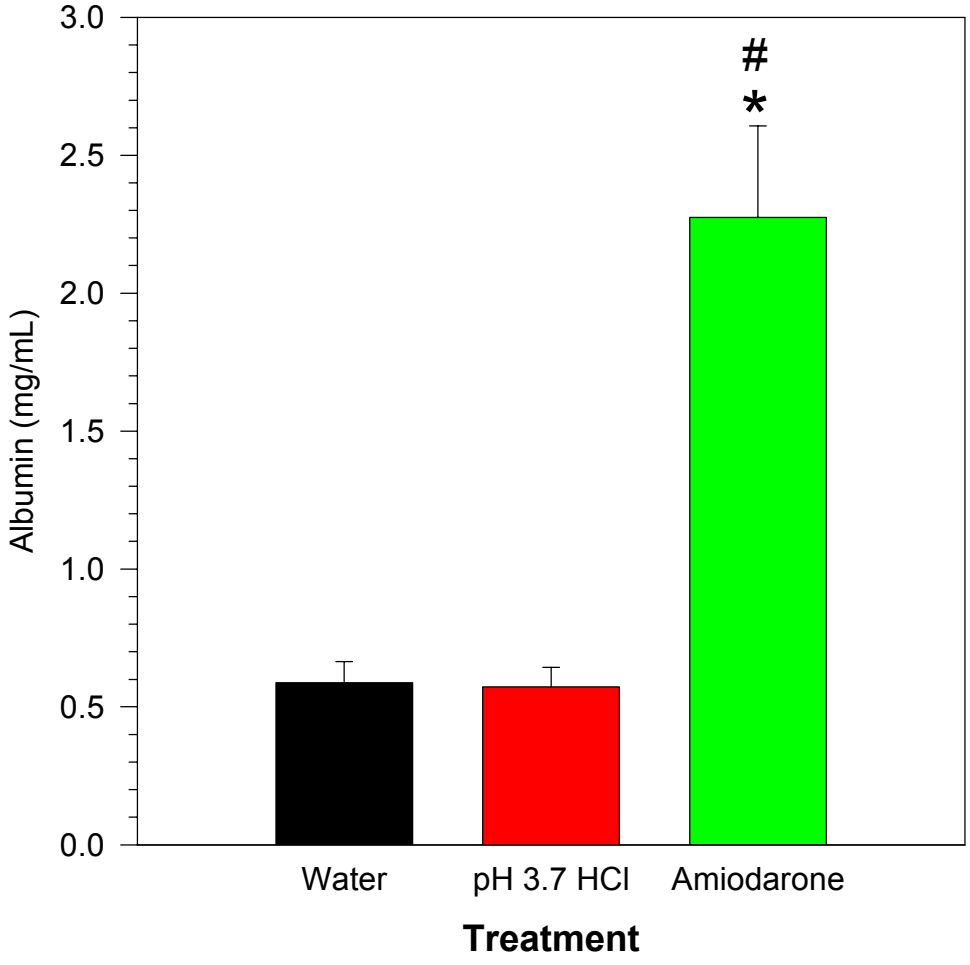

Figure 23: Albumin in the first BAL fraction on day 3 following intratracheal amiodarone, vehicle, or acidic vehicle treatment on days 0 and 2. Rats were given i.t. AD (6.25 mg/kg), sterile water, or sterile water adjusted to pH 3.7 with HCl to match the pH of the amiodarone solution on days 0 and 2. Rats were lavaged on day 3 and albumin levels were measured in the first BAL fraction. Values are means ± SEM. N=6-11. *Significantly different from sterile water control ($p<0.05$). #Significantly different from acidic water control.

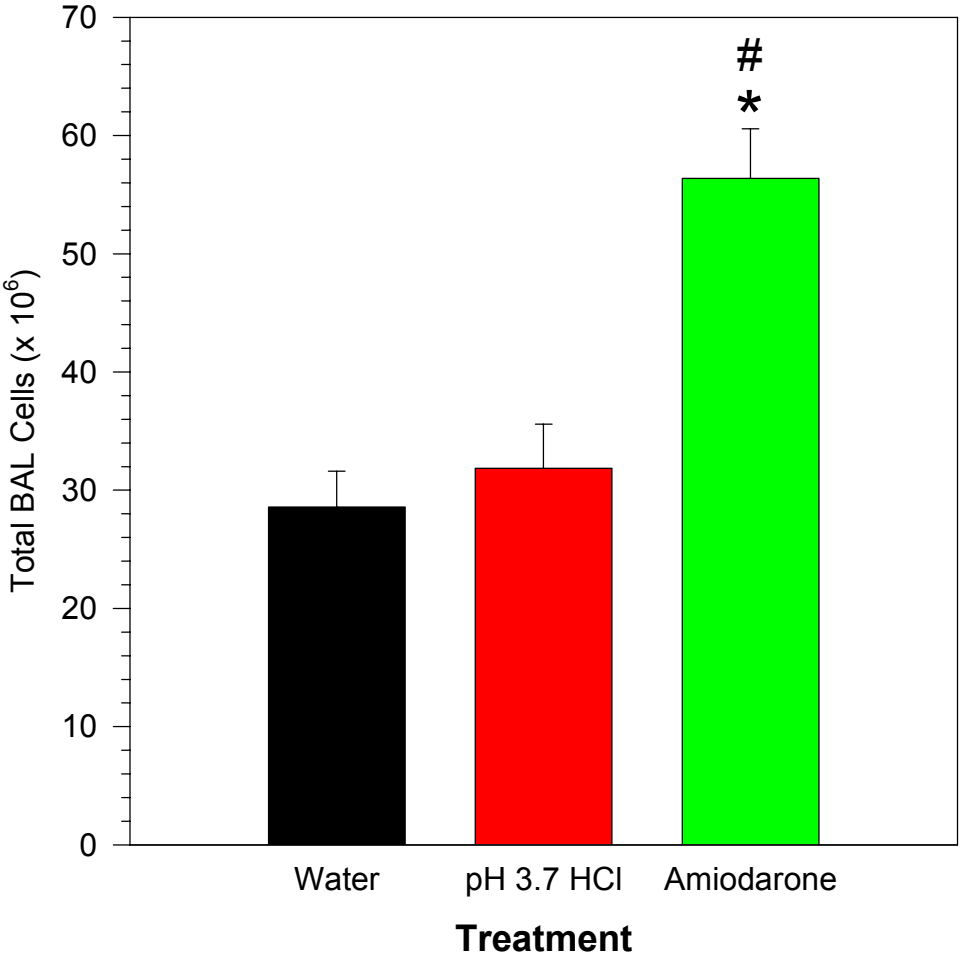

Figure 24: Total BAL cells recovered on day 3 following intratracheal amiodarone, vehicle, or acidic vehicle treatment on days 0 and 2. Rats were given i.t. AD (6.25 mg/kg), sterile water, or sterile water adjusted to pH=3.7 with HCl to match the pH of the amiodarone solution on days 0 and 2. Rats were lavaged on day 3 and the BAL cells were counted and differentiated. Values are means ± SEM. N=6-11. *Significantly different from sterile water control ($p<0.05$). #Significantly different from acidic water control.

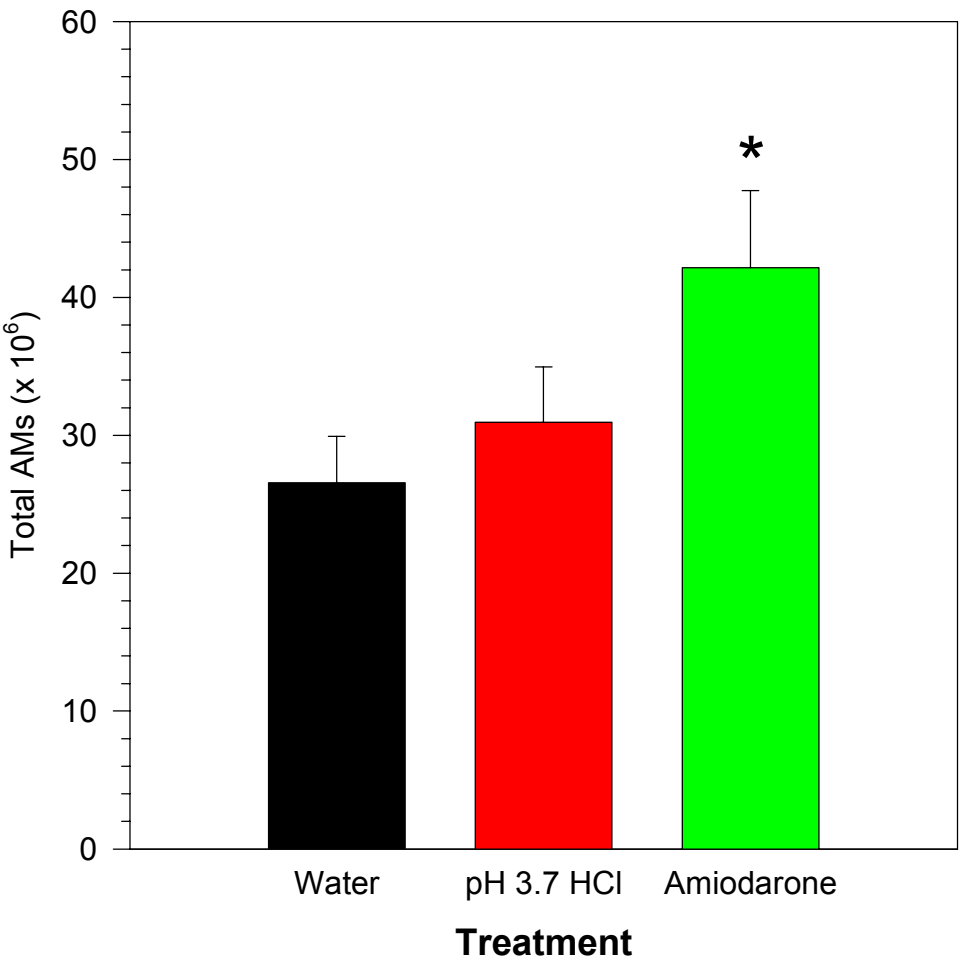

Figure 25: Total alveolar macrophages recovered on day 3 following intratracheal amiodarone, vehicle, or acidic vehicle treatment on days 0 and 2. Rats were given i.t. AD (6.25 mg/kg), sterile water, or sterile water adjusted to pH=3.7 with HCl to match the pH of the amiodarone solution on days 0 and 2. Rats were lavaged on day 3 and the BAL cells were counted and differentiated. Values are means ± SEM. N=6-11. *Significantly different from sterile water control ($p<0.05$).

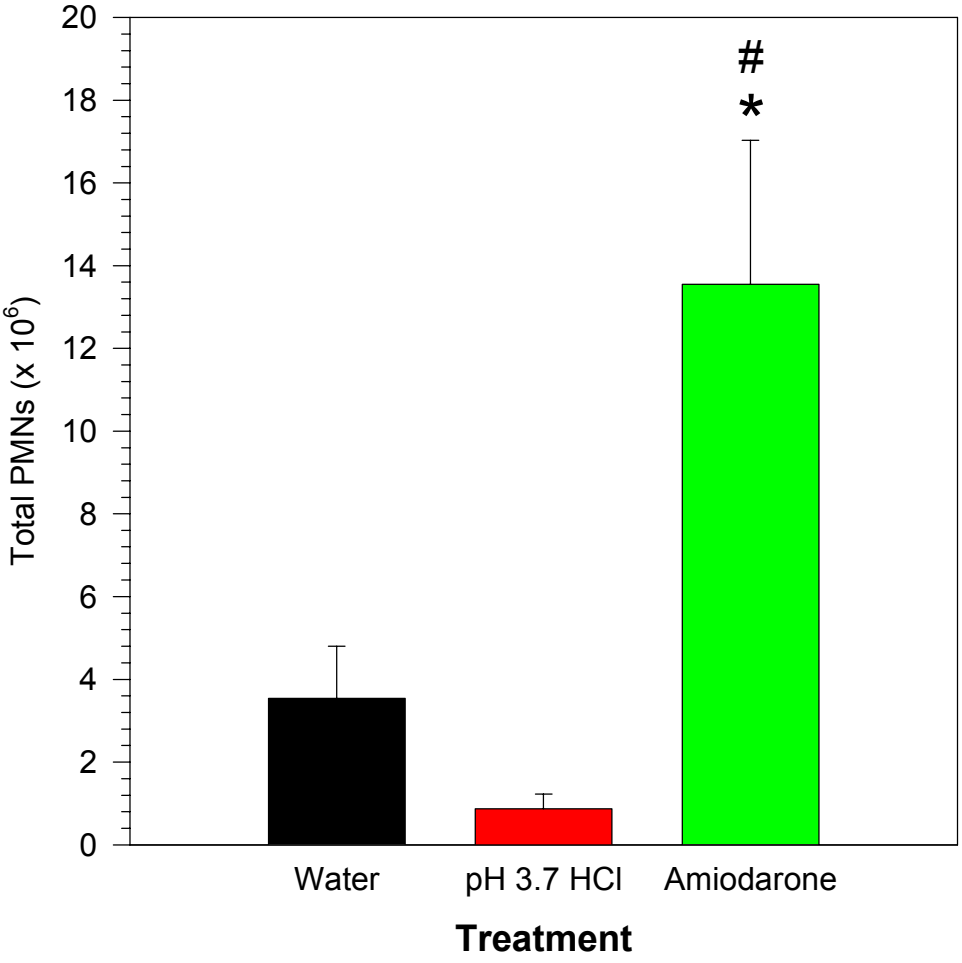

Figure 26: Total neutrophils (PMNs) recovered on day 3 following intratracheal amiodarone, vehicle, or acidic vehicle treatment on days 0 and 2. Rats were given i.t. AD (6.25 mg/kg), sterile water, or sterile water adjusted to pH=3.7 with HCl to match the pH of the amiodarone solution on days 0 and 2. Rats were lavaged on day 3 and the BAL cells were counted and differentiated. Values are means ± SEM. N=6-11. *Significantly different from sterile water control ($p<0.05$). #Significantly different from acidic water control.

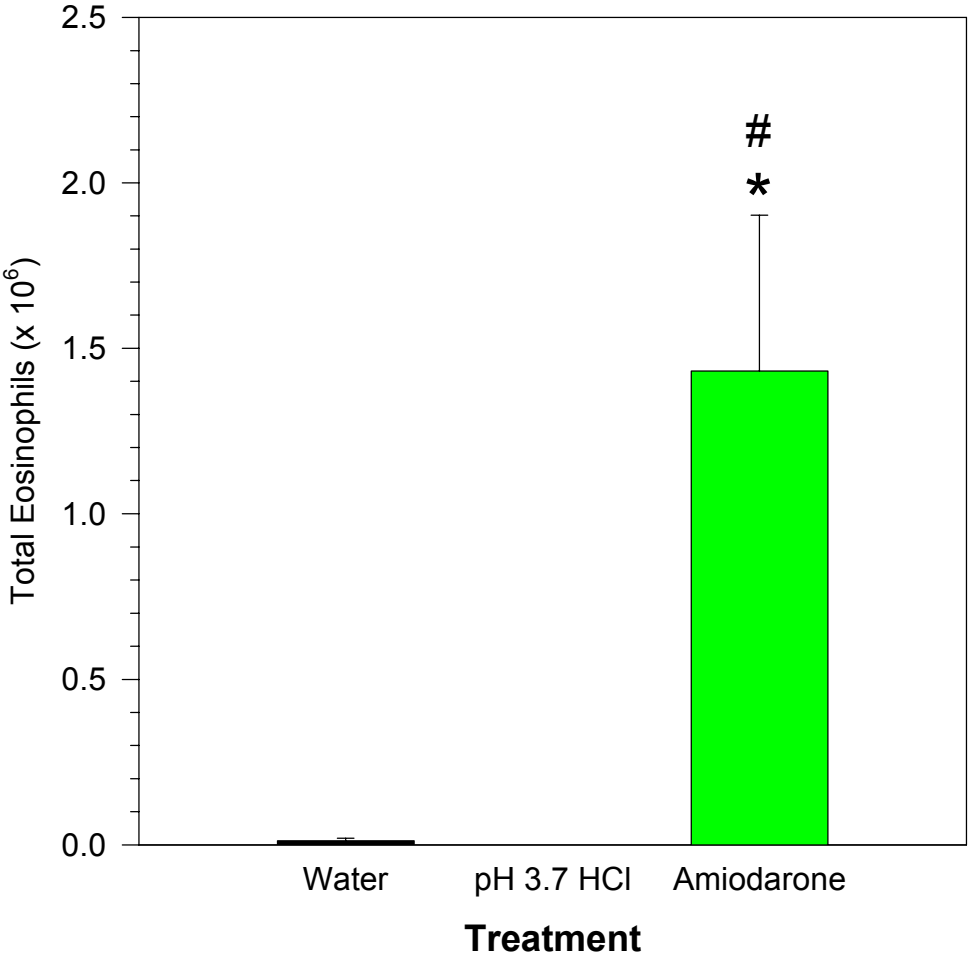

Figure 27: Total eosinophils recovered on day 3 following intratracheal amiodarone, vehicle, or acidic vehicle treatment on days 0 and 2. Rats were given i.t. AD (6.25 mg/kg), sterile water, or sterile water adjusted to pH=3.7 with HCl to match the pH of the amiodarone solution on days 0 and 2. Rats were lavaged on day 3 and the BAL cells were counted and differentiated. Values are means ± SEM. N=6-11. *Significantly different from sterile water control ($p<0.05$). #Significantly different from acidic water control.

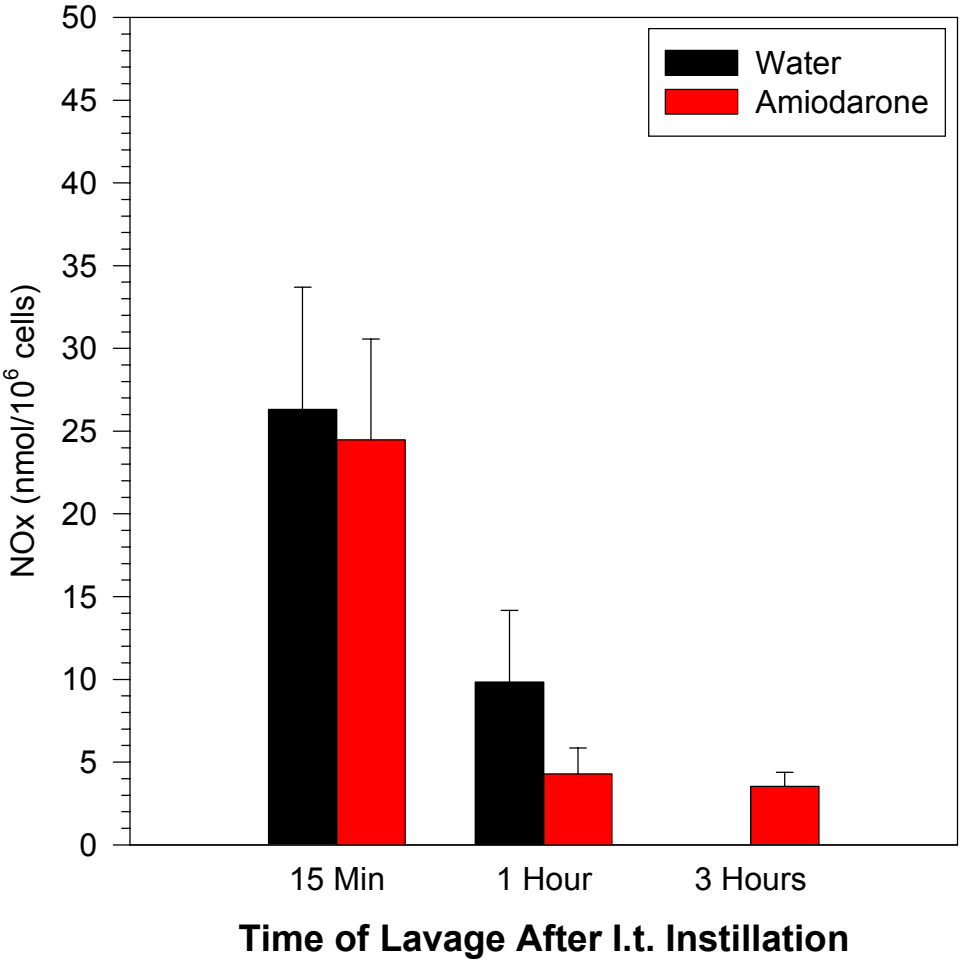

Figure 28A: Non-LPS-stimulated NOx production from cultured BAL cells lavaged at various time-points following intratracheal instillation of amiodarone or vehicle. Rats were given either a single i.t. dose of AD (6.25 mg/kg) or sterile water and lavaged at 15 minutes, 1 hour, 3 hours, or given the i.t. doses at day 0 and 2 and lavaged on day 3. The BAL cells were then cultured (without LPS addition) 24 hours, after which the media was assayed for nitrate (NO_3) and nitrite (NO_2), collectively referred to as NOx, which are the stable products of NO in solution. Values are means ± SEM. N=3-9. No significant differences from control ($p<0.05$).

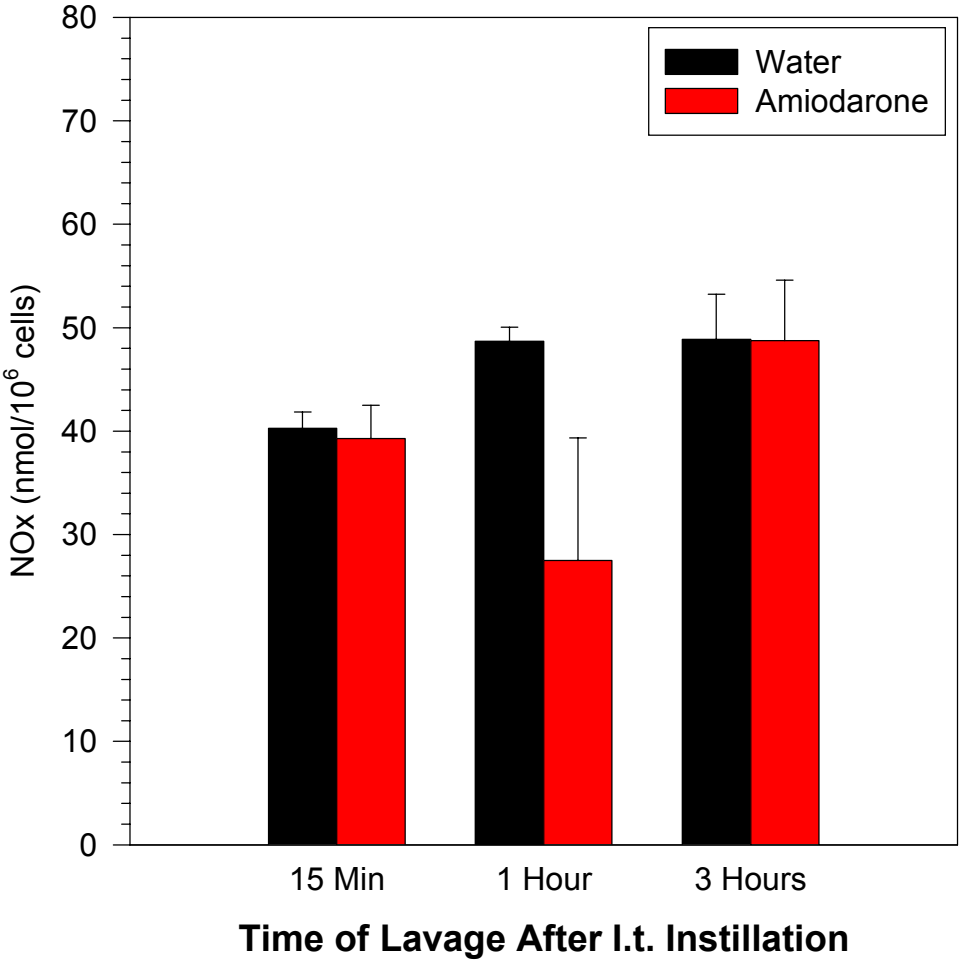

Figure 28B: LPS-stimulated NOx production from cultured BAL cells lavaged at various time-points following intratracheal instillation of amiodarone or vehicle. Rats were given either a single i.t. dose of AD (6.25 mg/kg) or sterile water and lavaged at 15 minutes, 1 hour, 3 hours, or given the i.t. doses at day 0 and 2 and lavaged on day 3. The BAL cells were then cultured (with LPS added) 24 hours, after which the media was assayed for nitrate (NO_3) and nitrite (NO_2), collectively referred to as NOx, which are the stable products of NO in solution. Values are means ± SEM. N=3-9. No significant differences from control ($p<0.05$).

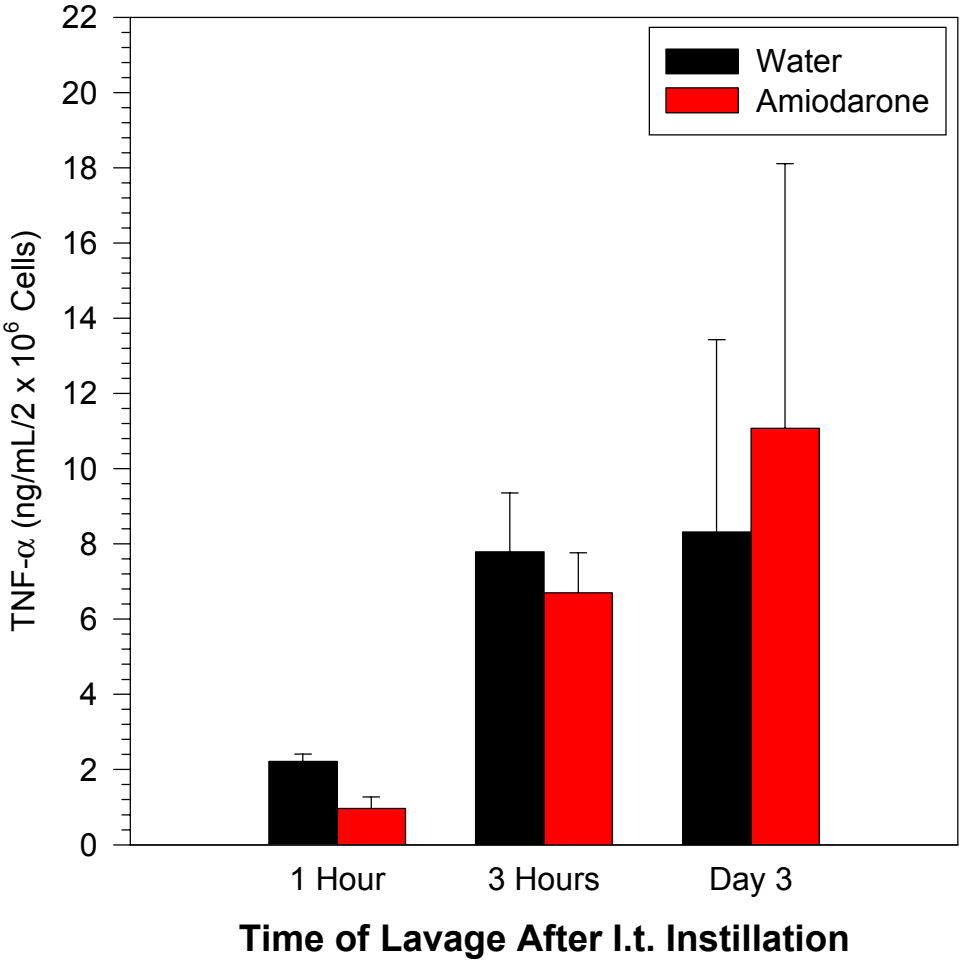

Figure 29A: Non-LPS-stimulated TNF-α production from cultured BAL cells lavaged at various time-points following intratracheal instillation of amiodarone or vehicle. Rats were given either a single i.t. dose of AD (6.25 mg/kg) or sterile water and lavaged at 1 hour or 3 hours, or given the i.t. doses at day 0 and 2 and lavaged on day 3. The BAL cells were then cultured 24 hours without LPS, after which the media was assayed for TNF-α. Values are means ± SEM. N=3-4. No significant differences from control ($p<0.05$).

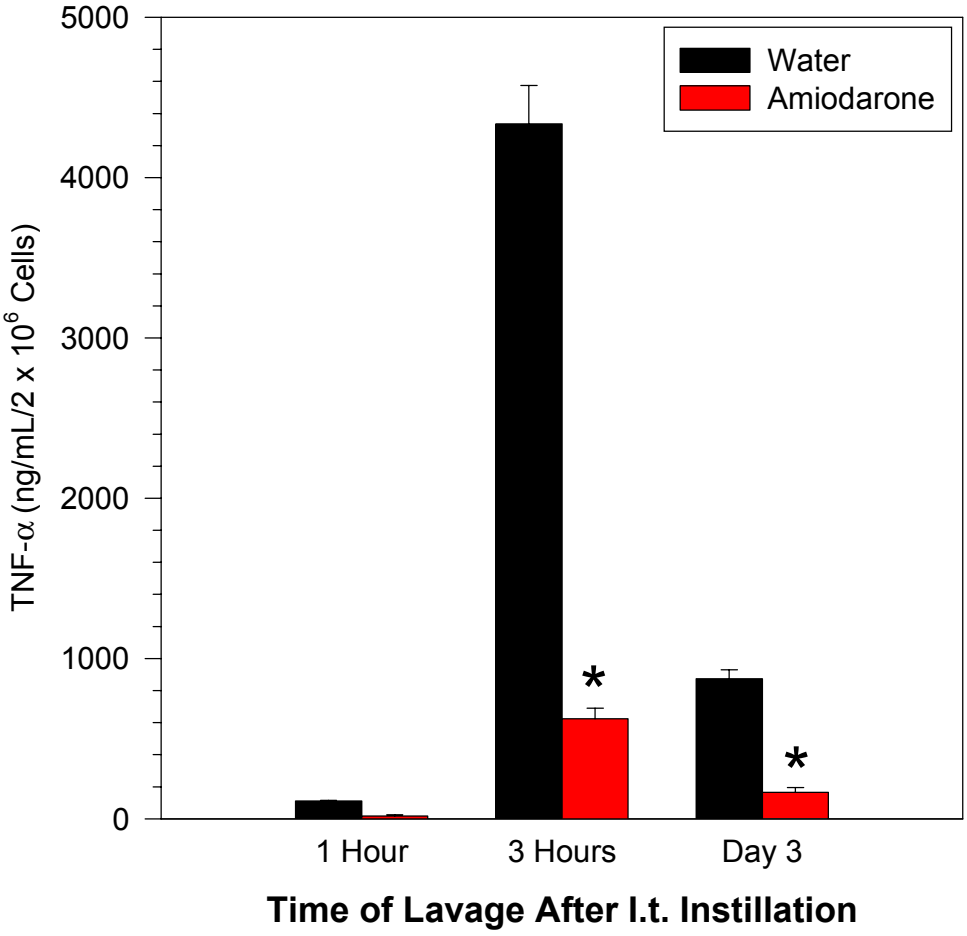

Figure 29B: LPS-stimulated TNF-α production from cultured BAL cells lavaged at various time-points following intratracheal instillation of amiodarone or vehicle. Rats were given either a single i.t. dose of AD (6.25 mg/kg) or sterile water and lavaged at 1 hour or 3 hours, or given the i.t. doses at day 0 and 2 and lavaged on day 3. The BAL cells were then cultured 24 hours with LPS, after which the spent media was assayed for TNF-α. Values are means ± SEM. N=3-4. *Significantly different from control ($p<0.05$).

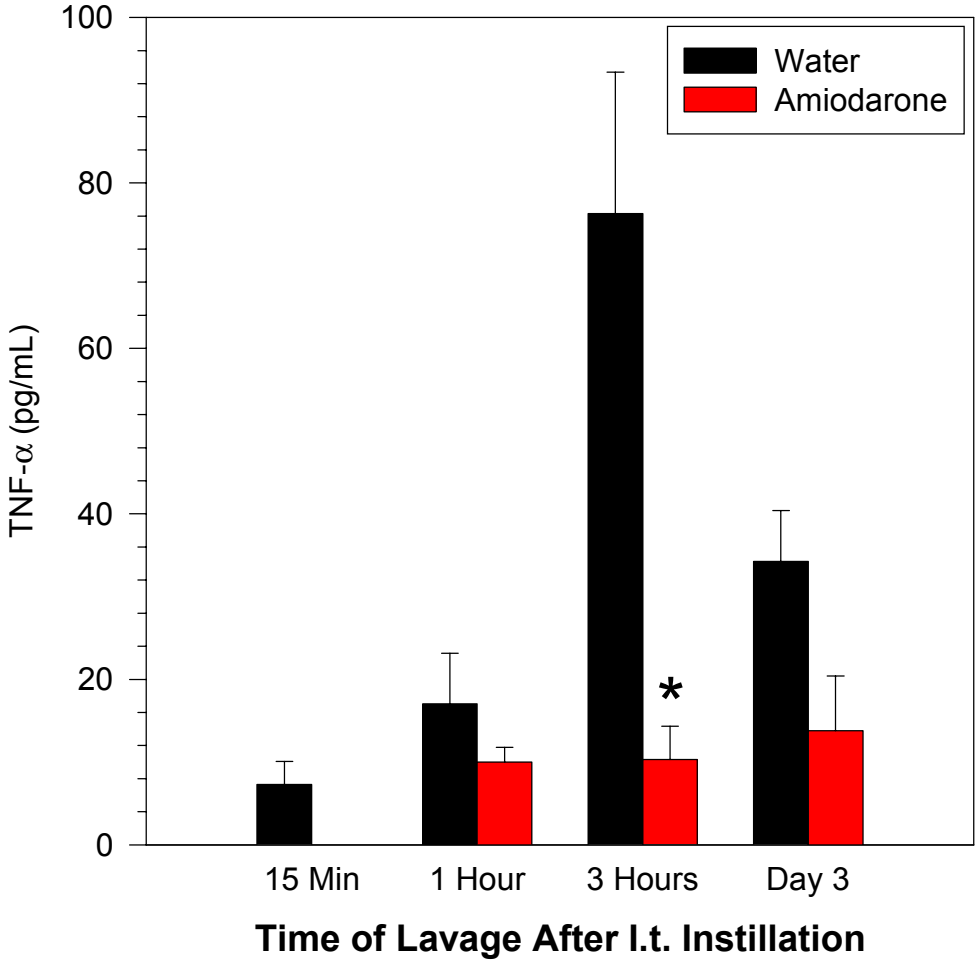

Figure 30: TNF-α levels in the first BAL fraction at various time-points following instillation of amiodarone or vehicle. Rats were given either a single i.t. dose of AD (6.25 mg/kg) or sterile water and lavaged at 15 minutes, 1 hour, 3 hours, or given the i.t. doses at day 0 and 2 and lavaged on day 3. TNF-α levels were determined in the first BAL fraction. Values are means ± SEM. N=2-4. *Significantly different from control ($p<0.05$).

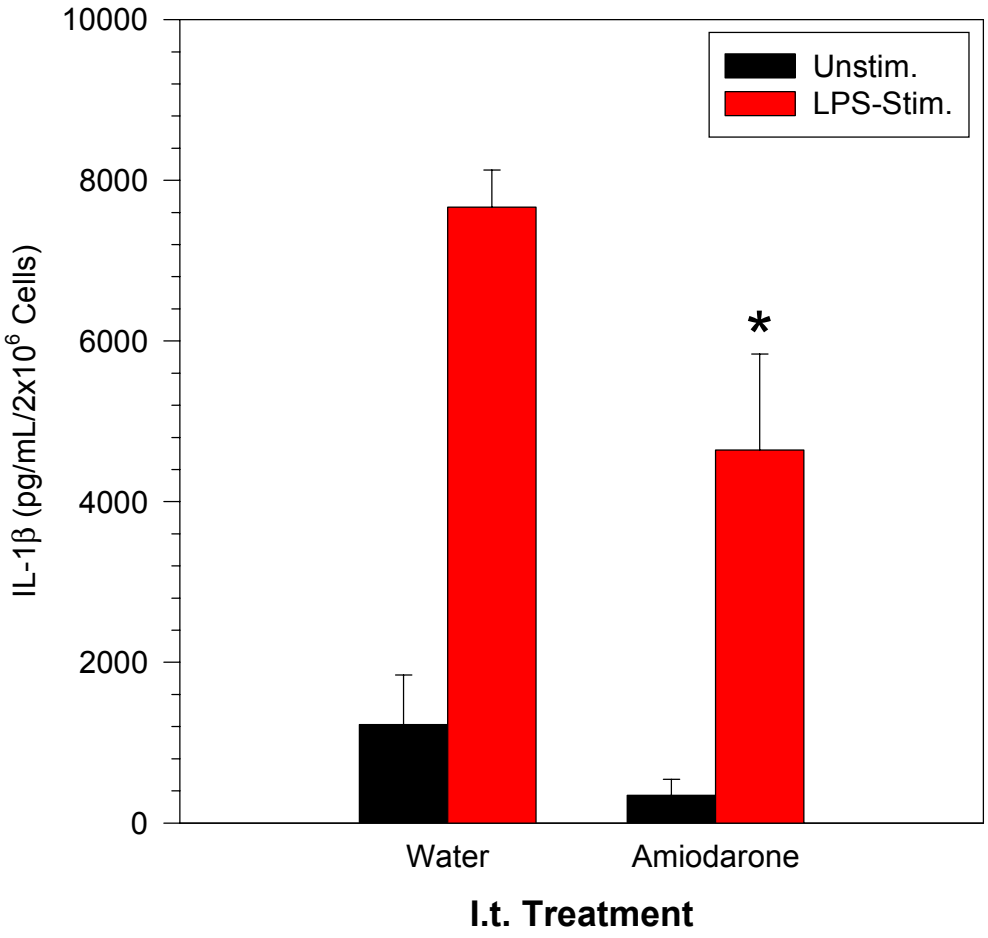

Figure 31: IL-1β production from cultured BAL cells recovered by lavage 3 hours following intratracheal amiodarone or vehicle treatment. Rats were given a single i.t. dose of AD (6.25 mg/kg) or sterile water and subjected to BAL 3 hours later. BAL cells were then cultured 24 hours with and without LPS. IL-1β levels were determined in the culture media. Values are means ± SEM. N=4. *Significantly different from control with LPS ($p<0.05$).

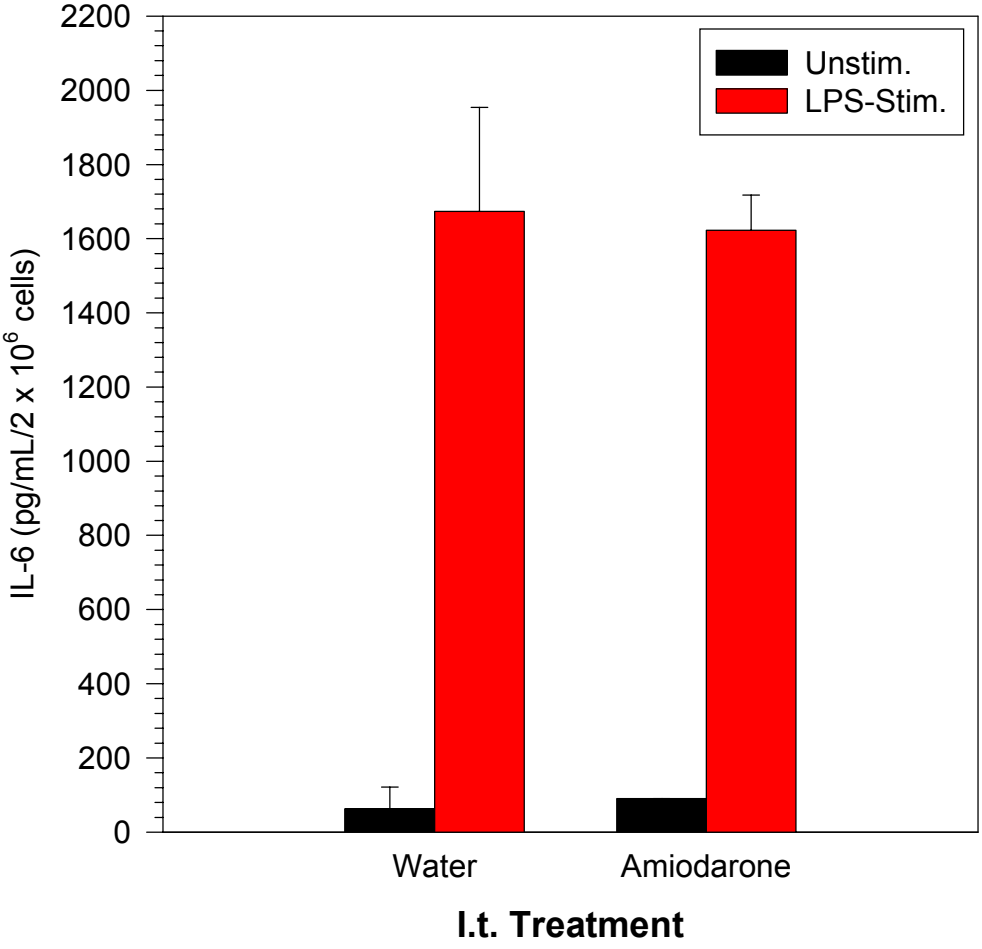

Figure 32A: IL-6 production from BAL cells recovered by lavage 15 minutes following i.t. instillation of amiodarone or vehicle and cultured 24 hours. Rats were given a single i.t. dose of AD (6.25 mg/kg) or sterile water and subjected to BAL 15 minutes later. BAL cells were then cultured 24 hours with and without LPS. IL-6 levels were determined in the culture media. Values are means ± SEM. N=2-4. No significant differences from control ($p<0.05$).

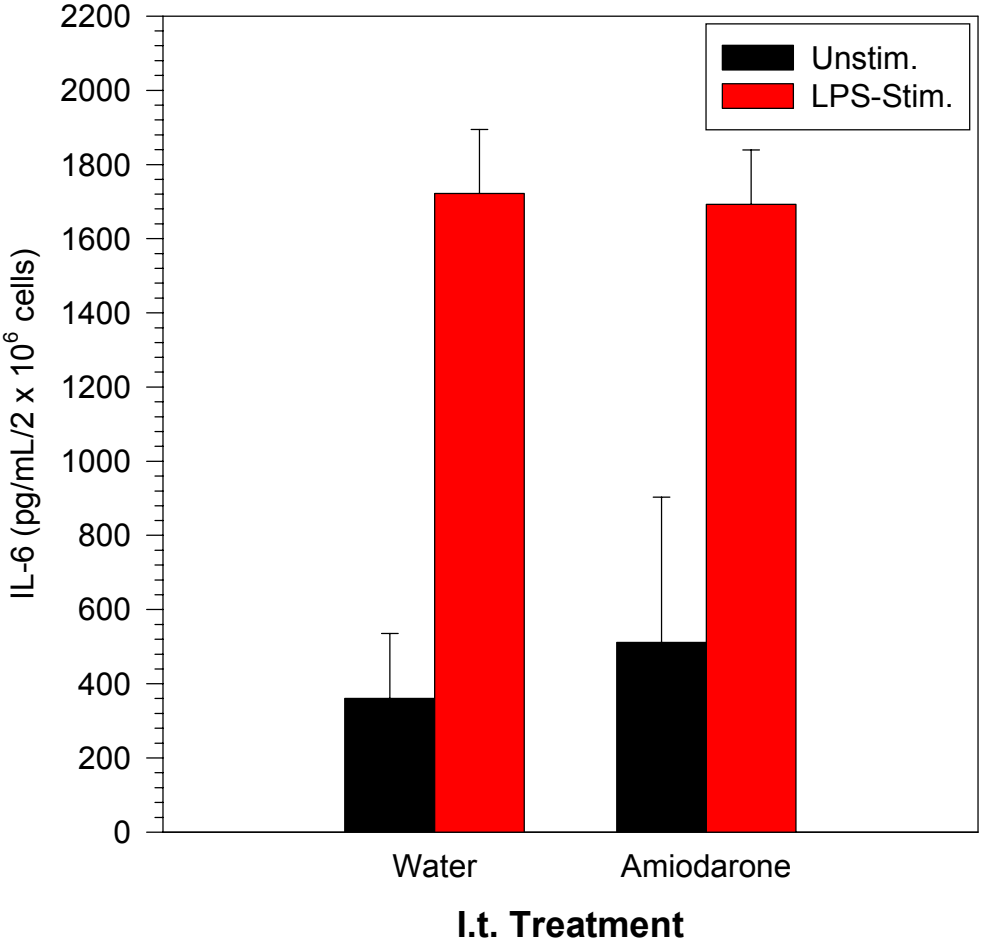

Figure 32B: IL-6 production from BAL cells recovered by lavage on day 3 following i.t. instillation of amiodarone or vehicle and cultured 24 hours. Rats were given i.t. AD (6.25 mg/kg) or sterile water on days 0 and 2 and subjected to BAL on day 3. BAL cells were then cultured 24 hours with and without LPS. IL-6 levels were determined in the culture media. Values are means ± SEM. N=2-4. No significant differences from control ($p<0.05$).

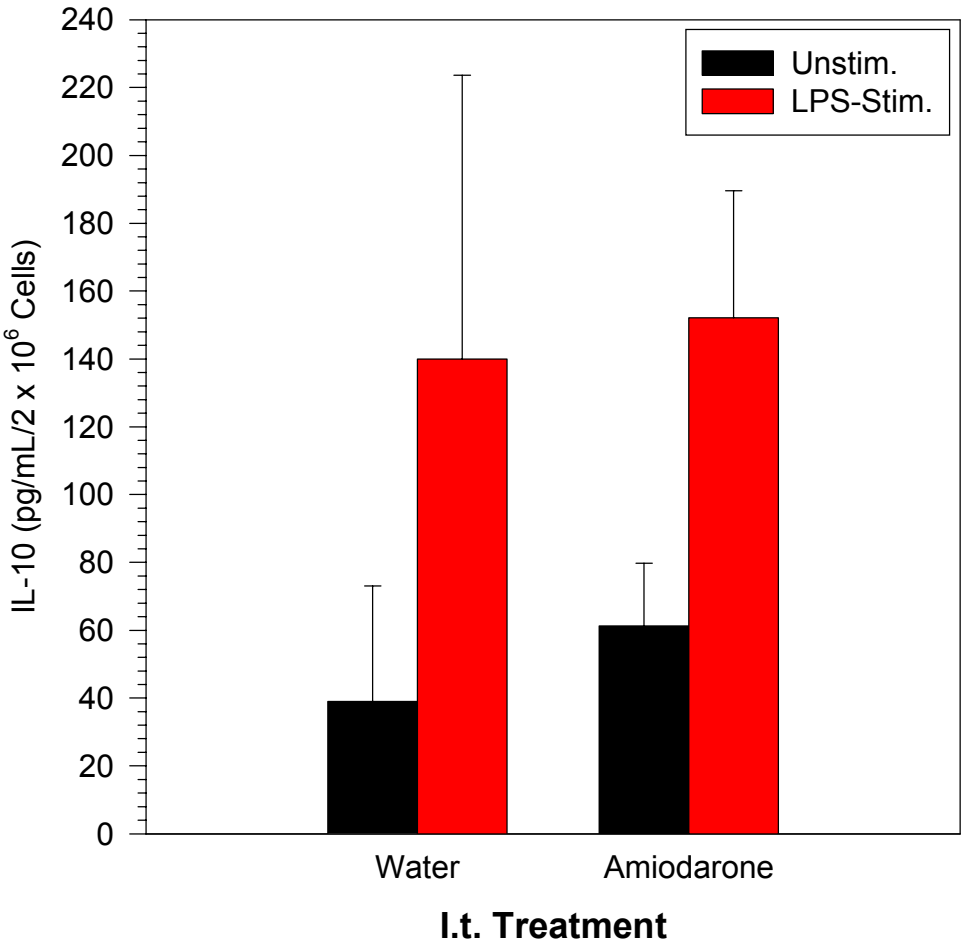

Figure 33A: IL-10 production from BAL cells recovered by lavage 15 minutes following i.t. instillation of amiodarone or vehicle and cultured 24 hours. Rats were given a single i.t. dose of AD (6.25 mg/kg) or sterile water and subjected to BAL 15 minutes later. BAL cells were then cultured 24 hours with and without LPS. IL-10 levels were determined in the culture media. Values are means ± SEM. N=2-4. No significant differences from control ($p<0.05$).

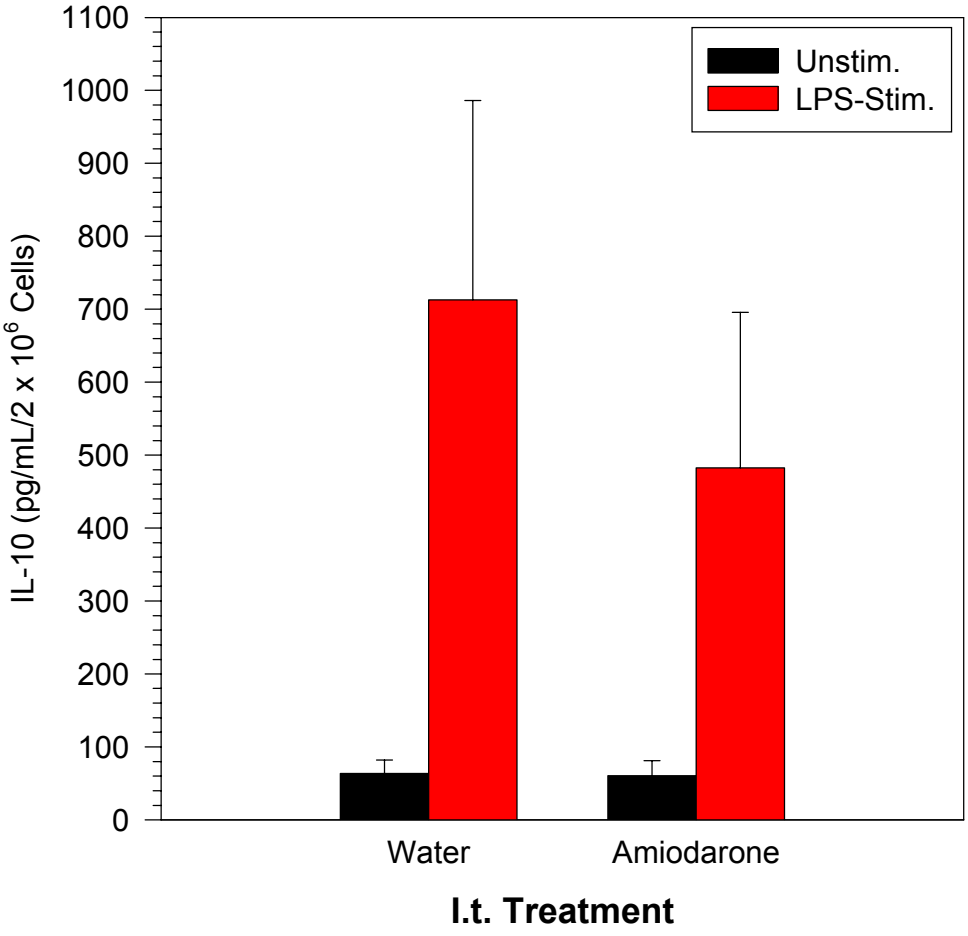

Figure 33B: IL-10 production from BAL cells recovered by lavage on day 3 following i.t. instillation of amiodarone or vehicle and cultured 24 hours. Rats were given i.t. AD (6.25 mg/kg) or sterile water on days 0 and 2 and subjected to BAL on day 3. BAL cells were then cultured 24 hours with and without LPS. IL-10 levels were determined in the culture media. Values are means ± SEM. N=2-4. No significant differences from control ($p<0.05$).

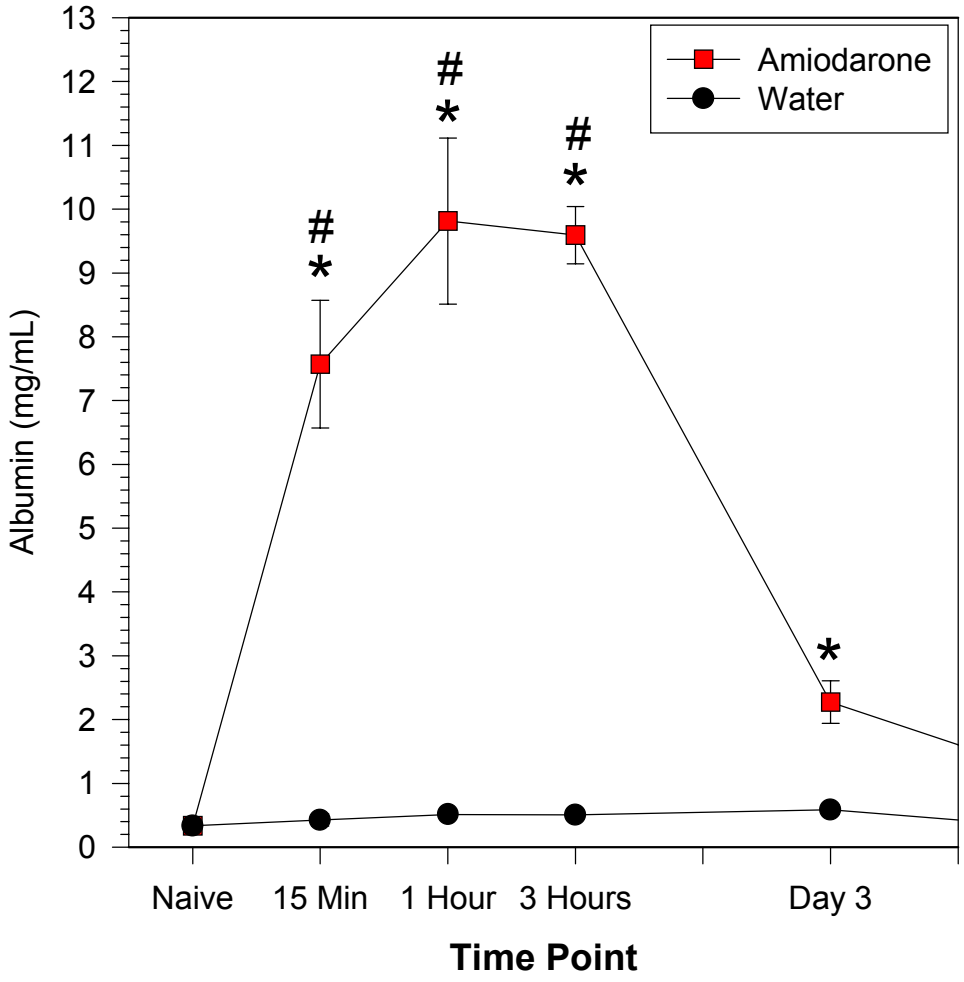

Figure 34: Albumin in the first BAL fraction at various time-points following intratracheal amiodarone or vehicle treatment. Rats were either given a single i.t. dose of AD (6.25 mg/kg) or sterile water and subjected to BAL after 15 minutes, 1 hour, or 3 hours, or were given i.t. doses of AD or water on days 0 and 2 and subjected to BAL on day 3. Albumin was measured in the first BAL fraction. Naïve values are represented at day 0. Values are mean ± SEM. N=5-9. *Significantly different from control ($p<0.05$). #Significantly different than AD-treated day 3 level ($p<0.05$).

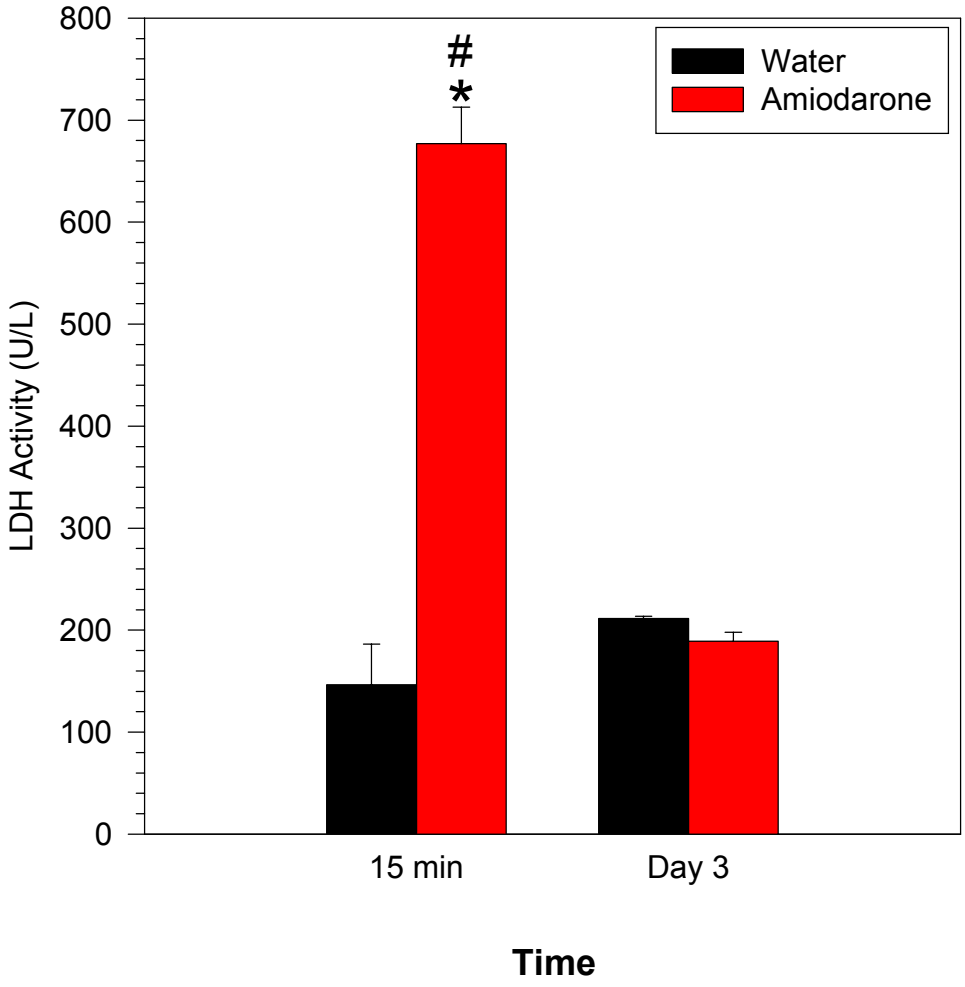

Figure 35: LDH Activity in the first BAL fraction at two time-points following intratracheal amiodarone or vehicle treatment. Rats were either given a single i.t. dose of AD (6.25 mg/kg) or sterile water and subjected to BAL after 15 minutes or given i.t. doses of AD or water on days 0 and 2 and subjected to BAL on day 3. LDH activity was measured in the first BAL fraction. Values are mean ± SEM. N=5-6. *Significantly different from control ($p<0.05$). #Significantly different than AD-treated day 3 level ($p<0.05$).

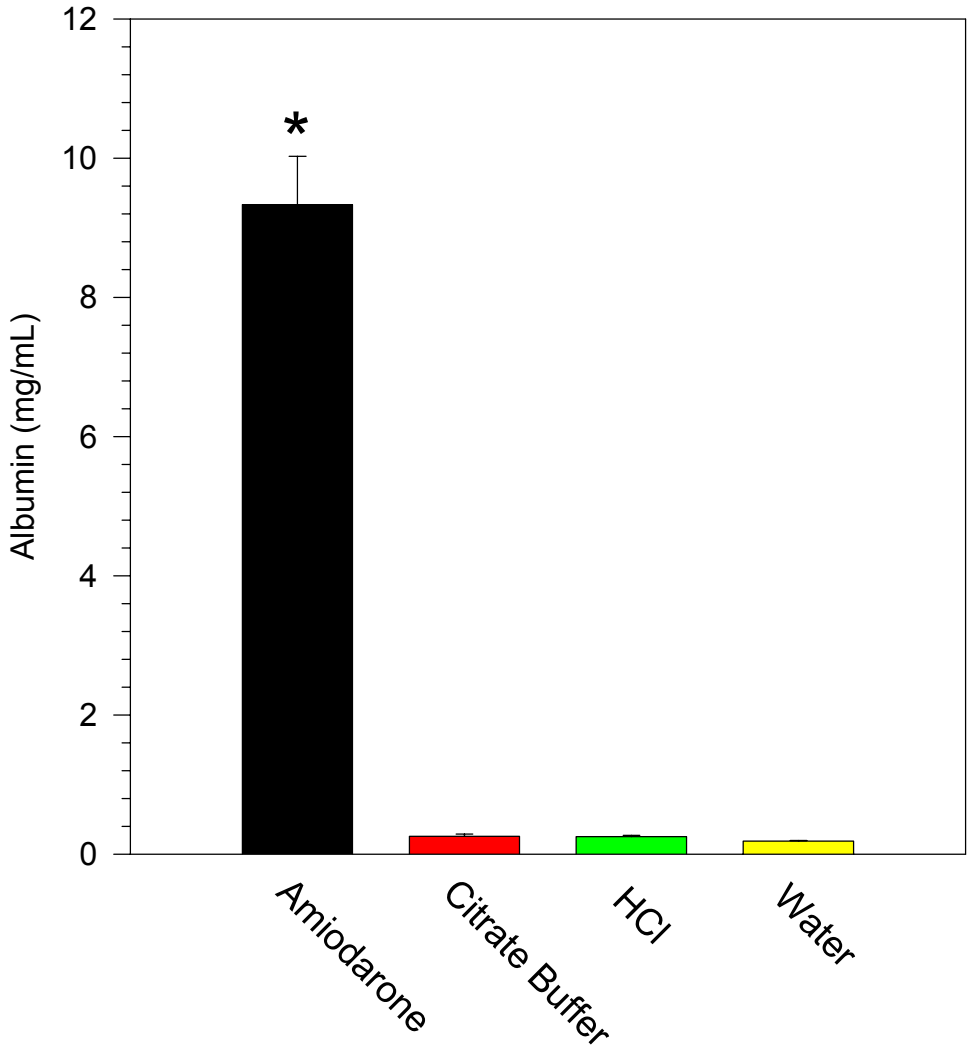

Figure 36A: Effect of AD, citrate buffer, or HCl on albumin in the first BAL fraction at 15 min. Rats were instilled intratracheally with AD (6.25 mg/kg) or an equivalent volume of citrate buffer (pH 3.7; equal to AD solution), HCl (equimolar concentration to AD-HCl), or sterile water and albumin was measured in the first BAL fraction. Values are means ± SEM. N=4-5. *Significantly different from water ($p<0.05$).

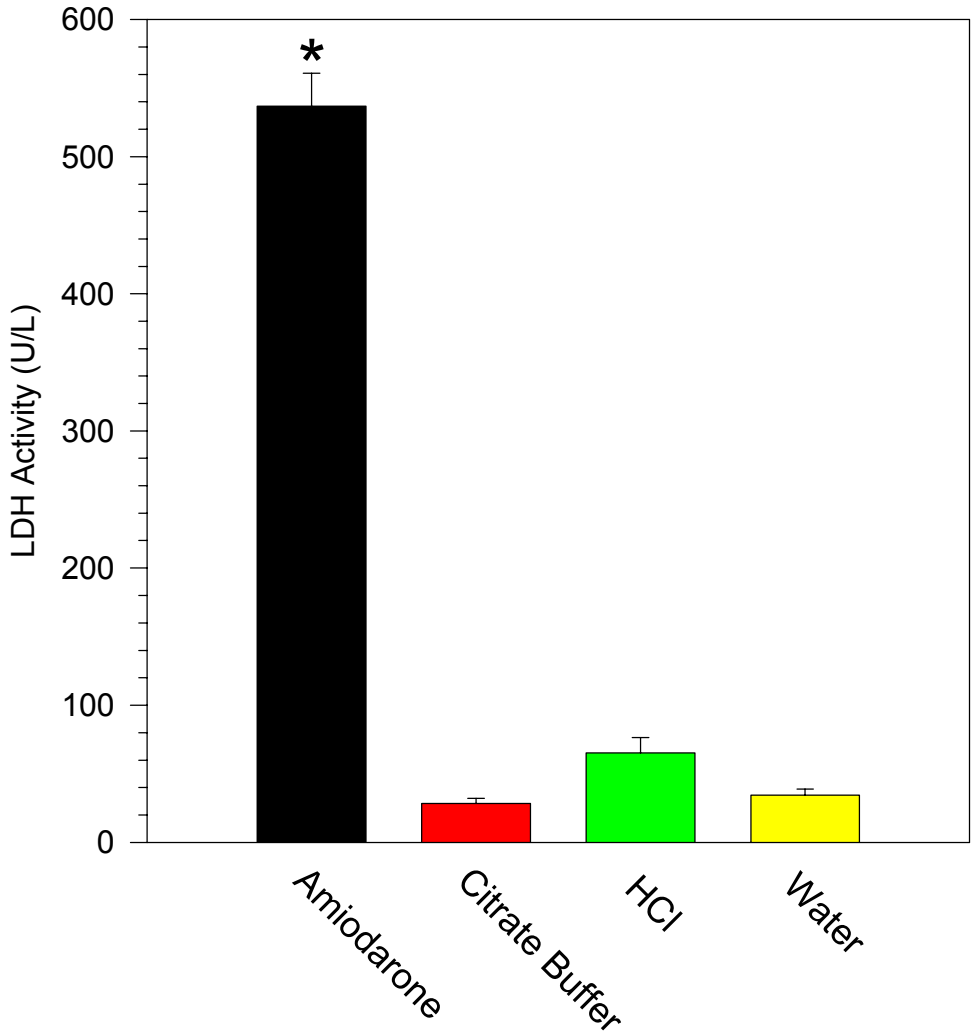

Figure 36B: Effect of AD, citrate buffer, or HCl on LDH activity in the first BAL fraction at 15 min. Rats were instilled intratracheally with AD (6.25 mg/kg) or an equivalent volume of citrate buffer (pH 3.7; equal to AD solution), HCl (equimolar concentration to AD-HCl), or sterile water and LDH activity was measured in the first BAL fraction. Values are means ± SEM. N=3-5. *Significantly different from water ($p<0.05$).

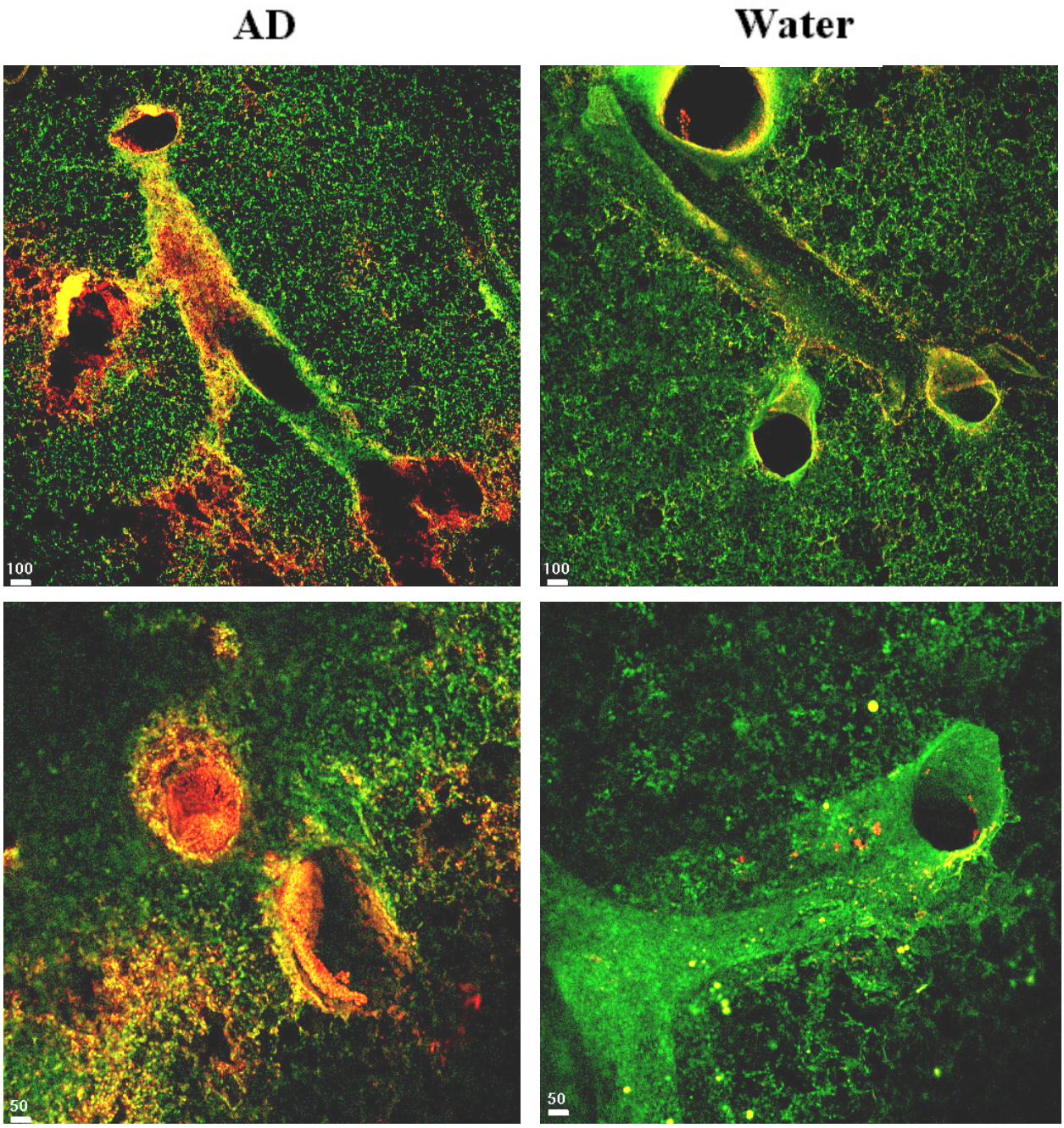

Figure 37A: Representative images obtained by LSCM of the effect of AD on cellular viability *in situ* at 15 min. Rats were given a single i.t. dose of AD (6.25 mg/kg) or sterile water and in situ viability was examined in lung tissue with LSCM at 15 min. Cells that have lost membrane integrity stain ethidium-positive and are displayed as red. Cells that have not taken up ethidium are stained green with Yo-Pro-1. Cells with both stains present may appear yellow and are also ethidium-positive. Scale bars indicate size in μm.

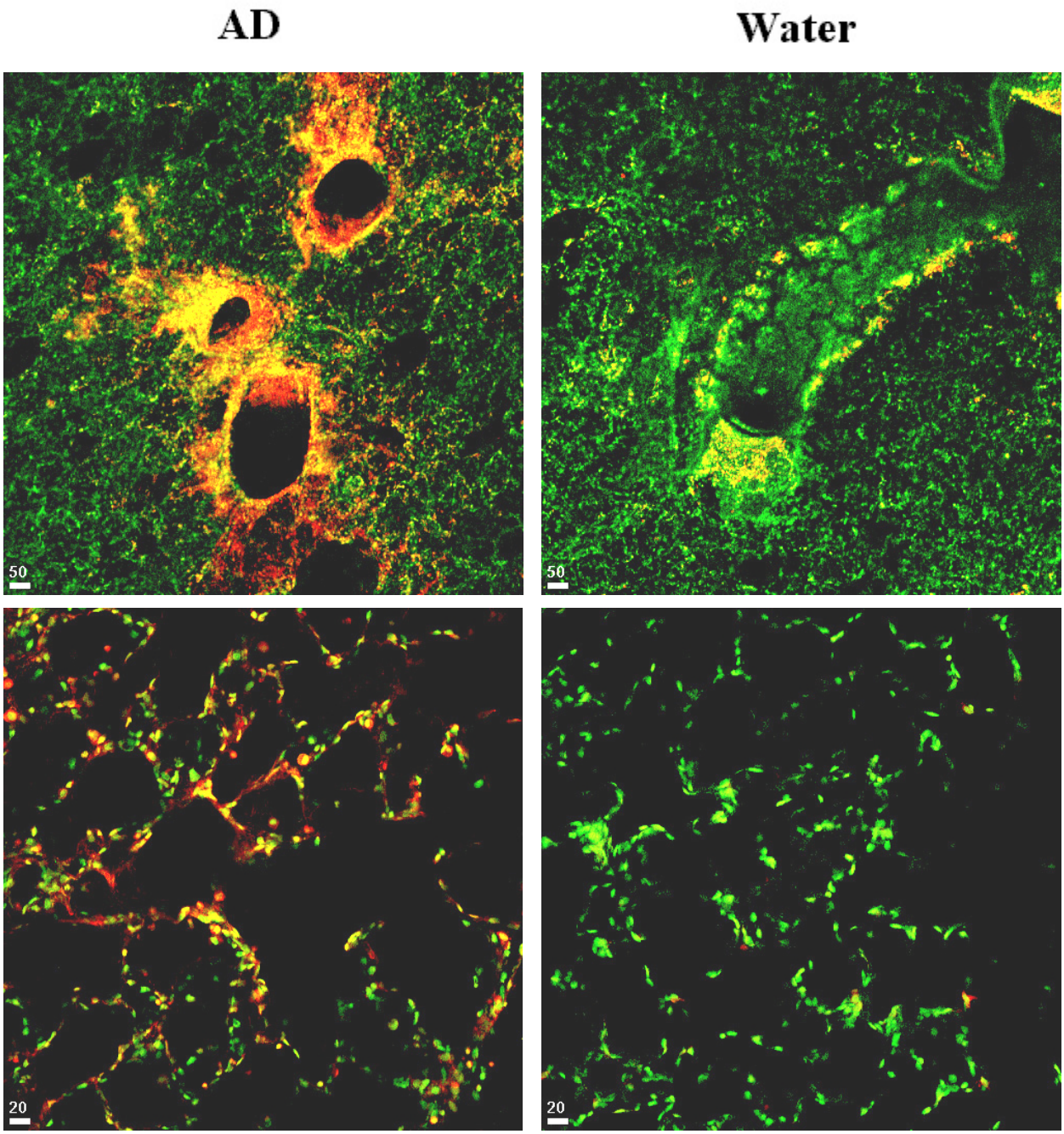

Figure 37B: Representative images obtained by LSCM of the effect of AD on cellular viability *in situ* at 3 hours. Rats were given a single i.t. dose of AD (6.25 mg/kg) or sterile water and in situ viability was examined in lung tissue with LSCM at 3 hours. Cells that have lost membrane integrity stain ethidium-positive and are displayed as red. Cells that have not taken up ethidium are stained green with Yo-Pro-1. Cells with both stains present may appear yellow and are also ethidium-positive. Scale bars indicate size in μm.

AD

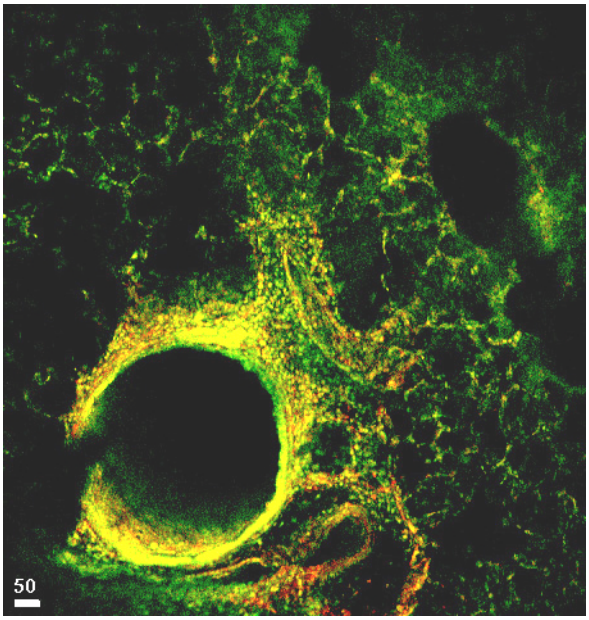

Water

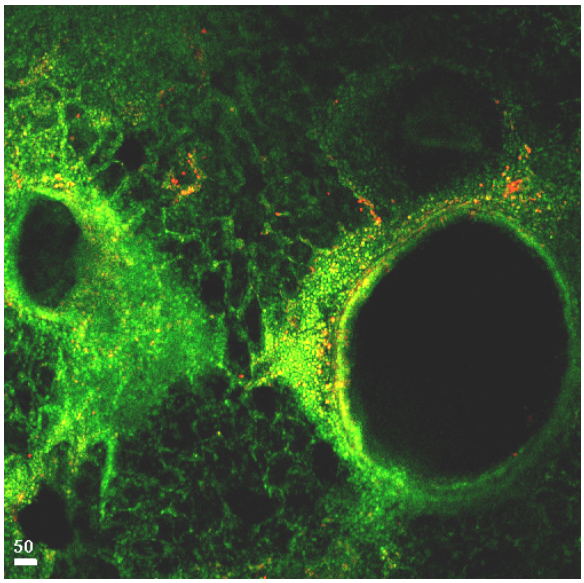

Figure 37C: Representative images obtained by LSCM of the effect of AD on cellular viability *in situ* at day 3. Rats were given i.t. AD (6.25 mg/kg) or sterile water on days 0 and 2 and in situ viability was examined in lung tissue with LSCM at day 3. Cells that have lost membrane integrity stain ethidium-positive and are displayed as red. Cells that have not taken up ethidium are stained green with Yo-Pro-1. Cells with both stains present may appear yellow and are also ethidium-positive. Scale bars indicate size in μm.

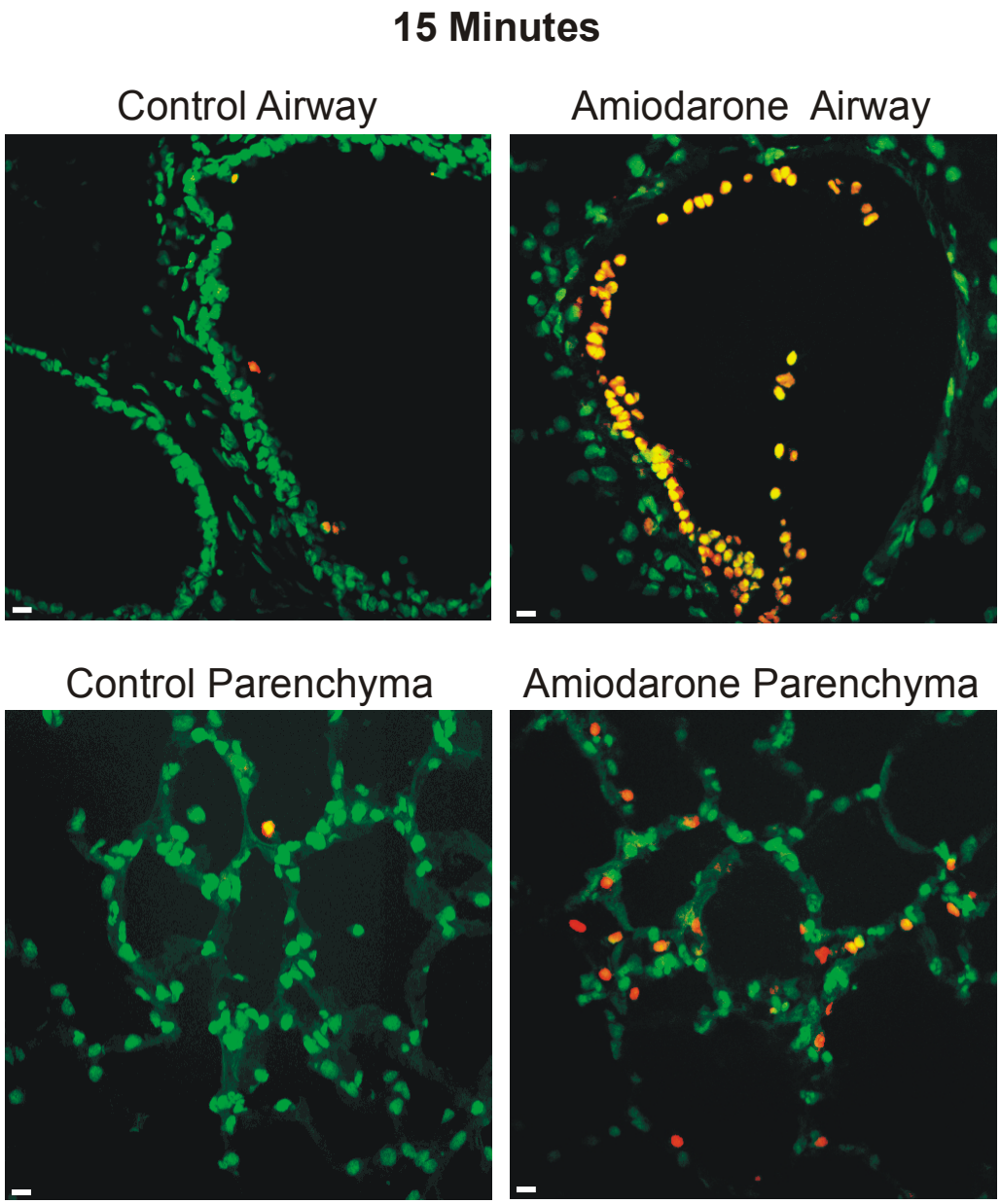

Figure 38: Representative micrographs of thin sections obtained by LSCM for *in situ* quantification of the effect of AD on cellular viability at 15 min. Rats were instilled intratracheally with AD (6.25 mg/kg) or sterile water and *in situ* cellular viability was determined at 15 min. Cells that have lost membrane integrity stain ethidium-positive and are displayed as red. Cells that have not taken up ethidium are stained green with Yo-Pro-1. Cells with both stains may appear yellow and are also ethidium-positive.

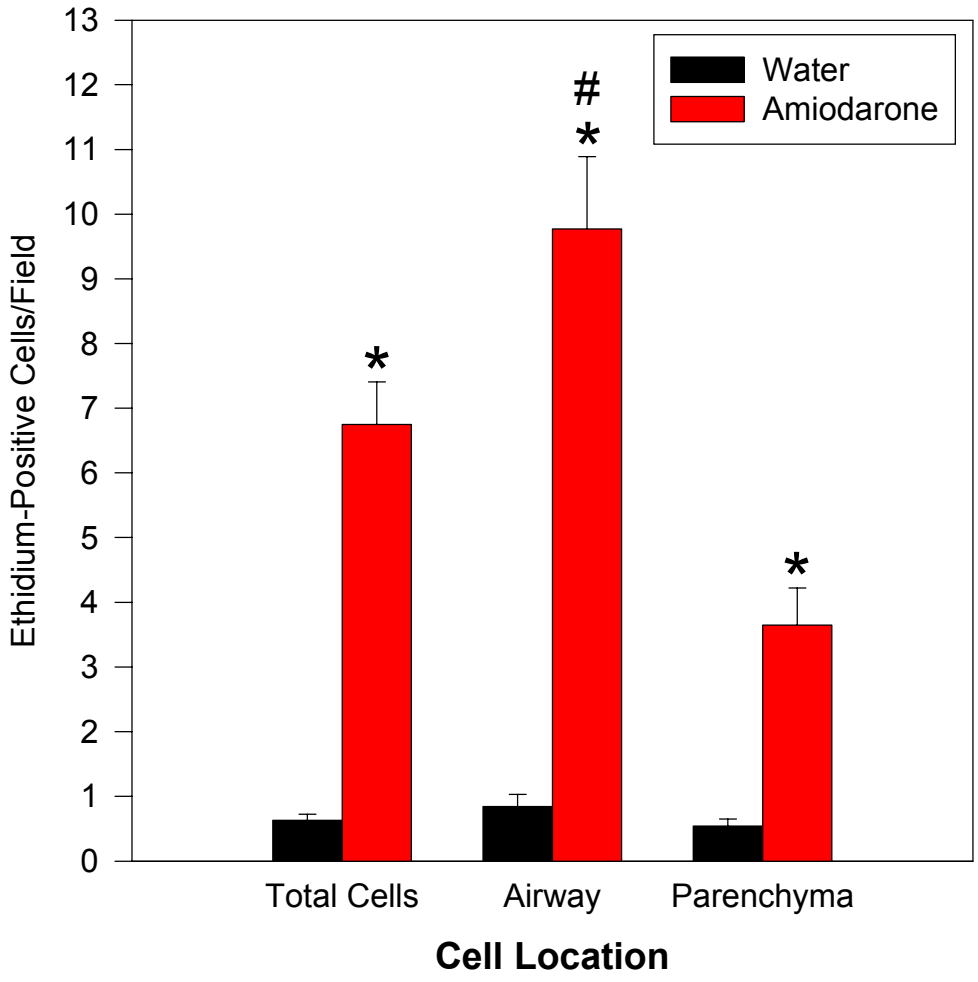

Figure 39A: Effect of AD on ethidium staining of airway and parenchymal cells at 15 min. Rats were instilled with i.t. AD (6.25 mg/kg) or sterile water and the number and location of ethidium-positive cells/field was determined. Values are means ± SEM. N=200-250 fields per treatment group. *Significantly different from water ($p<0.05$). #Significantly different from AD parenchyma ($p<0.05$).

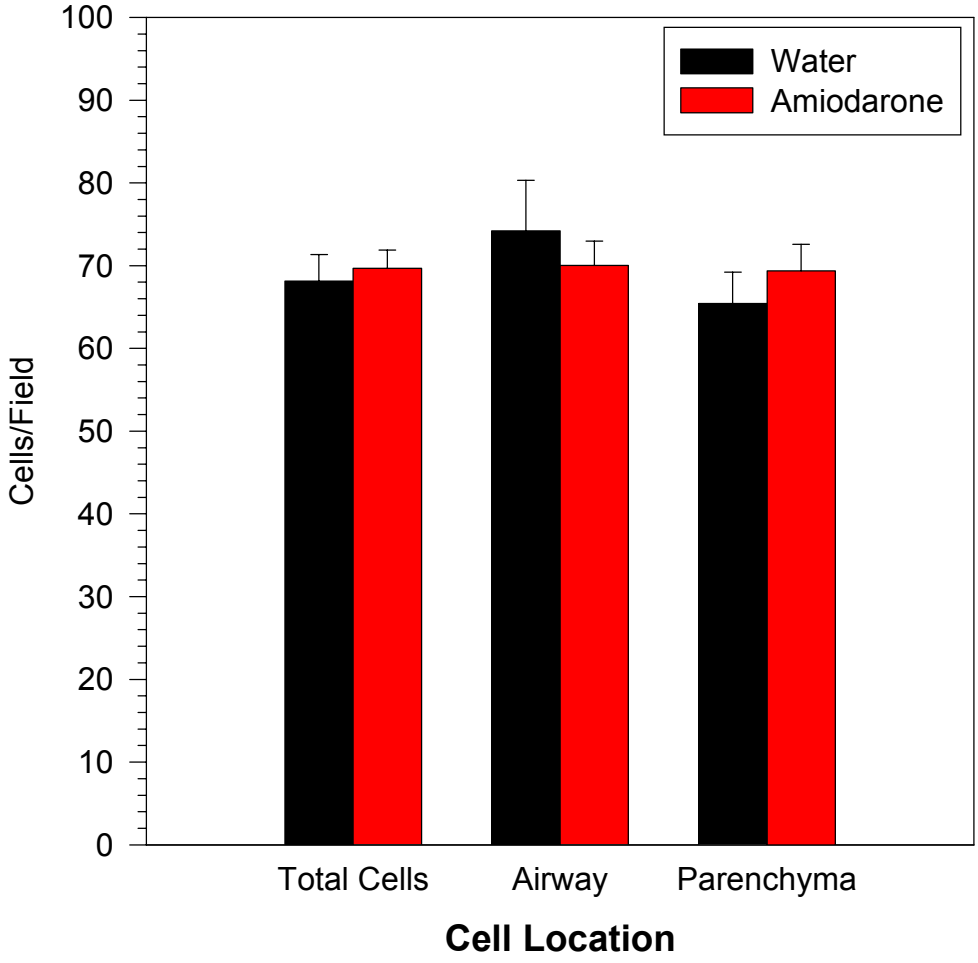

Figure 39B: Overall total cells, total airway cells, and total parenchymal cells per field at 15 min. Rats were instilled with i.t. AD (6.25 mg/kg) or sterile water and the number and location of total (ethidium-positive and Yo-Pro-1-positive) cells/field was determined. Values are means ± SEM. N=200-250 fields per treatment group. No significant differences were found ($p<0.05$).

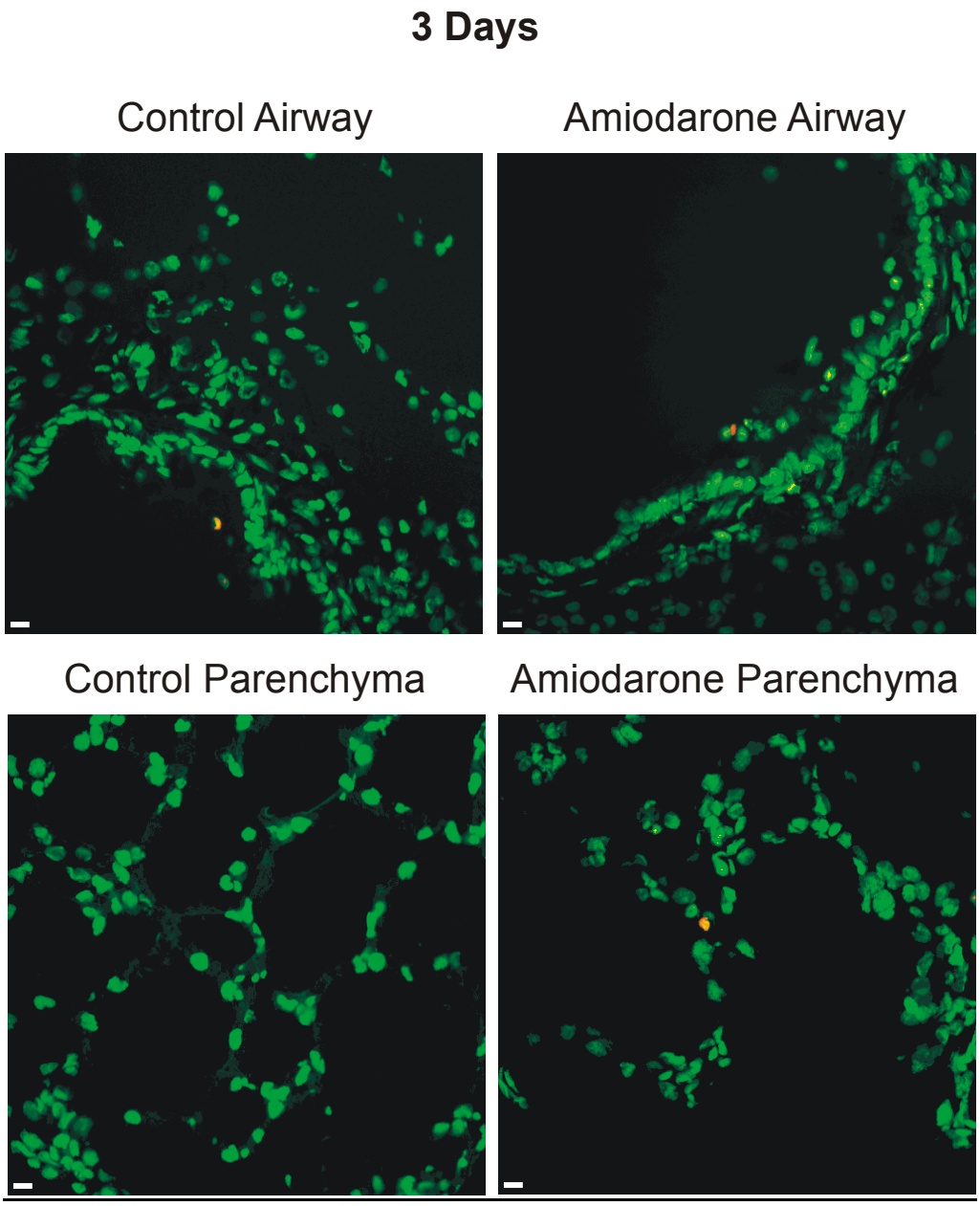

Figure 40: Representative micrographs of thin sections obtained by LSCM for *in situ* quantification of the effect of AD on cellular viability at day 3. Rats were instilled intratracheally with AD (6.25 mg/kg) or sterile water and on days 0 and 2 and *in situ* cellular viability was determined at day 3. Cells that have lost membrane integrity stain ethidium-positive and are displayed as red. Cells that have not taken up ethidium are stained green with Yo-Pro-1. Cells with both stains may appear yellow and are also ethidium-positive.

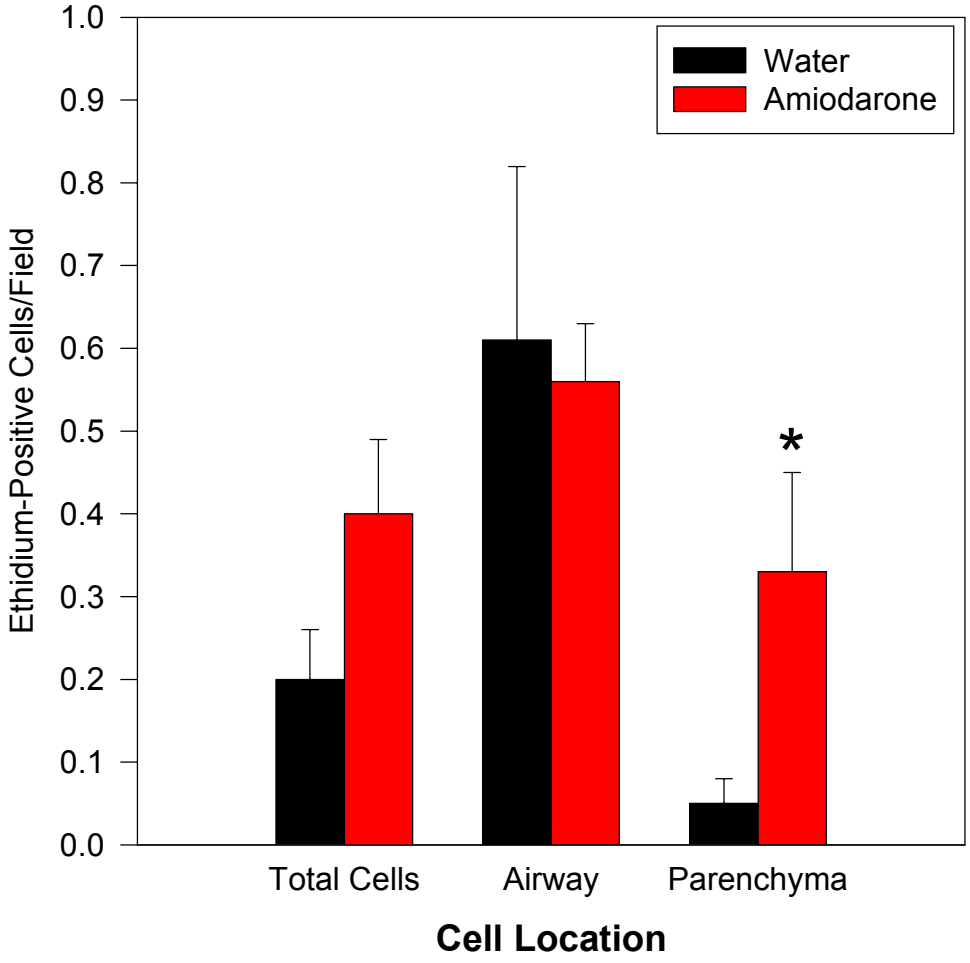

Figure 41A: Effect of AD on ethidium staining of airway and parenchymal cells at day 3. Rats were instilled with i.t. AD (6.25 mg/kg) or sterile water on days 0 and 2 and the number and location of ethidium-positive cells/field was determined. Values are means ± SEM. N=150-250 fields per treatment group. *Significantly different from water parenchyma ($p<0.05$).

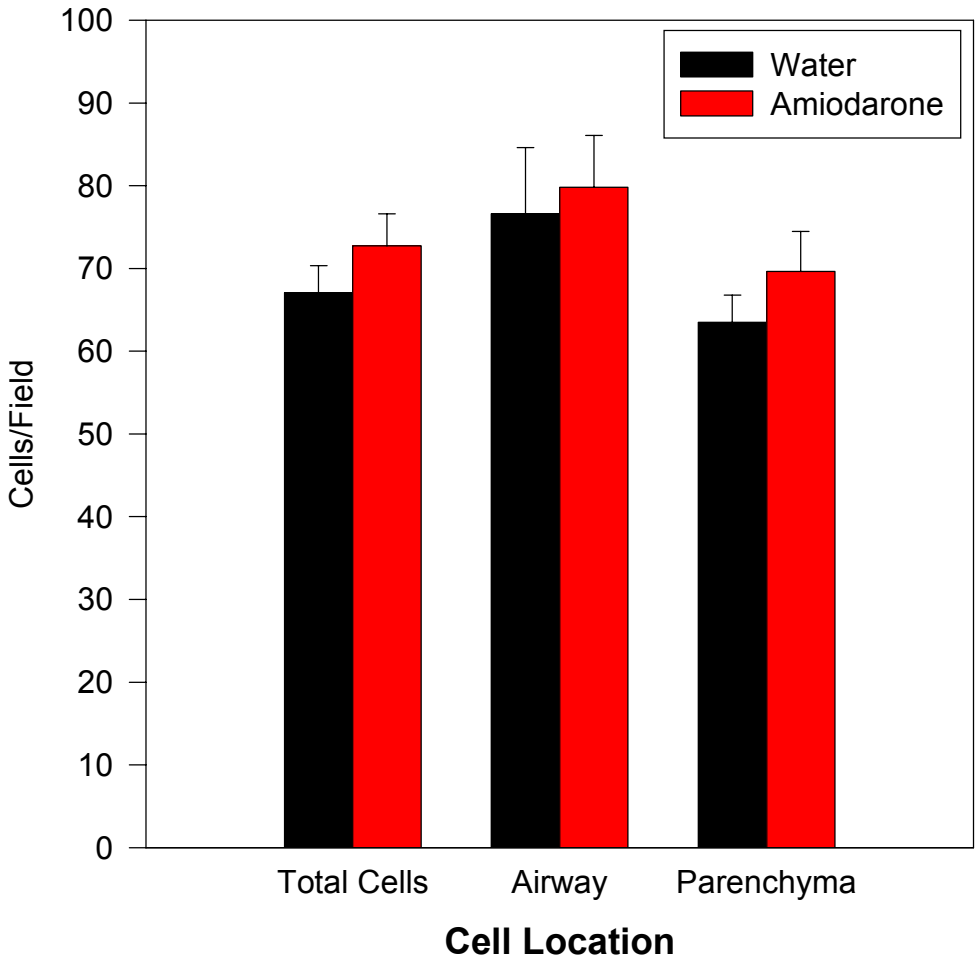

Figure 41B: Overall total cells, total airway cells, and total parenchymal cells per field at day 3. Rats were instilled with i.t. AD (6.25 mg/kg) or sterile water on days 0 and 2 and the number and location of total (ethidium-positive and Yo-Pro-1-positive) cells/field was determined. Values are means ± SEM. N=150-250 fields per treatment group. No significant differences were found ($p<0.05$).

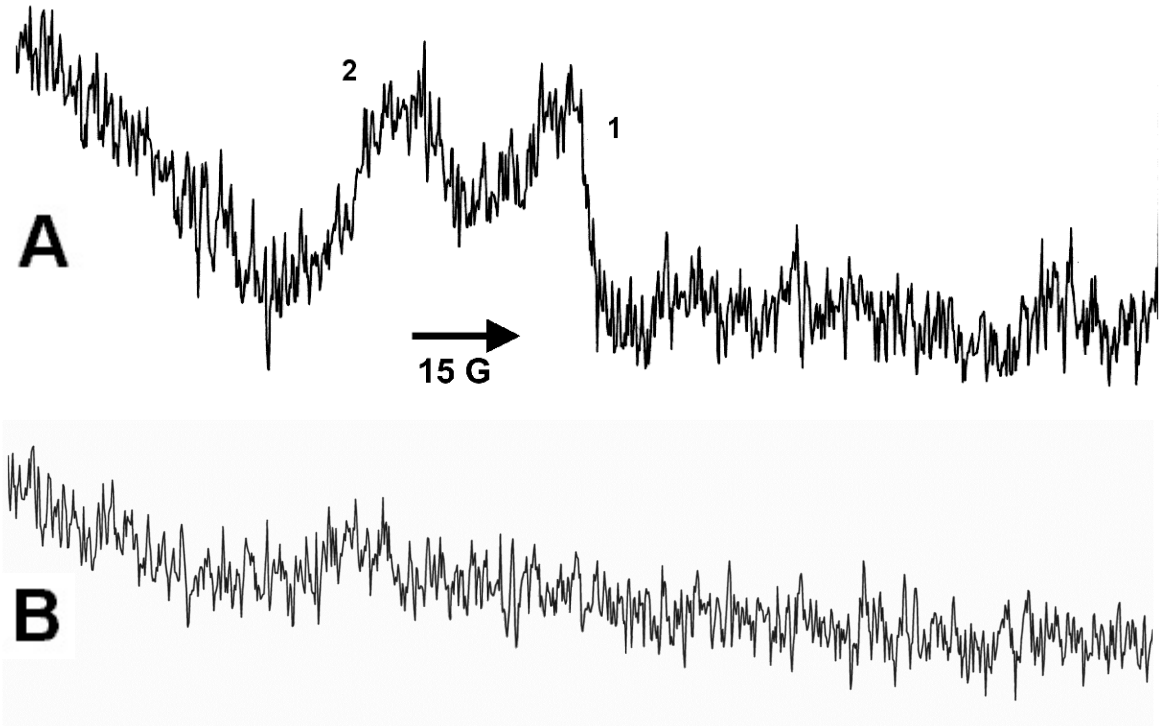

Figure 42: ESR spectra of AD solution without spin-trapping. A) AD (25 mg/mL) in water without DMPO showing the presence of a carbon-based radical (1) and an unknown radical (2). B) AD (100 mg/mL) in water without DMPO showing the elimination of radical signal with increased AD concentration. Arrow indicates 15 Gauss width and direction of scanning.

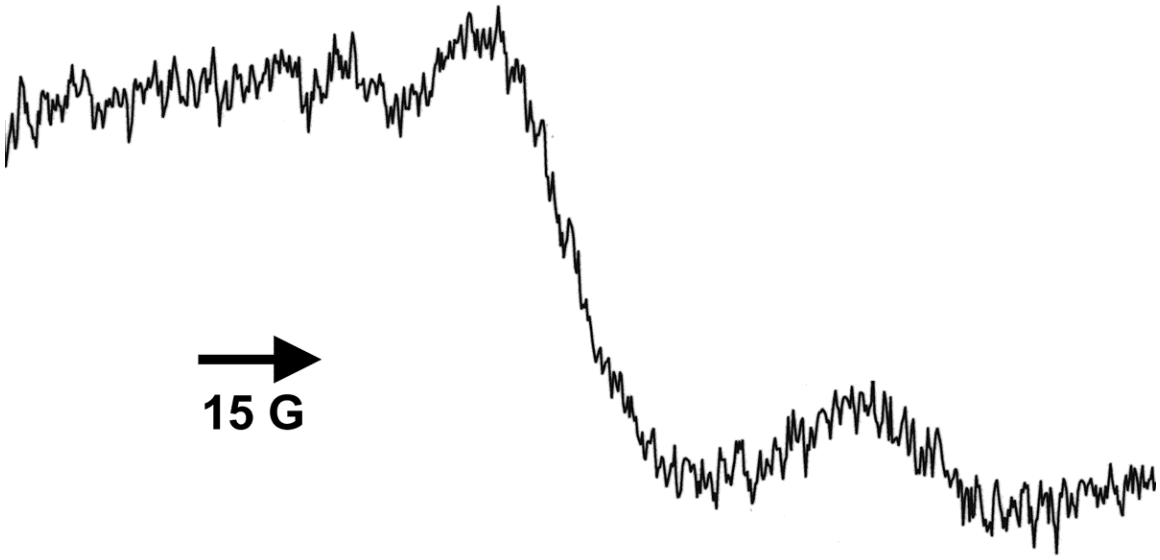

Figure 43: ESR spectrum of AD powder. Spectra of dry AD powder showing the presence of a carbon-based radical. Arrow indicates 15 Gauss width and direction of scanning.

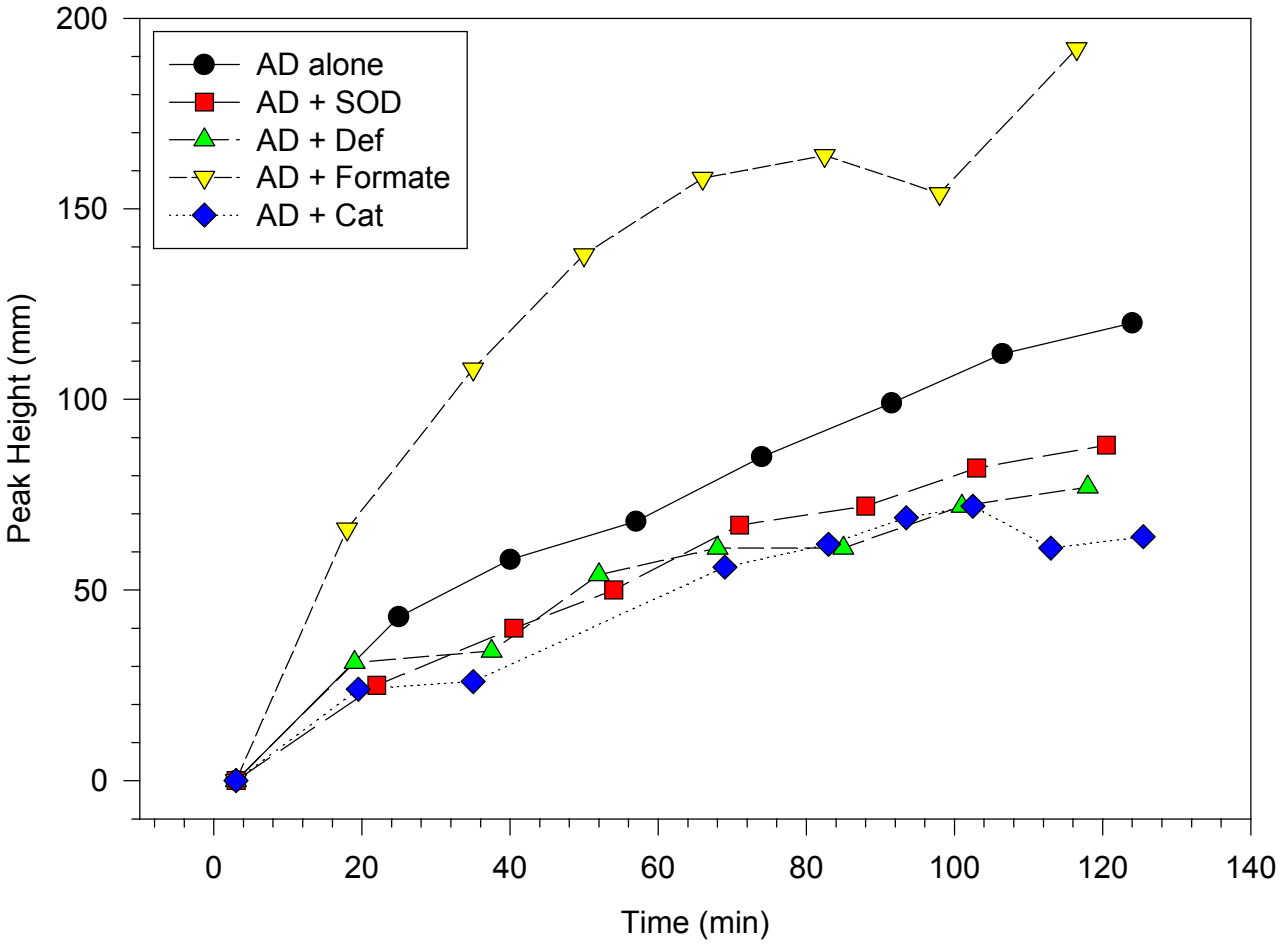

Figure 44: Time course of AD-induced DMPO peak formation in water; effects of inhibitors and exogenous chemicals. DMPO was added to AD (3.125 mg/mL) in water to trap hydroxyl radicals with and without inhibitors and exogenous chemicals. The samples were analyzed at various time-points with ESR, and the two center peaks (doublets) of the hydroxyl-DMPO signal were measured and averaged for each spectrum. Inhibitors and chemicals (and final concentrations) used were: DMPO (.33 M); superoxide dismutase (SOD; 5 mg/mL); catalase (Cat; 5000 U/L); deferoxamine (Def; 20 mM); formate (500 mM).

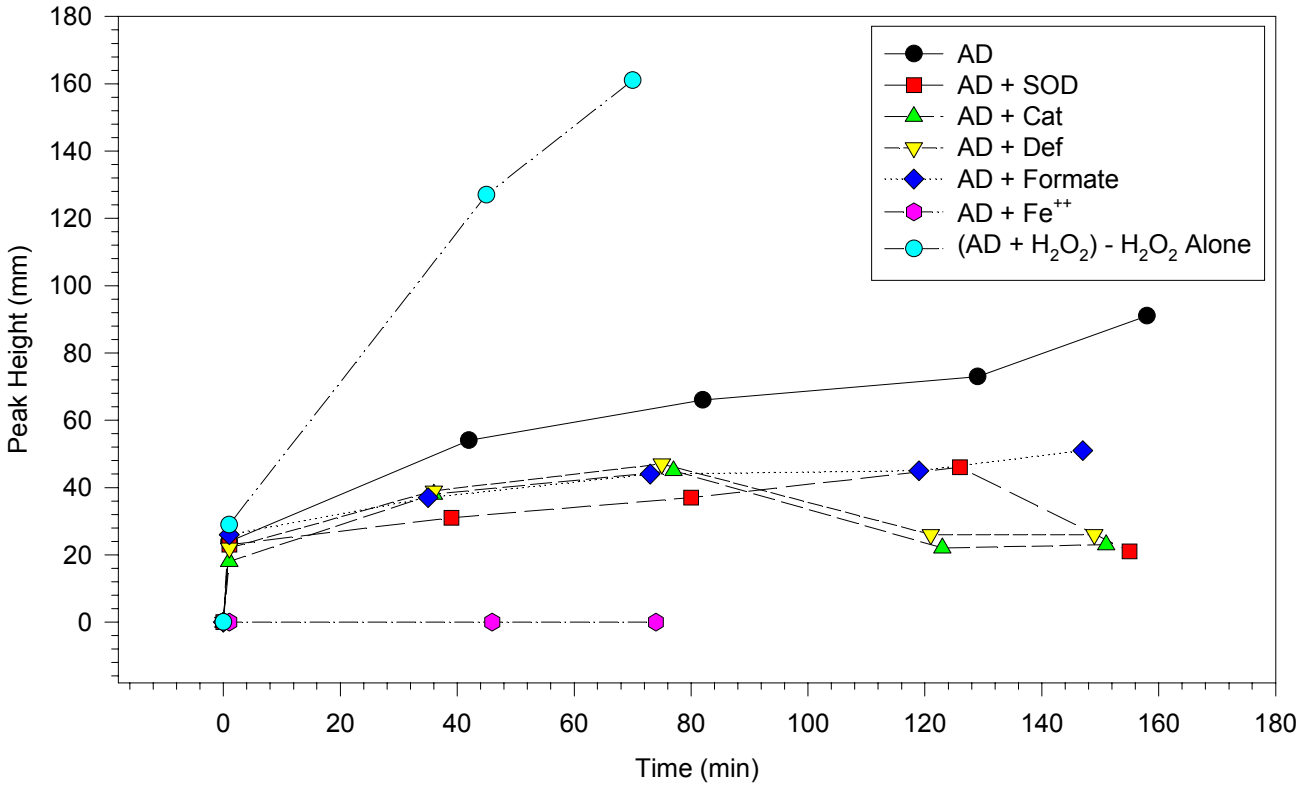

Figure 45A: Time course of AD-induced DMPO peak formation in PBS; effects of inhibitors and exogenous chemicals. DMPO was added to AD (3.125 mg/mL) in PBS to trap hydroxyl radicals with and without inhibitors and exogenous chemicals. The samples were analyzed at various time-points with ESR, and the two center peaks (doublets) of the hydroxyl-DMPO signal were measured and averaged for each spectrum. Inhibitors and chemicals (and final concentrations) used were: DMPO (.33 M); superoxide dismutase (SOD; 5 mg/mL); catalase (Cat; 5000 U/L); deferoxamine (Def; 20 mM); formate (500 mM); $FeSO_4$ (Fe^{++}; 1 mM); H_2O_2 (10 mM).

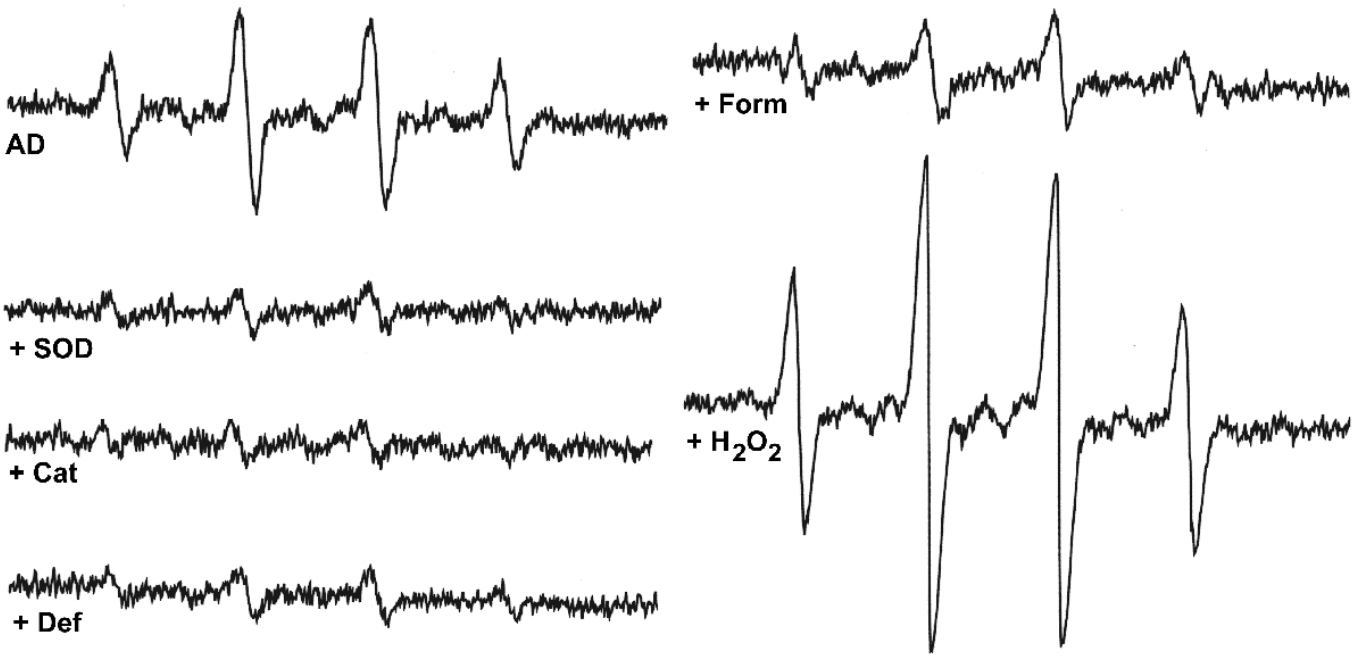

Figure 45B: Final spectra in the time course of AD-induced DMPO peak formation in PBS; effects of inhibitors and exogenous chemicals. DMPO was added to AD (3.125 mg/mL) in PBS to trap hydroxyl radicals with and without inhibitors and exogenous chemicals. The final spectrum of each sample is shown. Inhibitors and chemicals (and final concentrations) used were: DMPO (.33 M); superoxide dismutase (SOD; 5 mg/mL); catalase (Cat; 5000 U/L); deferoxamine (Def; 20 mM); formate (500 mM); H_2O_2 (10 mM).

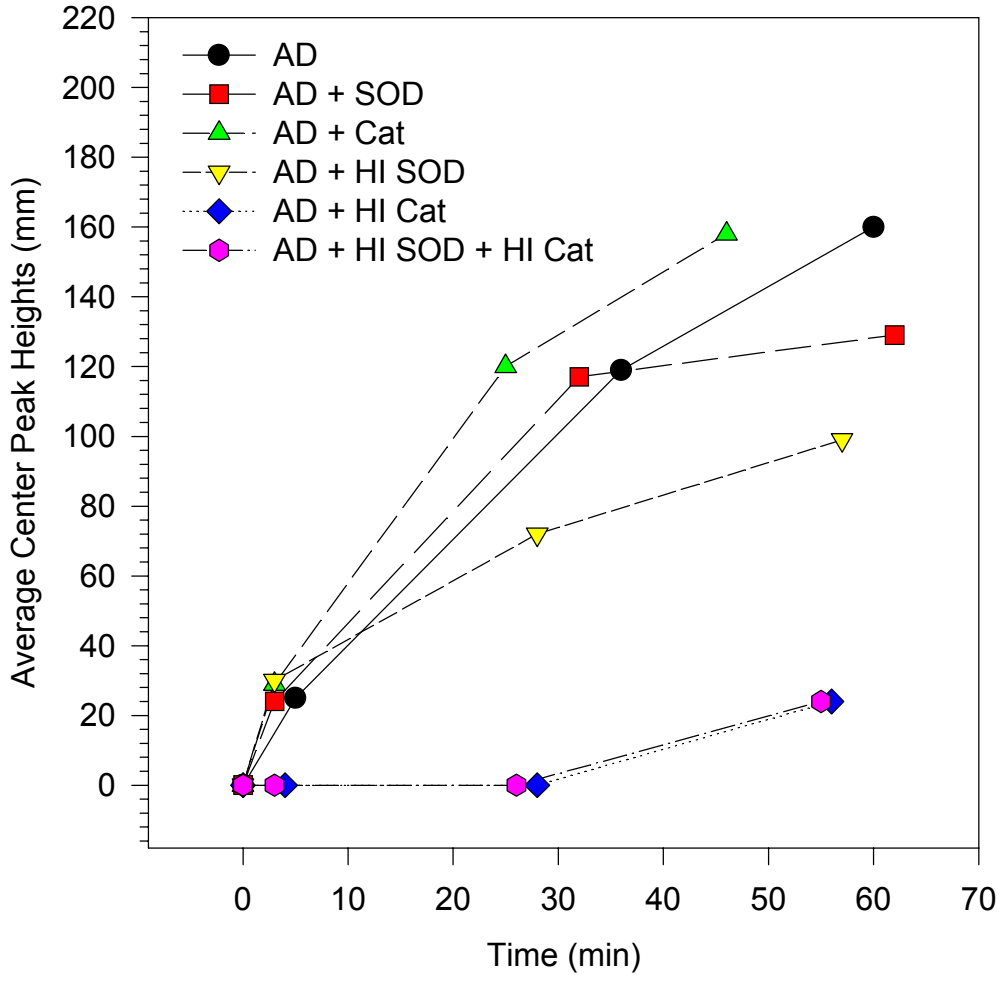

Figure 46: Time course of AD-induced DMPO peak formation in PBS; effect of heat-inactivation of inhibitor enzymes. DMPO was added to AD (3.125 mg/mL) in PBS to trap hydroxyl radicals with and without enzymes. The samples were analyzed at various time-points with ESR, and the two center peaks (doublets) of the hydroxyl-DMPO signal were measured and averaged for each spectrum. Enzymes indicated were heat-inactivated by being placed in a boiling water bath for 10-min. Enzymes (and final concentrations) used were: DMPO (.33 M); superoxide dismutase (SOD; 5 mg/mL); catalase (Cat; 5000 U/L); heat-inactivated SOD (HI SOD; 5 mg/mL); heat-inactivated Cat (HI Cat; 5000 U/L).

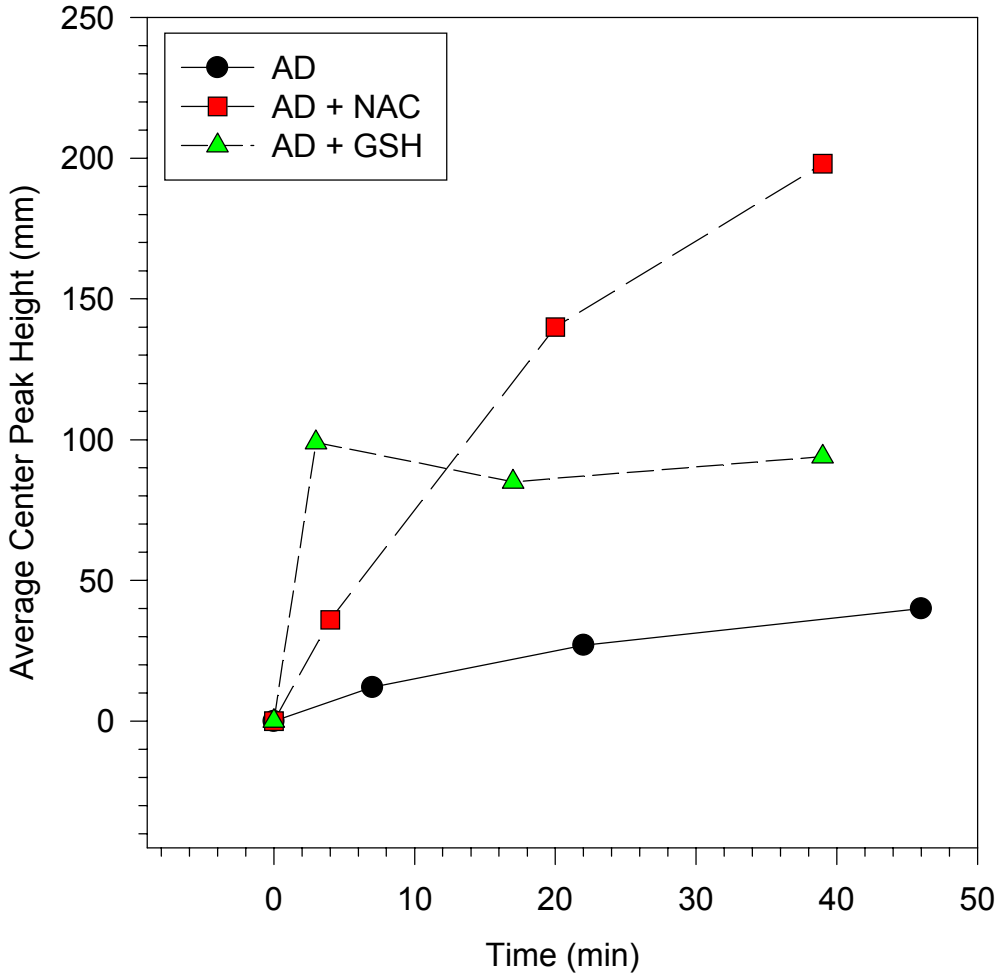

Figure 47: Time course of AD-induced DMPO peak formation in PBS; effects of thiol antioxidants. DMPO was added to AD (3.125 mg/mL; 4.5 mM) in PBS to trap hydroxyl radicals with and without thiol antioxidants. The samples were analyzed at various time-points with ESR, and the two center peaks (doublets) of the hydroxyl-DMPO signal were measured and averaged for each spectrum. Antioxidants and chemicals (and final concentrations) used were: DMPO (.33 M); *N*-acetyl cysteine (NAC; 9.0 mM); reduced glutathione (GSH; 9.0 mM).

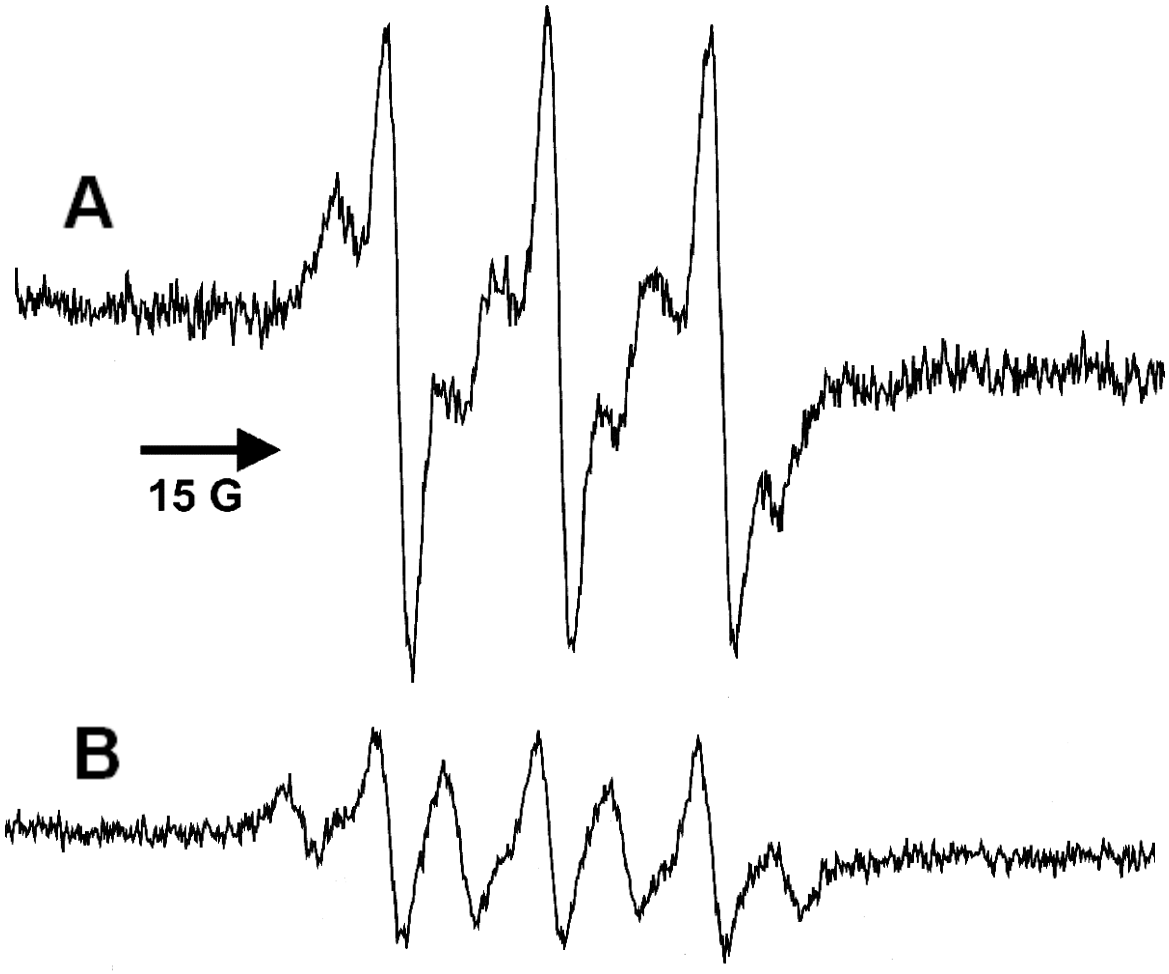

Figure 48: ESR spectra of AD solution in chloroform with spin-trapping at 3 min. A) AD (3.125 mg/mL) in chloroform with DMPO showing the presence an undetermined radical, presumably an AD radical. B) AD (3.125 mg/mL; 4.5 mM) in chloroform with NAC (9.0 mM) showing the presence of an *N*-acetyl cystyl radical splitting with the undetermined radical signal. Arrow indicates 15 Gauss width and direction of scanning.

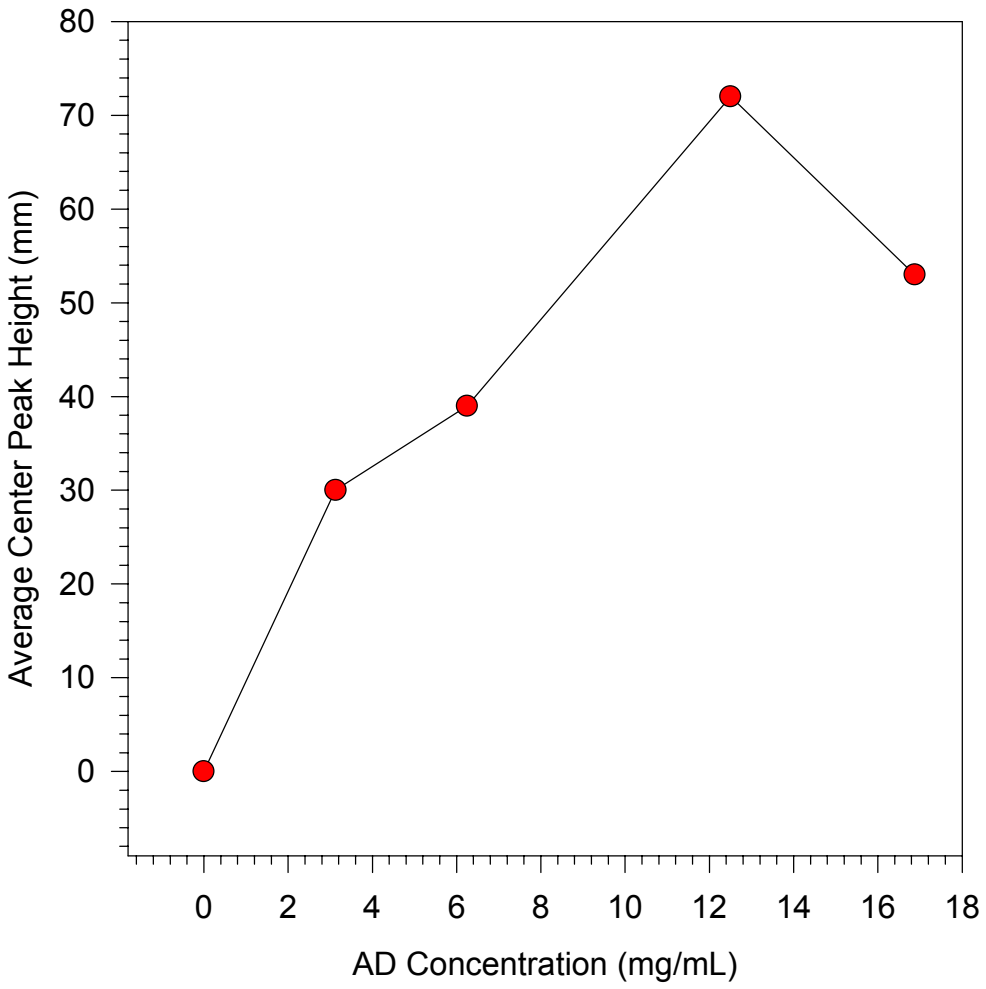

Figure 49: Effect of AD concentration on hydroxyl radical production at 30 min. AD at various concentrations was incubated with DMPO for 30 min before being analyzed by ESR. The two center peaks (doublets) of the hydroxyl-DMPO signal were measured and averaged for each spectrum.

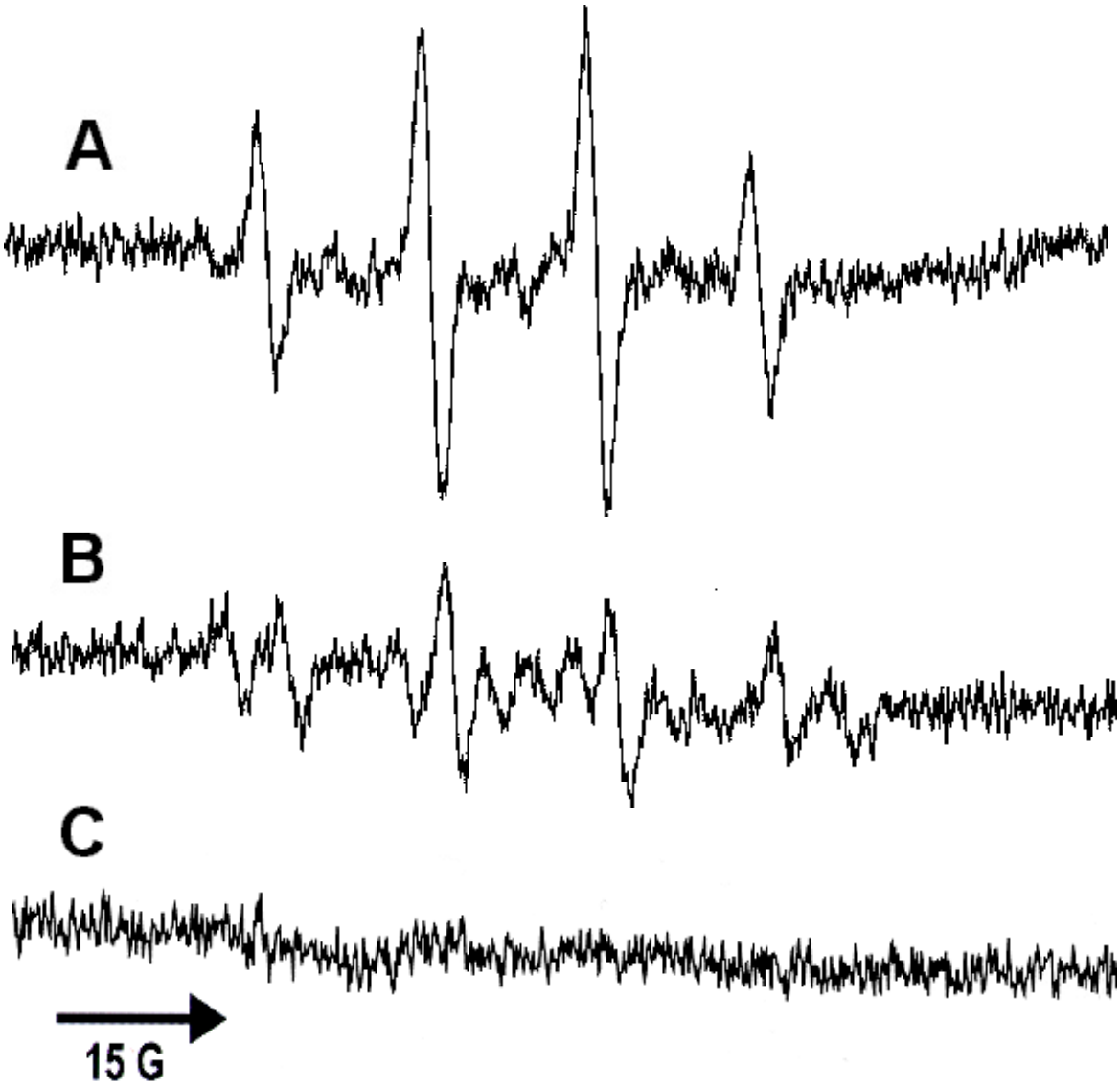

Figure 50: ESR spectra of AD solution in water with spin-trapping at 30 min.; effects of UV irradiation and antioxidants. A) AD (3.125 mg/mL) in water with DMPO at 30 min showing the presence of hydroxyl radical. B) AD (3.125 mg/mL) in water with DMPO at 30 min following UV irradiation during the first 10 min of incubation. C) AD (3.125 mg/mL; 4.5 mM) with DMPO, Trolox (45 mM), and ascorbate (22.5 mM) showing the elimination of radical signal. Arrow indicates 15 Gauss width and direction of scanning.

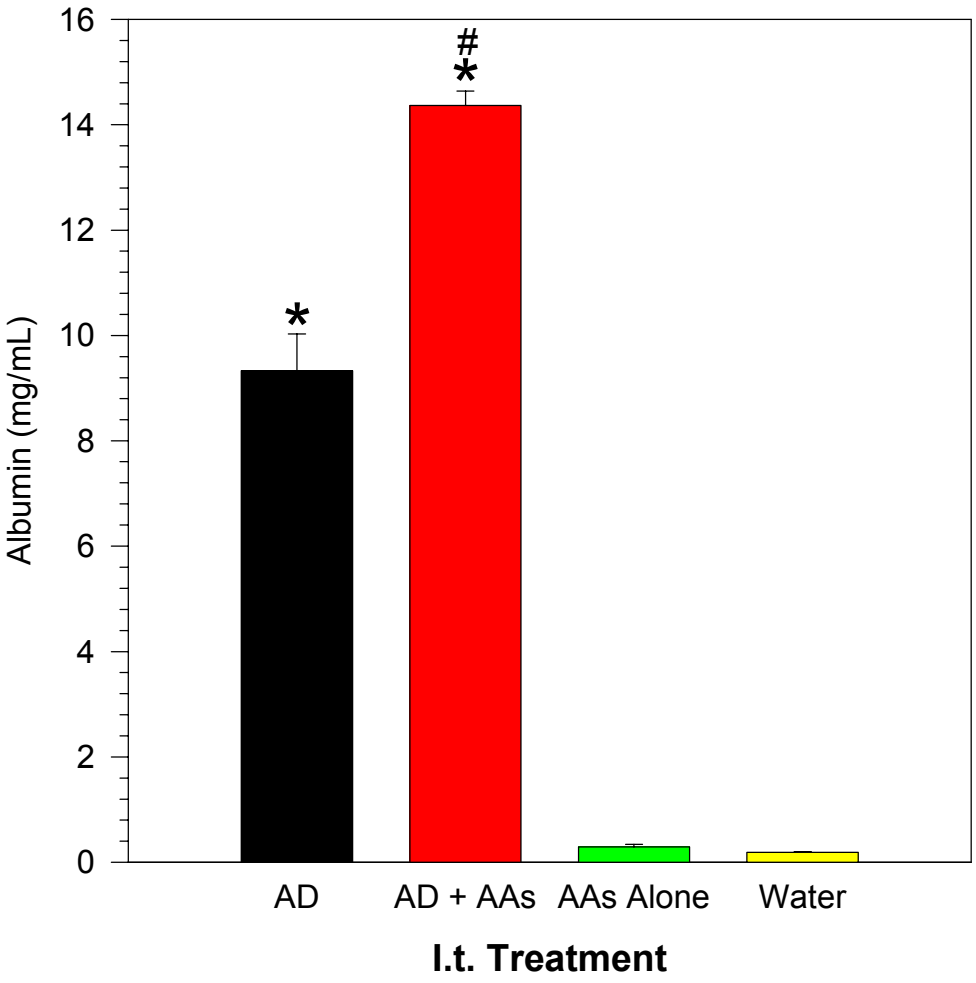

Figure 51A: Effect of AD with and without antioxidants on albumin in the first BAL fraction at 15 min. Rats were instilled intratracheally with AD (6.25 mg/kg) with or without antioxidants (AAs; Trolox [45 mM] and ascorbate [22.5 mM] in water) or an equivalent volume of the antioxidants alone or sterile water. Albumin was measured in the first BAL fraction at 15 min. Values are means ± SEM. N=4-6. *Significantly different from water ($p<0.05$). #Significantly different from AD.

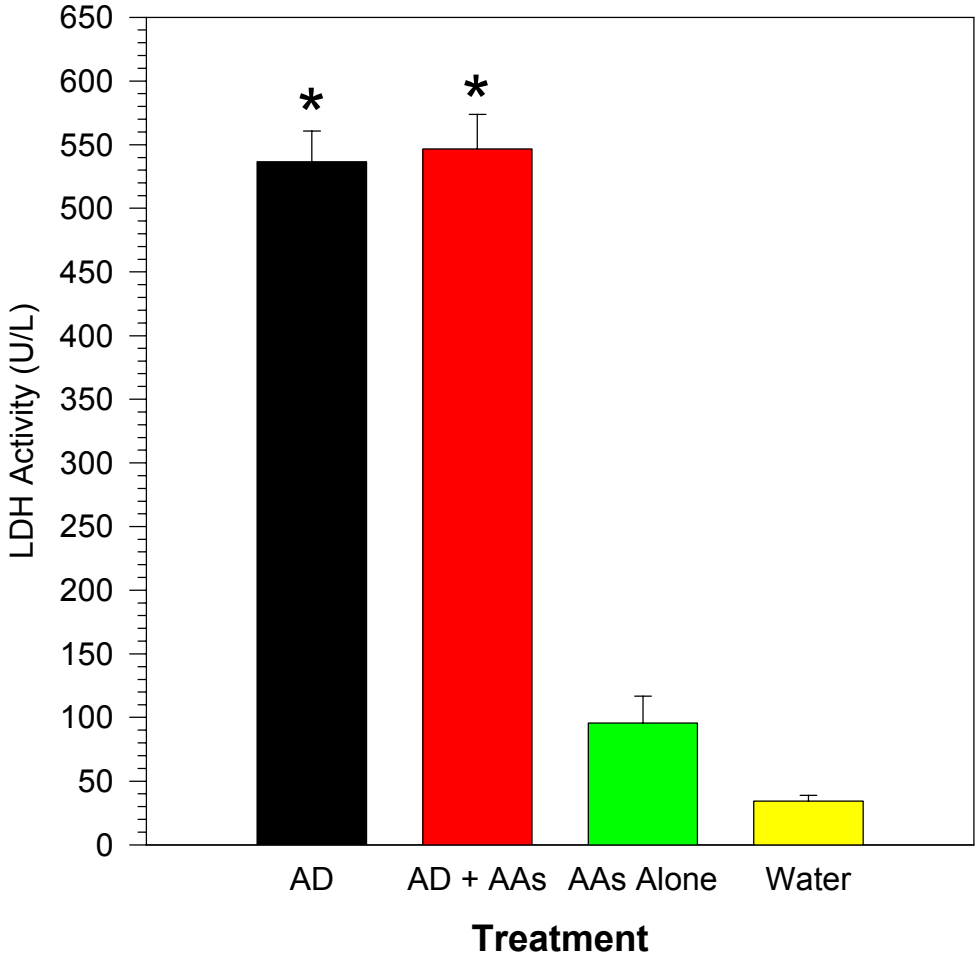

Figure 51B: Effect of AD with and without antioxidants on LDH activity in the first BAL fraction at 15 min. Rats were instilled intratracheally with AD (6.25 mg/kg) with or without antioxidants (AAs; Trolox [45 mM] and ascorbate [22.5 mM] in water) or an equivalent volume of the antioxidants alone or sterile water and LDH activity was measured in the first BAL fraction. Values are means ± SEM. N=4-6. *Significantly different from water ($p<0.05$).

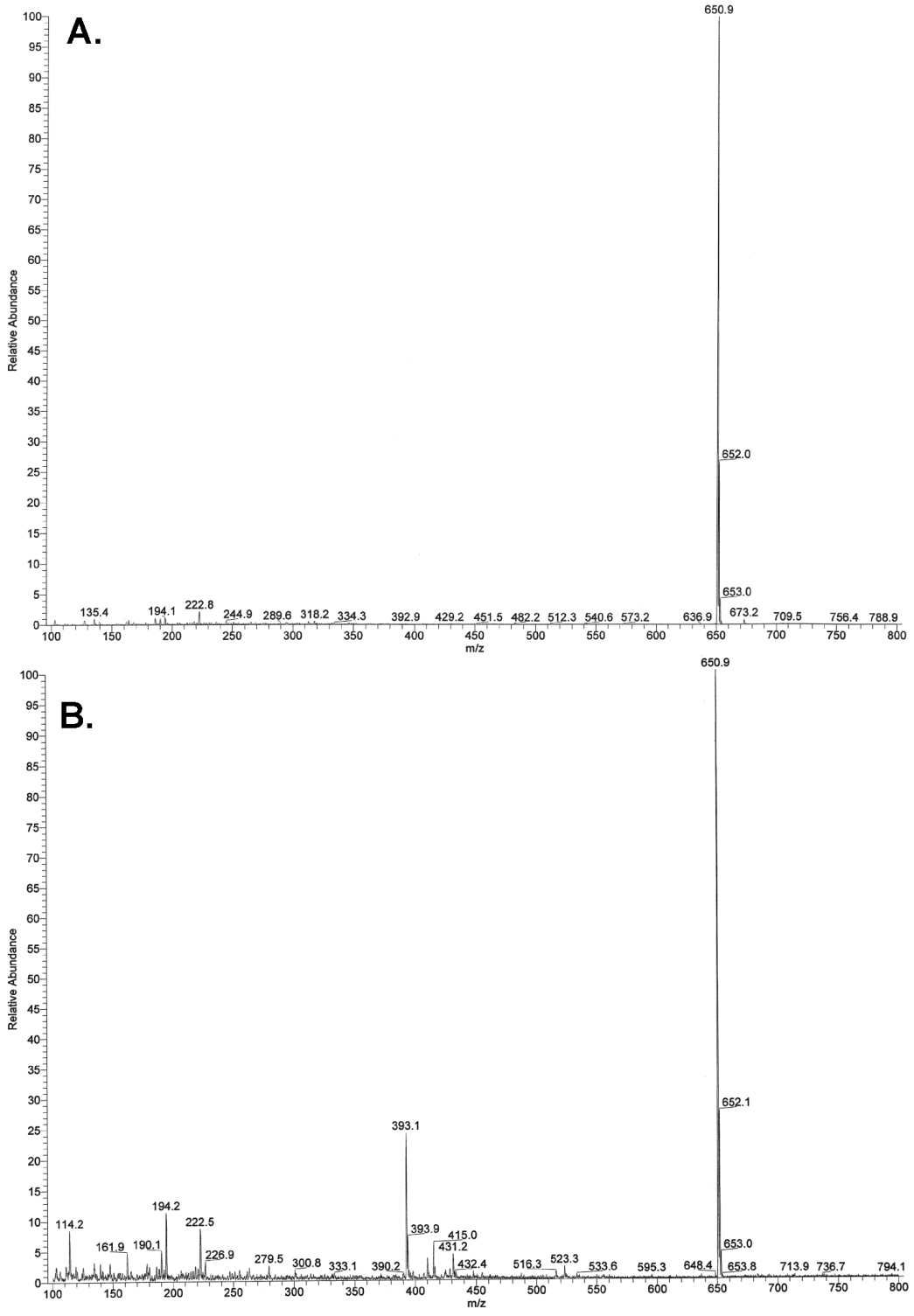

Figure 52A: Positive-ion electrospray mass spectra of AD in methanol and water. A) Spectrum of AD (4.5 µM diluted from 4.5 mM) dissolved in methanol showing parent-compound peaks. B) Spectrum of AD (4.5 µM diluted from 4.5 mM) dissolved in water showing parent compound peaks and peak(s) of possible breakdown products. No evidence for a mono-deiodination of AD [~518 Da] is shown, but a possible di-deiodinated AD [~393 Da] is shown.

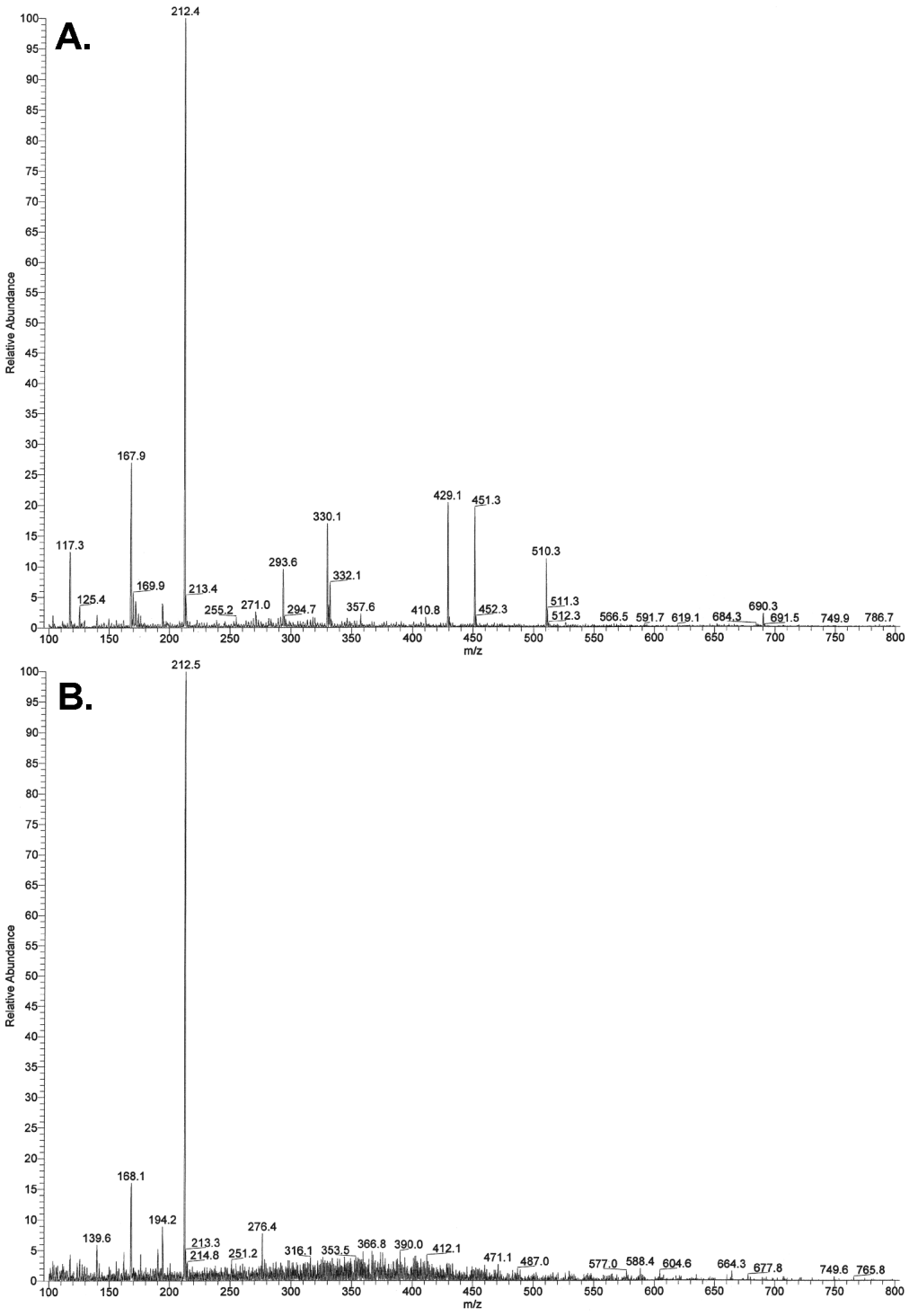

Figure 52B: Negative-ion electrospray mass spectra of AD in methanol and water. A) Spectrum of AD (4.5 µM diluted from 4.5 mM) dissolved in methanol showing no evidence of deiodination (I^- [127 Da], I_2 [254 Da], or I_3 [381 Da]). B) Spectrum of AD (4.5 µM diluted from 4.5 mM) dissolved in water showing no evidence of deiodination (I, I_2, or I_3). The peaks at 167.8 and 212.6 Da in both negative-ion spectra are known contaminants of the analysis system.

Discussion

The overall objective of this research project was to develop and characterize a rat model of AIPT. It was anticipated that the study of such a model would aid in identifying the underlying causes of AIPT. Once the mechanisms of disease development are elucidated, specific treatments directed against these mechanisms could be developed. To accomplish this goal, a rat model for AIPT was developed and characterized. This model incorporated the more damaging aspects of AIPT of inflammation and fibrosis. However, the early damage to the lungs done by the drug solution directly does not mimic the pathology of AIPT in humans.

The project may be divided into three main objectives. The first was to examine existing animal models in order to identify the most useful, or if none were adequate, to develop one that was. The second was to characterize the chosen model, with attention to the endpoints of inflammation and fibrosis, as well as possible mechanisms that may cause or contribute to the toxicity. The third was to examine the initial events that occur soon after the drug is administered, focusing primarily on the temporal relationships between the production of inflammatory cytokines, the appearance of inflammatory cells, and the initial damage to the alveolar-capillary barrier and cellular death. The direct role of AD in this damage and cellular death was also examined, as were properties of the drug that could contribute to toxicity.

As previously stated, two primary routes of administration exist in the literature for animal models of AIPT. Oral dosing of animals leads to a marked phospholipidosis in lung cells and tissue, but does not produce a consistent inflammatory or fibrotic response. Conversely, i.t. dosing of animals produces an initial inflammation

subsequently followed by fibrosis without producing the drug accumulation and phospholipidosis characteristic of the oral route. Thus the i.t. route has become favored in studies that examine the inflammatory and/or fibrotic aspects of AIPT, which are the aspects of the toxicity that are more serious and potentially fatal. The i.t. AD model was based on the development of an i.t. model of bleomycin-induced pulmonary fibrosis, even though the pathology between oral and i.t. bleomycin-induced fibrosis were subsequently found to be different. The use of the i.t. AD model has continued because of the lack of inflammation and fibrosis in oral animal models of AIPT.

Much of the research thus far has utilized hamsters as the test animal. Models that involve the i.t. dosing of hamsters with AD have been characterized with regards to the inflammatory and fibrotic responses. However, attempts to elucidate the signaling mechanisms involved may have been hindered by the lack of widely available molecular tools and reagents for hamsters. Researchers would have to generate specific antibodies against hamster proteins and develop their own ELISAs for each signaling protein they were interested in, a process that is time-consuming and labor-intensive, and still carries a risk of failure. However, many of these reagents are commercially available for rats, making rats a more attractive species for the study of signaling molecules. While it has been reported that an i.t. dose of AD leads to fibrosis in rats (Reinhart et al, 1996), little information exists about the development of inflammation or any other early events in the progression of the toxicity. Thus the potential exists for a rat model of AIPT to be helpful in elucidating the events that occur in the development of the toxicity as well as to identify the signaling molecules directing the responses.

The first objective was to define the animal model and select the dosing protocol to be subsequently fully characterized. To accomplish this, rats were treated either orally and intratracheally with AD so a comparison of responses could be made. As expected, the oral treatment led to phospholipidosis and an accumulation of AD and dAD in BAL cells without producing significant inflammation when dosed 7 or 14 days. A single i.t. dose of AD did lead to inflammation at day 5 without phospholipidosis or drug accumulation. Furthermore, the cells recovered on day 5 from i.t. AD-treated rats produced more NO in culture and more LDCL counts over 20 minutes than cells from control rats. Cells from rats treated orally for 7 days did not produce more NO or LDCL than controls, indicating that the cells from the i.t. AD-treated rats were activated to produce more oxidants while cells from oral-AD-treated rats were not primed. Because the oral treatment was reported not to lead to fibrosis (confirmed later in this study) and the i.t. treatment did, these findings were consistent with the hypothesis that i.t. treatment activates the cells to produce more oxidants, possibly causing lung damage and subsequent fibrosis, while the oral treatment does not activate cells. Thus the i.t. model was further examined as a potential model of AIPT to fully characterize.

Amiodarone is not extremely water-soluble, and will not dissolve in an ionic solution such as saline at neutral pH. It will, however, dissolve in water when heated to about 70^{o}C, but will immediately precipitate if saline is added in an attempt to make the solution physiological. While the report of fibrosis in rats used AD dissolved in water, a previous study in the hamster model used AD suspended in saline for instillations (Blake and Reasor, 1995a). An experiment to compare cellular activation via LDCL using AD either dissolved in water or suspended in saline revealed that AD in water stimulated the

cells more than AD in saline. AD in water may be able to penetrate cells more readily than AD in a particulate form, thus activating the cells more, or AD in solution may be more reactive if participating in radical reactions. Because of this finding, and to avoid any complications of instilling AD in particulate form in saline, AD dissolved in water was chosen as the preparation for subsequent intratracheal dosing. However, the ultimate state of AD once it is in the ionic but surfactant-rich fluid lining of the lungs is unknown.

Since it was desirable that the model included a fibrotic endpoint, studies to confirm the fibrosis reported earlier by this dosing technique (Reinhart et al, 1996) were performed. Surprisingly, the single i.t. dose of AD did not lead to a consistent elevation of right-lung hydroxyproline levels of fibrosis histopathologically. To achieve a significant increase in hydroxyproline following AD treatment, a second dose of AD or control vehicle was added to the regimen. To identify the appropriate time to give the second dose, experiments comparing hydroxyproline levels at day 28 when the drug was given at days 0 and 2 or at days 0 and 7, the latter protocol previously reported in a hamster model (Blake and Reasor, 1995b). The protocol with doses at days 0 and 2 was more fibrogenic than that with day 0 and 7 dosing, meaning the day 0 and 2 protocol would be adopted for subsequent studies with AD. An experiment to identify the proper time-point for analysis of fibrosis revealed no differences between AD-induced hydroxyproline increases at 4 or 6 weeks; therefore the 4 week (28 day) time-point was chosen for any subsequent fibrosis analyses.

In a final attempt to elevate right-lung hydroxyproline levels even further, another dosing protocol was implemented combining both the i.t. and oral dosings in the same animals. This protocol has not been previously reported in the literature. Two groups of

animals were treated with two different protocols. The first group, referred to as concurrent, were administered both the first oral and first i.t. dose on day 0, and subsequently received the second i.t. dose on day 2 and daily oral doses through the entire treatment period. The second group, referred to as orally pretreated, was treated orally with AD or vehicle for 7 days before the first of two i.t. doses were given, and daily oral doses were given until analysis at day 28. Controls were weight-matched to the orally treated rats by withholding food to eliminate effects of body weight and size on right-lung hydroxyproline levels. Groups of i.t.-only and oral-only treatments were also included for comparison. The concurrent drug treatment failed to elevate hydroxyproline levels above those of the i.t.-only group, and in fact, the orally pretreated group was protected from a significant increase in hydroxyproline levels. This may be due to the presence of phospholipidosis that is present in one week as demonstrated by the previous studies using oral AD. The lipid material in the alveolar region may act as a sink for the relatively small amounts of drug instilled intratracheally, protecting the cells from activation and/or the lungs from direct damage. This lipid material could protect from radical-induced damage, whether the radicals are produced from activated cells or directly from the drug molecule. Since the oral treatment complicated the development of fibrosis without adding to the levels of hydroxyproline measured, the i.t.-only protocol was chosen to be characterized more thoroughly with regards to the development of inflammation, lung damage, and fibrosis.

The second objective of the study was to characterize the response of rats to day 0 and 2 i.t. doses of AD or water. This protocol produced a significant fibrosis as analyzed by three separate techniques. Traditional analysis of fibrosis usually includes a

biochemical analysis of fibrosis and/or a separate histopathologic analysis. There are advantages and disadvantages to each technique. Biochemical analysis allows quantification of the level of fibrosis, but because the lung tissue is completely digested during the analysis, no information can be gathered about the location of type of fibrosis involved. This technique also may not detect focal fibrosis that does not significantly add to the total lung hydroxyproline levels. Conversely, histopathological analysis allows localization and characterization of fibrosis, but quantitation with this technique is subjective at best. An attempt was made to use LSCM with lucifer yellow staining to both quantitate connective tissue and analyze the location and type of fibrosis. This technique may be useful in the examination of lung biopsy tissue, or any application where the amount of lung tissue for analysis is limited, for fibrosis. The increase in lung tissue area found in this study correlated with in increase in the amount of lung collagen, as was probably directly related. However, there are instances when septal thickening may occur in which fibrosis is not occurring, such as pulmonary edema and interstitial inflammation. Lucifer Yellow preferentially stains collagen, and therefore much of the area with edema (and therefore lightly stained) can be thresholded out. Masking tools exist in the software to remove inflammatory cells from quantitation, although this technique was not necessary in this study.

To examine the early responses involved in this model, rats were dosed intratracheally with either AD in sterile water (6.25 mg/mg in a 3.125 mg/mL solution) or the sterile water vehicle and were lavaged at various time-points. Specifically, damage to the alveolar-capillary barrier as well as the number, type, and level of activation of BAL cells were examined at days 3, 5, 6, 7, and 10. The elevated albumin levels found in the

first BAL fraction indicated an early damage to the alveolar-capillary barrier, allowing the protein from the blood to cross into the alveolar space. The integrity of the relatively delicate barrier between the air in the blood in the alveolar region of the lungs is a good indicator of lung damage. Damage is most prominent at day 3, and resolves quickly thereafter. Therefore, in this model, the development of fibrosis was associated with an early and transient damage to the alveolar-capillary barrier.

The total number of cells recovered by BAL from AD-treated rats was significantly elevated on days 3 and 5. This indicates a cellular response to the AD administration. When the cells were differentiated, most were found to be alveolar macrophages, which were also significantly elevated in number on days 3 and 5. The number of alveolar macrophages can be increased by recruitment from the surrounding tissue as well as from monocytes recruited from the blood (Sibille and Reynolds, 1990). Stimulated macrophages can play an instrumental role in directing an inflammatory reaction by releasing chemical mediators to direct the recruitment of inflammatory cells as well as releasing oxidants as part of the host-defense system (Laskin and Pendino, 1995). There is evidence that inflammatory cells are indeed recruited to the lungs after AD administration, as the number of polymorphonuclear leukocytes (PMNs) was increased at day 3. PMNs are important in the inflammatory response in that they can release a variety of inflammatory mediators as well as oxidant species when recruited and activated. PMNs are recruited in various types of inflammatory reactions (Sibille and Reynolds, 1990).

The eosinophil is another type of inflammatory cell recruited to the lung after AD administration. Eosinophils are more often recruited during inflammatory reactions

involving immune reactions, possibly implicating an immunological component to AIPT in this model. Elevated eosinophils have also been reported in a hamster model for AIPT (Blake and Reasor, 1995a) and in the lungs of some human patients with AIPT (Akoun et al., 1991). The basis for eosinophil recruitment in this model is not clear, although proteins altered by AD could be perceived as foreign and initiate an immune response. Eosinophils can participate in inflammatory reactions by releasing damaging enzymes and oxidant species (Giembycz and Lindsay, 1999).

To assess the capacity for activation of the cells recovered by BAL, the cells were subjected to LDCL with and without PMA stimulation. PMA-stimulated BAL cells from AD-treated rats produced significantly more LDCL counts over 20 minutes than PMA-stimulated cells from control animals at day 3, indicating more oxidants were being produced. This indicates that the BAL cells from AD-treated rats can be activated to produce more oxidant species on a per-cell basis on day 3 than BAL cells from control animals. Since the total cell number was also elevated at day 3, the potential total oxidant burden was calculated by multiplying the PMA-stimulated LDCL counts, which were on a per-cell basis, by the total number of BAL cells recovered. Thus, on day 3, there is a much greater potential oxidant burden on the lungs of AD-treated animals than in the lungs of control animals.

In an attempt to identify the oxidant species involved in the LDCL response at day 3, specific inhibitors were utilized. L-NAME was used as an inhibitor of NO production while SOD was used as a scavenger of superoxide radicals. L-NAME alone significantly inhibited LDCL production from BAL cells from AD-treated rats. SOD also significantly inhibited light production presumably by scavenging superoxide anions

produced by BAL cells. Therefore, much of the light response was dependent on superoxide production. Even though SOD inhibited more light than L-NAME, L-NAME is a charged molecule that may not penetrate the cell membrane well enough to reach maximally effective inhibitory concentrations in the cytosol. Furthermore, when SOD and L-NAME were combined, light production from PMA-stimulated BAL cells was inhibited to the level of non-PMA-stimulated cells. Increased NO production was also shown from cells cultured from AD-treated animals. Since superoxide and NO readily combine to form the powerful oxidant peroxynitrite, it is possible that peroxynitrite production is increased from BAL cells from AD-treated rats. The conclusion from these experiments was that AD administration might lead to elevated oxidant stress in the lungs resulting from elevated production of oxidant species by an increased number of cells in the lungs soon after the drug doses. This may cause damage to the lung tissue that, when subsequently repaired, leads to increased collagen deposition and pulmonary fibrosis. However, the direct role of the drug in the early damage had not yet been explored.

Another goal of the study was to identify a biomarker that could easily be measured in the serum and could potentially aid in the diagnosis of AIPT. If applicable to humans, it would be important that this material could be obtained easily and monitored serially from the beginning of AD treatment. Also, it should correlate with the early aspects of the toxicity, such as pulmonary inflammation, so that a proper diagnosis can be made and the patient treated before the onset of irreversible and potentially fatal pulmonary fibrosis. It was found that serum levels of SP-D, a surfactant-associated protein, were elevated during the inflammatory stage of the response and through day 7. Therefore, SP-D levels in humans may serve as a useful marker for the onset of AIPT and

may aid in its initial diagnosis, which is often difficult (Martin and Rosenow, 1988b). Currently diagnosis is made using non-specific symptoms and chest imaging without specific diagnostic features, and can be complicated by the presence of other disorders (Martin and Rosenow, 1988b; Butler and Smathers, 1985; Delany et al., 1993). Substances previously proposed as biomarkers for AIPT may lack pulmonary specificity. SP-D may prove useful as an indicator of the lung-specific damage that occurs early in the development of AIPT. SP-D levels would need to be measured in patients taking amiodarone over time, and if increased would provide a signal that damage is occurring. Research to characterize changes in serum SP-D levels is required before it could be adopted as a biomarker in humans. However, serum SP-D increases have been correlated with the development of adult respiratory distress syndrome (ARDS) (Greene et al., 1999), pulmonary alveolar proteinosis (PAP), idiopathic pulmonary fibrosis (IPF), and interstitial pneumonia with collagen vascular diseases (IPCD) in humans (Kuroki et al., 1998). Therefore there is potential for elevated serum SP-D levels in patients developing AIPT. However, because of the massive damage that occurs to the alveolar-capillary barrier in this model, the clinical relevance of these findings is unknown. The monitoring of SP-D levels in patients taking amiodarone is necessary to determine its usefulness as a biomarker for AIPT.

To elucidate the effects that the low pH of the AD solution may have been having on the cellular differentials and albumin leakage at day 3, sterile water adjusted to the same pH as AD solution with HCl was instilled on days 0 and 2. The BAL results on day 3 were compared to animals treated with AD and non-adjusted sterile water (the normal control). "Acidic water" (same pH as AD solution) did not induced increases in total

cells, macrophages, PMNs, or eosinophils that is seen with the AD treatment. Acidic water also did not elevate albumin levels in the first BAL fraction, indicating those responses were drug-specific.

The third objective was to examine the initial events that occur soon after the drug is administered, focusing primarily on the temporal relationships between the production of inflammatory cytokines, the appearance of inflammatory cells, and the direct role of the drug in the initial damage to the alveolar-capillary barrier. By examining both *ex vivo* cytokine production and cytokine levels in the first BAL fraction, it was apparent that the inflammation resulting from i.t. AD dosing did not follow the traditional pattern of an initial increase in TNF-α, followed by and increase in IL-1β. Instead, TNF-α production was inhibited after AD administration both in cells cultured from AD-treated rats and directly in the lavage fluid of AD-treated rats. While the inhibition of TNF-α production at the early time-points may be due to the killing of the cells that produce it, the findings of inhibited LPS-stimulated TNF-α production at day 3 are free from viability issues (viability of cells recovered at day 3 is >90%). This implicates an inhibition of the TNF-α production process. This is in agreement with a study of human peripheral blood monocytes which showed a decrease in TNF-α production following treatment with AD (Matsumori et al., 1997). It is likely that the inhibition of TNF-α production following i.t. AD is not permanent, however. A study (Reinhart and Gairola, 1997) in which rats were subjected to a single i.t. dose of AD (6.25 mg/kg) or water and then lavaged at 1, 3, or 6 weeks afterwards revealed that cultured BAL cells from AD-treated rats produced significantly more TNF-α than cells from control rats at the 3- and 6-week time points,

but not at the 1 week time-point. Thus TNF-α may play a role in the development of pulmonary fibrosis seen at the 6-week time point in that study.

In an attempt to identify any other cytokines that may be have a role in AD-induced inflammation, IL-1β production was also analyzed from cultured BAL cells at 3 hours post-i.t. LPS-stimulated IL-1β levels were significantly decreased in the media of cells from AD-treated animals. This finding is consistent with the hypothesis that IL-1β levels are dependent in the initial increase of TNF-α. Without the TNF-α rise, production of IL-1β is not stimulated. It could also be an effect of the mortality rate of the BAL cells at this time-point. IL-6 production was examined to determine if a cytokine involved in the specific immune response was elevated following AD treatment. However, no changes were found in IL-6 production after AD treatment. The same is true for IL-10 production, an anti-inflammatory cytokine. However, the role of cytokines in the AD-induced inflammation became much less significant when it became apparent that the drug solution itself was causing massive damage to the lungs as early as 15 min. The subsequent cellular responses were probably a non-specific reaction to the damage, with activated phagocytes engulfing cellular debris. The presence of the eosinophils still hint at an immune response in the lungs following AD treatment, possibly through AD-protein hapten formation. However, the relatively low number of recruited eosinophils compared to macrophages suggests a very small role any immunological mechanisms may be having in the recruitment of cells in this model.

Ethidium homodimer is a vital stain; it cannot cross intact cell membranes due to its positive charge. However, when cell membranes are disrupted, as in significant membrane damage or cell death, the ethidium homodimer is able to enter the cell,

intercalate in the DNA, and fluoresce. The use of LSCM to examine *in situ* viability found focal areas of massive damage soon after i.t. AD, as well as relatively undamaged areas. These differences probably reflect the drug distribution following i.t. administration.

Because substantial ethidium staining and elevated albumin and LDH levels in the first BAL fraction from AD-treated rats were present as early as 15 min, this time-point was chosen for subsequent characterization of the direct effect of the drug solution in the toxicity. To assess the role of hydrogen ions in the AD solution (3.125 mg/mL; 4.5 mM; pH 3.7) in the toxicity at 15 min, citrate buffer (pH 3.7) and HCl (4.5 mM; pH 2.5) were used as control solutions. Neither acidic control significantly elevated albumin or LDH activity in the first BAL fraction. Analysis of ethidium staining in an animal treated with HCl (4.5 mM) also revealed no qualitative differences from water control. Therefore the hydrogen ions in the AD solution do not appear to be the cause of the damage seen after i.t. AD administration.

In order to quantitate ethidium staining, thin sections of ethidium-stained tissue were made 15 min following a single i.t. AD or water administration, or on day 3 following i.t. treatments on days 0 and 2. Using computer software, the number of ethidium-positive and total cells/random field were obtained. By categorizing the field as either airway or parenchymal tissue, AD-induced damaged was localized. While both airways and parenchyma were affected 15 min post-i.t. AD, more airway cells/field were damaged. This indicated that AD is damaging the epithelial cells lining the airways as a result of the i.t. route of administration. This damage is repaired by day 3, either by replacement or simply removal of the damaged cells by phagocytes. At day 3 more

parenchymal cells in AD-treated animals stain ethidium-positive, possibly as a result of damage from activated inflammatory cells in the alveolar regions, although ethidium staining in general at day 3 is much less than at 15 min. This LSCM technique confirms the findings of the damage indicators that massive damage involving cell death is present soon after i.t. AD administration. The localization of damage in the airways suggests that the damage is much different than the pathology of AIPT in human patients. Human patients do not undergo a massive cytotoxic event, but rather progress through a gradual lung-drug accumulation that leads to inflammation and fibrosis. The inflammation and fibrosis observed in this model are most likely direct results of the route of administration of the AD, and thus are not necessarily relevant to the human condition.

The direct damage caused by AD was surprising because AD was not thought to be a reactive compound. Free radical formation had been postulated as being involved in AD-induced phototoxicity, but studies of the free radical generation by AD involved irradiating the AD with UV light or ionizing radiation. Vereckei et al. (1993) speculated that the deiodination of AD would lead to the formation of a very reactive aryl radical. Experiments were performed in this study to test that hypothesis using ESR techniques to examine free radical production in solutions similar to that used to treat animals intratracheally (3.125 mg/ml; 4.5 mM). Without DMPO spin trapping, a carbon based free radical signal was indeed found in AD solution (25 mg/mL). This signal was reduced by increased concentration of AD (100 mg/mL), demonstrating possible autoquenching. Although AD would most likely need to be in solution to be deiodinated, a carbon-based free radical signal was also found in the dry AD powder, indicating that the responsible compound may be present before the drug is in solution.

By using DMPO as a spin trap, hydroxyl radicals were found in the AD solution (3.125 mg/mL) in water. Hydroxyl radicals were also trapped when a solution of i.v. AD was diluted to the same concentration (3.125 mg/mL), despite the fact that it was in solution for several months prior to analysis in the presence of benzyl alcohol and polysorbate 80, which were present but diluted during the analysis as well (data not shown). While pulmonary toxicity has not been associated with the short-term i.v. AD treatment used in cardiac emergencies, toxicity could be expected to blood vessels and other organs following the administration of a free radical producer. However, the extensive binding of AD by albumin may serve to protect these tissues from damage, as 5 mg/mL albumin greatly reduced the hydroxyl signal from AD (data not shown). The finding of hydroxyl

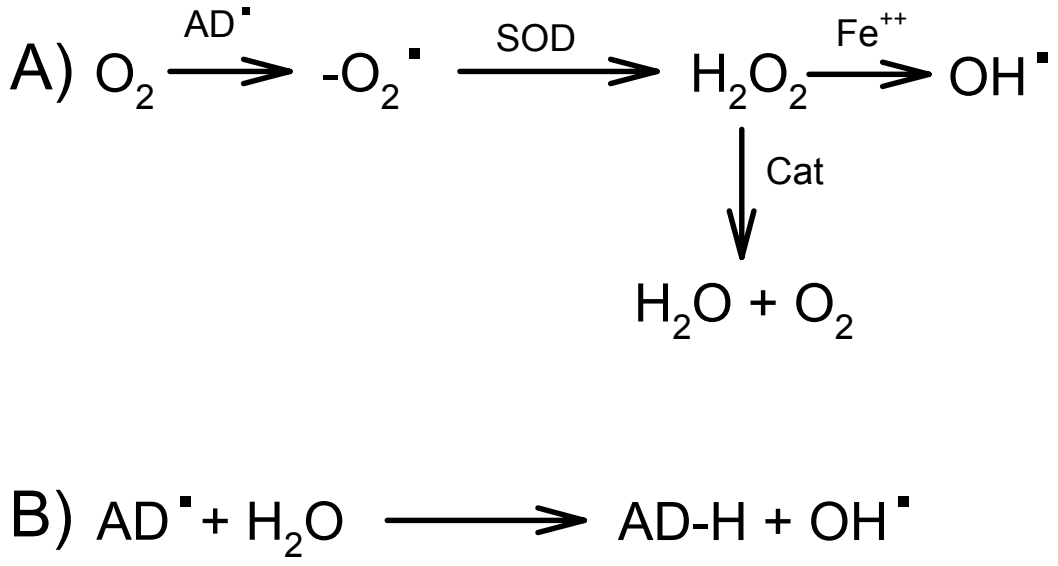

Figure 53: Possible pathways for AD-induced hydroxyl radical formation; the effects of exogenous enzymes and chemicals.

radical implies that a parent compound radical is present, and this radical interacts with constituents in the solution to produce hydroxyl radicals. Two possible pathways for hydroxyl production from molecular oxygen (A) and water (B) are presented in **Figure 53**. Experiments were done to determine the pathway of hydroxyl radical formation by the addition of exogenous chemicals and enzymes to the AD solution.

Hydroxyl production induced by AD (3.125 mg/mL) was first analyzed in water. If the pathway illustrated by Figure 53(A) is occurring, then SOD may enhance hydroxyl production, while Cat and Def (an iron chelator) should decrease the signal. All three compounds reduced the signal, indicating a non-specific effect of the compounds, or indicating that another pathway may be partly involved. Since formate changed the pH of the solution and changed the trapping efficiency of DMPO, this experiment was repeated in phosphate-buffered saline to maintain constant pH. Even though the AD partly came out of solution, hydroxyl radicals were still produced. SOD, Cat, Def, and formate all inhibited the signal without eliminating it, while the addition of exogenous H_2O_2 increased the hydroxyl signal. This finding implies that something is acting as a transition element, possibly a metal or the AD molecule itself. By adding Fe^{++}, the presence of H_2O_2 in AD solution was expected to be determined. An increased signal would indicate that H_2O_2 was involved. However, the charged ion forced AD completely out of solution and eliminated the hydroxyl signal. Formate caused both a reduction and a splitting of the hydroxyl signal, indicating that the hydroxyl was free in solution, since formate itself is a radical and competes for the DMPO.

To determine if the effects of the enzymes in the previous studies were specific for their actions, or an effect of exogenous protein, they were heat-inactivated and added

to the AD solution (3.125 mg/mL) in PBS. However, the enzymes did not produce the same inhibition as seen in previous experiments. Heat-inactivated SOD did inhibit to about the same level as did normal SOD in previous experiments, but heat inactivated Cat drastically reduced the signal. This may have been due to the denatured protein releasing its active site moiety into solution. The variable effects of the enzymes preclude definitive determination of the pathway of hydroxyl formation in solution. The incomplete inhibition by Def and Cat in the two previous experiments suggest that hydroxyl radical may be coming from molecular oxygen as well as direct hydrogen abstraction from water. However no measurable oxygen consumption was observed in a solution of AD (25 mg/mL) in water, indicating that molecular oxygen is not used to a great extent in this particular solution.

To determine if an aryl radical was present in the AD solution (4.5 mM; 3.125 mg/mL in water), thiol antioxidants were added in an attempt to adduct the aryl radical and eliminate the hydroxyl signal. However, more hydroxyl was trapped when either NAC (9.0 mM) or GSH (9.0 mM) was in the AD solution. This was not due to either compound altering the pH of the AD solution. An animal treated with AD (4.5 mM) and NAC (22.5 mM) in the same solution suffered hemorrhaging and subsequently died. To examine the possible oxidation of NAC, AD (3.125 mg/mL) and DMPO were placed into chloroform with and without NAC. Without water present, hydroxyl radicals are not formed, and the spectrum of the parent radical can be obtained. A radical signal was found in the AD solution, presumably the AD radical. The addition of NAC (9.0 mM) to AD and DMPO in chloroform produced a signal consistent with the field width of an *N*-acetyl cystyl radical, although the signal was split by the AD radical signal. This

indicated that the NAC was being oxidized into a radical itself, and by interacting with molecular oxygen or water, producing more hydroxyl radicals. While the exact nature of the parent compound radical could not be easily identified, the structure could be inferred in a computer simulation of the spectra. Since the hyperfine coupling that makes up the appearance of an ESR spectrum is determined by the atoms adjacent to the radical, it would be possible to simulate the spectra of AD with DMPO in chloroform and gain insight into the structure of the parent radical being trapped. This was not done in these studies, however, due to the lack of access of such capabilities.

Autoquenching of hydroxyl radical was explored by analyzing the hydroxyl-DMPO signal from increasing concentrations of AD. While the peak appeared to be reached around 12 mg/mL AD, further studies could not be completed due to a crosslinking or solidifying of the AD solution. This may indicate that AD is both a free-radical producer and scavenger on different parts of its structure. When one AD molecule is in the form of a radical, another may adduct with it, eliminating the radical signal. However, the importance of this characteristic *in vivo* is not clear. AD is accumulated to a high degree in lung cells and tissues, and autoquenching could explain why the cells are not damaged by radical production (if any occurs). This could help explain why animals treated with oral AD accumulate large amounts of drug without cellular activation. However, no evidence for an AD complex (i.e. an AD dimer, etc.) was found during HPLC analysis of AD levels in animals treated with oral AD.

Attempts to examine free radical production *in vivo* were unsuccessful. DMPO was instilled with AD into rats, and then withdrawn, but even the expected baseline hydroxyl-DMPO signal was absent. Protocols involving the treatment of excised lungs,

lung homogenates, and varying concentrations of BAL cells failed to yield any radical signals. This obviously could mean that radicals are not involved in the AD-induced damage. However, it is possible that the activated DMPO was actually quenched by endogenous and cellular antioxidants. Experiments with cells and tissues have to be carefully balanced to avoid the quenching of the spin trap while maintaining enough cells to affect. Therefore all experiments with animals, tissues, and cells were inconclusive.

To determine if an aryl radical could be formed and measured in AD solution (3.125 mg/mL) in water with DMPO, AD solution was analyzed with and without UV treatment. UV exposure for the first 10 min of the 30 min incubation produced a typical aryl-DMPO signal split with a hydroxyl-DMPO signal. Therefore it is possible for an aryl radical to be formed in AD solution. However, the importance of the aryl radical in the non-UV treated samples was not clear. It is possible that the hydroxyl signal was produced by a small amount of aryl radical in solution, or that a non-aryl radical pathway of AD-induced free radical production was occurring.

To determine if the hydroxyl signal could be eliminated, several antioxidants and combinations of antioxidants were tested in AD solution (3.125 mg/mL; 4.5 mM) with DMPO. While several antioxidants had varying effectiveness in eliminating the hydroxyl signal, a combination of Trolox (45 mM) and ascorbate (22.5 mM) completely inhibited the hydroxyl signal. This combination was chosen for an attempt to protect animals from i.t. AD-induced damage at 15 min. For the protection experiment, the antioxidants had to be at least partly water-soluble, as they would need to be in solution with AD to ensure equal distribution with the drug. However, if the drug partitioned into the lipid membrane, any protective effect of the water-soluble antioxidants could be lost. Trolox

is a water-soluble vitamin E derivative, and was chosen in an attempt to protect the lipid compartment. Ascorbate was chosen to protect the aqueous compartment, partly because of its ability to interact with vitamin E in other situations to scavenge radicals. However, the presence of these antioxidants in solution actually exacerbated the damage at 15 min. Effects were both qualitative (physical examination revealed worse hemorrhaging of the lungs and a greater amount of blood in the BAL fluid) and quantitative, as evidenced by increased albumin in the BAL fluid from animals given AD and antioxidants, as compared to animals given AD alone. Curiously the added apparent damage did not increase LDH activity in the BAL fluid of rats receiving AD with antioxidants. This could be due to the nature of the alveolar-capillary barrier. Type I epithelial cells that form this barrier are extremely thin, with little cytoplasm but a large surface area. Damage done to this region on the lungs may result in a greater leakage of albumin to the airways without significantly increasing the level of LDH in the BAL fluid due to the limited amount of cytoplasm of type I cells. It is possible that significantly more damage can be done to the alveolar-capillary barrier without a significant increase in cell death, if that cell death is occurring in the alveoli. Antioxidant solution alone had no effect on albumin or LDH activity in the first BAL fraction at 15 min as compared to sterile water.

The lack of protection by antioxidants from i.t. AD-induced damage does not resolve the issue of the involvement of free radicals in the damage. It could be possible that AD is causing damage through a non-radical pathway, and the radicals signals observed with ESR are incidental, caused by low-level deiodination and radical formation, but not to a level that induces damage. Or it is possible that the water-soluble antioxidants chosen could not protect cells from AD-radical induced damage in the lipid

compartment. Other possibilities for AD-induced damage that do not involve radicals do exist. While AD is a hydrochloride, the effect is mostly likely not due to the pH of the AD solution. Because of its amphiphilic structure, AD could simply be acting as a detergent, and as such could permeabilize cell membranes upon contact. Even though AD is instilled in solution, it could also have the effects of a particulate if it does not remain in solution in the fluid lining of the lungs. AD precipitating adjacent to cell membranes may have a damaging effect on those membranes. Further studies would be needed to control for each of these possibilities to determine the most likely mechanism for AD-induced damage. However, since the damage that occurs is not similar to the pathology of AIPT in human patients, there would be little clinical relevance of those studies. The role of direct cytotoxicity of AD in human AIPT has not been completely elucidated. The finding of elevated LDH activity in the serum of a patient with AIPT (Drent et al., 1998) could be attributed to AD-induced cytotoxicity, or cytotoxicity accompanying the acute inflammatory reaction.

To examine if deiodination of AD occurred when dissolved in water, solutions of AD dissolved in water and methanol were analyzed with electrospray mass spectroscopy with Robert Smith (Dept of Biochemistry, WVU). Intact AD was expected to have a molecular weight of ~645 Da. Instead, AD was found at 651, 652, and 653 Da. Electrospray analysis usually adds 1.0 Da to the molecular weight. This means that the AD in both methanol and water was either fully saturated with hydrogen, the technique added more than 1 Da to the apparent molecular weight, or that this particular AD has an unusual amount of ^{13}C in its structure. Whatever caused the discrepancy, conclusions can still be drawn from this experiment. No evidence was found for deiodinated AD, either

mono (~518 Da) or di-deiodinated (~393 Da) in the positive ion spectra from AD in methanol. However, possible di-deiodinated AD (~393 Da) was found in the AD-water solution. No evidence was found for a mono-deiodinated compound that would have been expected to be present as well in the solution, possibly in higher concentrations than the di-deiodinated compound. Also, no evidence for free iodine in solution (I^-, I_2, or I_3; ~127, ~254, and ~381 Da respectively) `was found in the negative ion spectra for AD in methanol or water. The peaks at 167.8 and 212.6 Da in both negative-ion spectra are known contaminants of the analysis system. Thus the ~393 Da peak could represent di-deiodinated AD, although no iodine or mono-deiodinated AD were found, or an unknown AD breakdown product, implying that dissolving AD in water may indeed change its structure. No evidence for this breakdown product was found utilizing HPLC analysis with a spectrometer, but the product might not absorb at the UV wavelength used to detect AD, especially if it was not di-deiodinated AD, which would have maintained its ring structure. The overall conclusions of the mass spectroscopy is that AD does not significantly deiodinate when dissolved in water, but may change structurally in some other undetermined fashion. This could imply that AD is able to generate free radicals in an as of a yet-undetermined mechanism, or it could mean that that the levels of mono-deiodination in solution are so small as to be undetectable by mass spectroscopic analysis, but enough to produce radical signals in ESR analysis. This latter scenario seems unlikely given the relatively greater sensitivity of mass spec vs. the relatively less-sensitive technique of ESR spin trapping. ^{1}H-Nuclear magnetic resonance analysis of the dry AD powder confirmed the expected structure of AD, which does not yield any insight

into what may have caused the carbon-based radical signal detected by ESR in the dry powder. Thus the mechanism for free radical production by AD remains unclear.

Intratracheal AD administration leads to a massive damage to the lungs within the first 15 min. This damage involves the death of airway and parenchymal cells, and results in leakage of albumin through the alveolar-capillary barrier as well as release of intracellular LDH. This damage seems to be a result of some aspect of the drug itself. At least a portion of the drug was found to be both a radical and capable of producing radicals in solution. The role of these radicals in the damage caused by i.t. AD remains unclear. The drug does not appear to undergo deiodination in solution, leaving the question of the exact mechanism of AD radical production unanswered. An undescribed mechanism of radical production from AD could be involved.

Because of the damage that i.t. AD causes soon after administration, this technique is not a relevant method to model human AIPT. If studies of AIPT are to continue, another animal model of the toxicity needs to be developed, one that hopefully employs an oral or i.v. route of administration. While rodents have been resistant to AIPT development when dosed orally, the search for another model can be expanded into other species. Even though the expense and technical considerations are greater for non-rodent species, including primates, the continued increase of the use of AD justifies those measures.

While modeling AIPT with intratracheal AD administration is not clinically relevant, some findings with this model warrant further consideration. The use of SP-D as a biomarker deserves further investigation. Even though the damage to the alveolar-capillary barrier induced by AD in this model could have allowed SP-D into the serum,

the successful use of this protein as a biomarker for other human lung toxicities warrants clinical trials in human patients. A biomarker could aid in the early diagnosis of AIPT and result in treatment of the condition rather than further development that could lead to death. The role of cytotoxicity in human AIPT also needs to be further explored. The large amount of cytotoxicity from relatively low drug levels begs the question of the effects of AD in the much higher concentrations seen in the lung *in vivo*. Finally, the ability of AD to readily generate radicals in solution is an important finding. Because the mechanism of AD radical generation may not be as hypothesized in the literature, the mechanism of free radical production without AD deiodination needs to be explored. The possibility of radical formation has implications for some of the side effects seen with AD treatment in patients. Skin photosensitivity could be due in part to the direct activation by sunlight of the drug stored in skin and subcutaneous tissues, leading to radical formation and skin damage. The accumulation of AD in the cornea could lead to activation that causes the oxidation of proteins there, causing opacity and inflammation. It is clear that stored AD in other tissues does not regularly undergo deiodination and activation induced by UV light, but these studies suggest that deiodination may not be necessary for radical production. It is therefore possible that in at least some cases of human AIPT, low levels of radical formation by non-bound drug in lung tissue could cause damage and lead to the persistent inflammation observed. Also, any proteins modified by radical damage or AD-hapten formation could then be seen as foreign and initiate the immune response seen in some individuals. As other cationic amphiphilic drugs are known to cause phospholipidosis without the widespread reports of

inflammation and fibrosis as with AIPT, it is possible that radical formation is unique to AD and possibly involved it the more damaging aspects of the toxicity.

It is hoped that these studies will contribute to the eventual determination of the mechanisms involved in AIPT development, if by nothing else sparing further study on animal models involving i.t. AD administration.

References

Adams, P.C., Gibson, G.J., Morley, A.R., et al. Amiodarone pulmonary toxicity: clinical and subclinical features. *Q.J.Med.* 59:449-471, 1986.

Adams, P.C., Holt, D.W., Storey, G.C., Morley, A.R., Callaghan, J. and Campbell, R.W. Amiodarone and its desethyl metabolite: tissue distribution and morphologic changes during long-term therapy. *Circulation* 72:1064-1075, 1985.

Agoston M., Cabello R., Blazovics A., Feher J., and Vereckei A. The effect of amiodarone and/or antioxidant treatment on splenocyte blast transformation. *Clin.Chem.Acta*. 303(1-2):87-94, 2001.

Akoun, G.M., Cadranel, J.L., Blanchette, G., Milleron, B.J. and Mayaud, C.M. Bronchoalveolar lavage cell data in amiodarone-associated pneumonitis. Evaluation in 22 patients. *Chest* 99:1177-1182, 1991.

Akoun, G.M., Gauthier-Rahman, S., Milleron, B.J., Perrot, J.Y. and Mayaud, C.M. Amiodarone-induced hypersensitivity pneumonitis. Evidence of an immunological cell-mediated mechanism. *Chest* 85:133-135, 1984.

Akoun, G.M., Liote, H.A., Milleron, B.J. and Mayaud, C.M. Amiodarone pulmonary toxicity [letter]. *Chest* 89:7681986.

American Heart Assosication. Cardiovascular disease statistics. Available at: http://www.americanheart.org/statistics/07other.html. Accessed 1-10-2000.

Ames, B.N., and Dubin, B.T. The role of polyamines in the neutralization of deoxyribonucleic acid. *J.Biol.Chem.* 235:769-775, 1960.

Antonini, J.M., Charron, T.G., Roberts, J.R., Lai, J., Blake, T.L. and Rogers, R.A. Application of laser scanning confocal microscopy in the analysis of particle-induced pulmonary fibrosis. *Toxicol.Sci.* 51:126-134, 1999.

Antonini, J.M., Van Dyke, K., Ye, Z., DiMatteo, M. and Reasor, M.J. Introduction of luminol-dependent chemiluminescence as a method to study silica inflammation in the tissue and phagocytic cells of rat lung. *Environ.Health Perspect.* 102 Suppl 10:37-42, 1994.

Bauman, J.L. Class III antiarrhythmic agents: the next wave. *Pharmacotherapy.* 17:76S-83S, 1997.

Blake, T.L. and Reasor, M.J. Acute pulmonary inflammation in hamsters following intratracheal administration of amiodarone. *Inflammation* 19:55-65, 1995a.

Blake, T.L. and Reasor, M.J. Pulmonary responses to amiodarone in hamsters: comparison of intratracheal and oral administrations. *Toxicol.Appl.Pharmacol.* 131:325-331, 1995b.

Blake, T.L. and Reasor, M.J. Dexamethasone protects hamsters from fibrosis but not inflammation induced by intratracheal amiodarone. *Tox.Sub.Mech.* 16:51-62, 1997.

Brien,J.F., Jimmo,S., Brennan,F.J., Ford,S.E., and Armstrong,P.W. Distribution of amiodarone and its metabolite, desethylamiodarone, in human tissues. *Can.J.Physiol.Pharmacol.* 65(3):360-364, 1987.

Butler, S., and Smathers, R.L. Computed tomography of amiodarone pulmonary toxicity. *J.Comput.Assist.Tomogr*. 9:375-376, 1985.

Camus, P. and Jeannin, L. Re: Speculation on the mechanism for amiodarone-induced pneumonitis [letter]. *Radiology* 150:279-280, 1984.

Cantor, J.O., Osman, M., Cerreta, J.M., Suarez, R., Mandl, I. and Turino, G.M. Amiodarone-induced pulmonary fibrosis in hamsters. *Exp.Lung Res.* 6:1-10, 1984.

Card, J.W., Leeder, R.G., Racz, W.J., Brien, J.F., Bray, T.M. and Massey, T.E. Effects of dietary vitamin E supplementation on pulmonary morphology and collagen deposition in amiodarone- and vehicle-treated hamsters. *Toxicology* 133:75-84, 1999.

Carvalho, C.R., Kairalla, R.A., Capelozzi, V.L., Amato, M.B. and Saldiva, P.H. Chronic amiodarone ingestion induces pulmonary toxicity in rats. *Braz.J.Med.Biol.Res.* 29:779-791, 1996.

Connolly, S.J. Evidence-based analysis of amiodarone efficacy and safety. *Circulation* 100:2025-2034, 1999.

Crouch, E.C. Structure, biologic properties, and expression of surfactant protein D (SP-D). *Biochim.Biophys.Acta* 1408:278-289, 1998.

D'Amico, D.J. and Kenyon, K.R. Drug-induced lipidoses of the cornea and conjunctiva. *Int.Ophthalmol.* 4:67-76, 1981.

Daniels, J.M., Brien, J.F. and Massey, T.E. Pulmonary fibrosis induced in the hamster by amiodarone and desethylamiodarone. *Toxicol.Appl.Pharmacol.* 100:350-359, 1989.

Delany, S.G., Taylor, D.R., Restieaux, N., and Doyle, T.C. Amiodarone pulmonary toxicity: its radiological features. *Australas.Radiol*. 37**:**47-49, 1993.

Devine, P.L., Siebert, W.J., Morton, S.L., Scells, B., Quin, R.J., Heddle, W.F., Zimmerman, P.V., and Donohoe, P.J. Serum mucin antigen (CASA) as a marker of amiodarone-induced pulmonary toxicity. *Dis.Markers* 14:169-175, 1998.

Drent, M., Cobben, N.A., Van Dieijen-Visser, M.P., Braat, S.H., and Wouters, E.F. Serum lactate dehydrogenase activity: indicator of the development of pneumonitis induced by amiodarone [letter]. *Eur.Heart* J. 19: 969-970, 1998.

Driscoll, K.E., Costa, D.L., Hatch, G., Herderson, R., Oberdorster, G., Salem, H., and Schlesinger, R.B. Intratracheal Instillation as an exposure technique for the evaluation of respiratory tract toxicity: uses and limitations. *Toxicol.Sci*. 55:24-35, 2000.

Fan, K., Bell, R., Eudy, S. and Fullenwider, J. Amiodarone-associated pulmonary fibrosis. Evidence of an immunologically mediated mechanism. *Chest* 92:625-630, 1987.

Folch, J., Lees, M., and Sloane-Stanley, G.H. A simple method for the isolation and purification of total lipds from animal tissues. *J.Biol.Chem.* 226:496-509, 1957.

Giembycz, M.A. and Lindsay, M.A. Pharmacology of the eosinophil. *Pharmacol.Rev.* 51:213-340, 1999.

Gill, J., Heel, R.C. and Fitton, A. Amiodarone. An overview of its pharmacological properties, and review of its therapeutic use in cardiac arrhythmias. *Drugs* 43:69-110, 1992.

Greene, K.E., Wright, J.R., Steinberg, K.P., Ruzinski, J.T., Caldwell, E., Wong, W.B., Hull, W., Whitsett, J.A., Akino, T., Kuroki, Y., Nagae, H., Hudson, L.D., and Martin, T.R. Serial changes in surfactant-associated proteins in lung and serum before and after onset of ARDS. *Am.J.Respir.Crit.Care Med*. 160:1843-1850, 1999.

Green, L.C., Wagner, D.A., Glogowski, J., Skipper, P.L., Wishnok, J.S. and Tannenbaum, S.R. Analysis of nitrate, nitrite, and [15N]nitrate in biological fluids. *Anal.Biochem.* 126:131-138, 1982.

Han, J.H., Beutler, B. and Huez, G. Complex regulation of tumor necrosis factor mRNA turnover in lipopolysaccharide-activated macrophages. *Biochim.Biophys.Acta* 1090:22-28, 1991.

Harris, L., McKenna, W.J., Rowland, E., Holt, D.W., Storey, G.C.A., and Krikler, D.M. Side effects of long-term amiodarone therapy. *Circulation* 67:45-51, 1983.

Hasan, T., Kochevar, I.E., and Abdulah, D. Amiodarone phototoxicity to human erythrocytes and lymphocytes. *Photochem. Photobiol*. 40:715-719, 1984.

Heath, M.F., Costa-Jussa, F.R., Jacobs, J.M. and Jacobson, W. The induction of pulmonary phospholipidosis and the inhibition of lysosomal phospholipases by amiodarone. *Br.J.Exp.Pathol.* 66:391-397, 1985.

Hesse, D.G., Tracey, K.J., Fong, Y., Manogue, K.R., Palladino, M.A.,Jr, Cerami, A., Shires, G.T., and Lowry, S.F. Cytokine appearance in human endotoxemia and primate bacteremia. *Surg.Gynecol.Obstet.* 166:147-153, 1988.

Hogan, S.P. and Foster, P.S. Cytokines as targets for the inhibition of eosinophilic inflammation. *Pharmacol.Ther.* 74:259-283, 1997.

Honda, Y., Kuroki, Y., Matsuura, E., Nagae, H., Takahashi, H., Akino, T., and Abe, S. Pulmonary surfactant protein D in sera and bronchoalveolar lavage fluids. *Am.J.Respir.Crit.Care Med*. 152:1860-1866, 1995.

Honegger, U.E., Scuntaro, I. and Wiesmann, U.N. Vitamin E reduces accumulation of amiodarone and desethylamiodarone and inhibits phospholipidosis in cultured human cells. *Biochem.Pharmacol.* 49:1741-1745, 1995.

Honegger, U.E., Zuehlke, R.D., Scuntaro, I., Schaefer, M.H., Toplak, H. and Wiesmann, U.N. Cellular accumulation of amiodarone and desethylamiodarone in cultured human cells. Consequences of drug accumulation on cellular lipid metabolism and plasma membrane properties of chronically exposed cells. *Biochem.Pharmacol.* 45:349-356, 1993.

Ide T., Tsutsui H., Kinugawa S., Utsumi H., and Takeshita A. Amiodarone protects cardiac myocytes against oxidative injury by its free radical scavenging action. *Circulation* 100:690-692, 1999.

Joelson, J., Kluger, J., Cole, S. and Conway, M. Possible recurrence of amiodarone pulmonary toxicity following corticosteroid therapy. *Chest* 85:284-286, 1984.

Kachel, D.L., Moyer, T.P. and Martin, W.J. Amiodarone-induced injury of human pulmonary artery endothelial cells: protection by alpha-tocopherol. *J.Pharmacol.Exp.Ther.* 254:1107-1112, 1990.

Kennedy, J.I., Myers, J.L., Plumb, V.J. and Fulmer, J.D. Amiodarone pulmonary toxicity. Clinical, radiologic, and pathologic correlations. *Arch.Intern.Med.* 147:50-55, 1987.

Kennedy, T.P., Gordon, G.B., Paky, A., et al. Amiodarone causes acute oxidant lung injury in ventilated and perfused rabbit lungs. *J.Cardiovasc.Pharmacol.* 12:23-36, 1988.

Kishimoto, T., and Hirano, T. Molecular regulation of B lymphocyte response. *Annu.Rev.Immunol*. 6:485-512, 1988.

Kuroki, Y., Takahashi, H., Chiba, H., and Akino, T. Surfactant proteins A and D: disease markers. *Biochim.Biophys.Acta* 1408:334-345, 1998.

Laskin, D.L. and Pendino, K.J. Macrophages and inflammatory mediators in tissue injury. *Annu.Rev.Pharmacol.Toxicol.* 35:655-677, 1995.

Lasky, J.A., and Brody, A.R. Interstitial fibrosis and growth factors. *Environ.Health Persp*. 108(Supp 4):751-762, 2000.

Leeder, R.G., Brien, J.F. and Massey, T.E. Investigation of the role of oxidative stress in amiodarone-induced pulmonary toxicity in the hamster. *Can.J.Physiol.Pharmacol.* 72:613-621, 1994.

Leeder, R.G., Rafeiro, E., Brien, J.F., Mandin, C.C. and Massey, T.E. Evaluation of reactive oxygen species involvement in amiodarone pulmonary toxicity in vivo and in vitro. *J.Biochem.Toxicol.* 11:147-160, 1996.

Levy, A., Meyerstein, D., and Ottolenghi, M. Photodissociation of iodoaromatics in solution. *J.Phys.Chem.* 77:3044-3047, 1973.

Li, A.S.W. and Chignell C.F. Spectroscopic studies of cutaneous photosensitizing agents-IX. A spin trapping study of the photolysis of amiodarone and desethylamiodarone. *Photochem. Photobiol*. 45(2):191-197, 1987.

Lillie, R.D. Histopathologic Technique. Blackiston, Philadelphia, 1948.

Lindenschmidt, R.C., Tryka, A.F., Godfrey, G.A., Frome, E.L., and Witschi, H. Intratracheal versus intravenous administration of bleomycin in mice: acute effects. *Toxicol Appl Pharmacol*. 85:69-77, 1986.

Lindstein, T., June, C.H., Ledbetter, J.A., Stella, G. and Thompson, C.B. Regulation of lymphokine messenger RNA stability by a surface-mediated T cell activation pathway. *Science* 244:339-343, 1989.

Liu, F.L., Cohen, R.D., Downar, E., Butany, J.W., Edelson, J.D. and Rebuck, A.S. Amiodarone pulmonary toxicity: functional and ultrastructural evaluation. *Thorax* 41:100-105, 1986.

Luster, M.I., Simeonova, P.P., Gallucci, R. and Matheson, J. Tumor necrosis factor alpha and toxicology. *Crit.Rev.Toxicol.* 29:491-511, 1999.

Marchlinski, F.E., Gansler, T.S., Waxman, H.L. and Josephson, M.E. Amiodarone pulmonary toxicity. *Ann.Intern.Med.* 97:839-845, 1982.

Martin, W.J. Mechanisms of amiodarone pulmonary toxicity. *Clin.Chest Med.* 11:131-138, 1990.

Martin, W.J. and Howard, D.M. Amiodarone-induced lung toxicity. In vitro evidence for the direct toxicity of the drug. *Am.J.Pathol.* 120:344-350, 1985.

Martin, W.J. and Rosenow, E.C. Amiodarone pulmonary toxicity. Recognition and pathogenesis (Part 2). *Chest* 93:1242-1248, 1988a.

Martin, W.J. and Rosenow, E.C. Amiodarone pulmonary toxicity. Recognition and pathogenesis (Part I). *Chest* 93:1067-1075, 1988b.

Mason, J.W. Amiodarone. *N.Engl.J.Med.* 316:455-466, 1987.

Massey, T.E., Leeder, R.G., Rafeiro, E. and Brien, J.F. Mechanisms in the pathogenesis of amiodarone-induced pulmonary toxicity. *Can.J.Physiol.Pharmacol.* 73:1675-1685, 1995.

Matsumori, A., Ono, K., Nishio, R., Nose, Y. and Sasayama, S. Amiodarone inhibits production of tumor necrosis factor-alpha by human mononuclear cells: a possible mechanism for its effect in heart failure. *Circulation* 96:1386-1389, 1997.

Nakazawa, H., Genka, C. and Fujishima, M. Pathological aspects of active oxygens/free radicals. *Jpn.J.Physiol.* 46:15-32, 1996.

Nicholson, A.A., and Hayward, C. The value of computed tomography in the diagnosis of amiodarone-induced pulmonary toxicity. *Clin.Radiol*. 40:564-567, 1989.

Paillous N. and Verrier, M. Photolysis of amiodarone, an antiarrhythmic drug. *Photochem.Photobiol*. 47(3):337-343, 1988.

Paine, R. III, and Ward, P.A. Cell Adhesion molecules and pulmonary fibrosis. *Am.J.Med*. 107:268-279, 1999.

Pitcher, W.D. Amiodarone pulmonary toxicity. *Am.J.Med.Sci.* 303:206-212, 1992.

Poli, G. and Parola, M. Oxidative damage and fibrogenesis. *Free Radic.Biol.Med.* 22:287-305, 1997.

Quaresima, V. and Ferrari, M. Current status of electron spin resonance (ESR) for in vivo detection of free radicals. *Phys.Med.Biol.* 43:1937-1947, 1998.

Rafeiro, E., Leeder, R.G., Brien, J.F., Kabalka, G.W., Chatla, N. and Massey, T.E. Comparison of the in vivo pulmonary toxicity of amiodarone and des-oxo-amiodarone in the hamster. *Toxicol.Appl.Pharmacol.* 127:275-281, 1994.

Ramalingam, A., Hirai, A. and Thompson, E.A. Glucocorticoid inhibition of fibroblast proliferation and regulation of the cyclin kinase inhibitor p21Cip1. *Mol.Endocrinol.* 11:577-586, 1997.

Reasor, M.J. and Kacew, S. An evaluation of possible mechanisms underlying amiodarone-induced pulmonary toxicity. *Proc.Soc.Exp.Biol.Med.* 212:297-304, 1996.

Reasor, M.J., McCloud, C.M., DiMatteo, M., Schafer, R., Ima, A. and Lemaire, I. Effects of amiodarone-induced phospholipidosis on pulmonary host defense functions in rats. *Proc.Soc.Exp.Biol.Med.* 211:346-352, 1996.

Reasor, M.J., Ogle, C.L., Walker, E.R. and Kacew, S. Amiodarone-induced phospholipidosis in rat alveolar macrophages. *Am.Rev.Respir.Dis.* 137:510-518, 1988.

Reinhart, P.G. and Gairola, C.G. Amiodarone-induced pulmonary toxicity in Fischer rats: release of tumor necrosis factor alpha and transforming growth factor beta by pulmonary alveolar macrophages. *J.Toxicol.Environ.Health* 52:353-365, 1997.

Reinhart, P.G., Lai, Y.L. and Gairola, C.G. Amiodarone-induced pulmonary fibrosis in Fischer 344 rats. *Toxicology* 110:95-101, 1996.

Ribeiro, S.M., Campello, A.P., Nascimento, A.J., and Kluppel, M.L. Effect of amiodarone on the antioxidant enzymes, lipid peroxidation and mitochondrial metabolism. *Cell.Biochem.Funct*. 15:145-152. 1997.

Riva, E., Marchi, S., Pesenti, A., Bizzi, A., Cini, M., Veneroni, E., Tavbani, E., Boeri, R., Bertani, T., and Latini, R. Amiodarone induced phospholipidosis. Biochemical, morphological and functional changes in the lungs of rats chronically treated with amiodarone. *Biochem.Pharmacol.* 36:3209-3214, 1987.

Robledo, R., and Mossman, B. Cellular and molecular mechanisms of asbestos-induced fibrosis. *J.Cell.Phys*. 180:158-166, 1999.

Rogers, R.A., Oldmixon, E.H., and Brain, J.D. Enhanced contrast within embedded tissue by lucifer yellow CH: an ideal stain for laser scanning confocal microscopy. *Mol.Biol.Cell*. 3:185a, 1992.

Rosenbaum, M.B., Chiale, P.A., Halpern, M.S., Nau, G.J., Przybylski, J., Levi, R.J., Lazzari, J.O., and Elizari, M.V. Clinical efficacy of amiodarone as an antiarrhythmic agent. *Am.J.Cardiol.* 38:934-944, 1976.

Rosenbaum, M.B., Chiale, P.A., Ryba, D. and Elizari, M.V. Control of tachyarrhythmias associated with Wolff-Parkinson-White syndrome by amiodarone hydrochloride. *Am.J.Cardiol.* 34:215-223, 1974.

Rotmensch, H.H., Liron, M., Tupilski, M. and Laniado, S. Possible association of pneumonitis with amiodarone therapy [letter]. *Am.Heart J.* 100:412-413, 1980.

Ruch, R.J., Bandyopadhyay, S., Somani, P. and Klaunig, J.E. Evaluation of amiodarone free radical toxicity in rat hepatocytes. *Toxicol.Lett.* 56:117-126, 1991.

Shimizu, H., Fisher, J.H., Papst, P., Benson, B., Lau, K., Mason, R.J., and Voelker, D.R. Primary structure of rat pulmonary surfactant protein D. cDNA and deduced amino acid sequence. *J.Biol.Chem*. 267:1853-1857, 1992.

Sibille, Y. and Reynolds, H.Y. Macrophages and polymorphonuclear neutrophils in lung defense and injury. *Am.Rev.Respir.Dis.* 141:471-501, 1990.

Singh, B.N., A study of the pharmacological actions of certain drugs and hormones with particular reference to cardiac muscle [doctoral thesis]. Oxford, UK: University of Oxford, 1971.

Singh, B.N., Venkatesh, N., Nademanee, K., Josephson, M.A. and Kannan, R. The historical development, cellular electrophysiology and pharmacology of amiodarone. *Prog.Cardiovasc.Dis.* 31:249-280, 1989.

Snead, W. Drug Prototypes and Their Exploitations. John Wiley and Sons, New York. 1996.

Snider, G.L., Hayes, J.A., and Korthy, A.L. Chronic interstitial pulmonary fibrosis produced in hamsters by endotracheal bleomycin. *Am.Rev.Respir.Dis*. 117:1099-1108, 1978.

Suffredini, A.F., Fantuzzi, G., Badolato, R., Oppenheim, J.J. and O'Grady, N.P. New insights into the biology of the acute phase response. *J.Clin.Immunol.* 19:203-214, 1999.

Venet, A., Caubarrere, I. and Bonan, G. Five cases of immune-mediated amiodarone pneumonitis [letter]. *Lancet* 1:962-963, 1984.

Vereckei, A. The role of free radicals in the pathogenesis of amiodarone toxicity. *J.Cardiovasc.Electrophysiol.* 4:161-177, 1993.

Wang, Q., Hollinger, M.A. and Giri, S.N. Attenuation of amiodarone-induced lung fibrosis and phospholipidosis in hamsters by taurine and/or niacin treatment. *J.Pharmacol.Exp.Ther.* 262:127-132, 1992.

Wang, S., Leonard, S.S., Castranova, V., Vallyathan, V. and Shi, X. The role of superoxide radical in TNF-alpha induced NF-kappaB activation. *Ann.Clin.Lab.Sci.* 29:192-199, 1999.

Ward, P.A. and Hunninghake, G.W. Lung inflammation and fibrosis. *Am.J.Respir.Crit.Care Med.* 157:S123-S1291998.

Wilson, B.D., Clarkson, C.E. and Lippmann, M.L. Amiodarone-induced pulmonary inflammation. Correlation with drug dose and lung levels of drug, metabolite, and phospholipid. *Am.Rev.Respir.Dis.* 143:1110-1114, 1991.

Wilson, B.D., Clarkson, C.E. and Lippmann, M.L. Amiodarone causes decreased cell-mediated immune responses and inhibits the phospholipase C signaling pathway. *Lung* 171:137-148, 1993.

Wilson, B.D., Jaworski, A.J., Donner, M.E. and Lippmann, M.L. Amiodarone-induced pulmonary toxicity in the rat. *Lung* 167:301-311, 1989.

Wilson, B.D. and Lippmann, M.L. Amiodarone pulmonary toxicity in the rat is associated with increased lavage immunoglobulin and alveolar macrophages primed for increased interleukin-1 secretion. *Am.J.Respir.Cell Mol.Biol.* 9:295-299, 1993.

Winkle, R.A. Amiodarone and the American Way [editorial]. *J.Am.Coll.Cardiol.* 6:822-824, 1985.

Witschi, H.P., Tryka, A.F. and Lindenschmidt, R.C. The many faces of an increase in lung collagen. *Fundam.Appl.Toxicol.* 5:240-250, 1985.

Wroblewski, F. and LaDue, J.S. Lactate dehydrogenase activity in blood. *Soc.Exp.Biol.Med*. 90:210-213.

Curriculum Vitae

Michael Douglas Taylor

Department of Pharmacology and Toxicology
Robert C. Byrd Health Sciences Center
West Virginia University
P.O. Box 9223
Morgantown, WV 26506-9223
(304) 293-4449
mtaylo17@wvu.edu

Education:

West Virginia University, Department of Pharmacology and Toxicology.
Pursuing a Ph.D. in Pharmacology and Toxicology.

West Virginia University.
B.A., Biology 1996.

Potomac State College of West Virginia University.
A.A., Biology 1994.

Research Experience:

8/96 - present: Graduate Research Assistant, Department of Pharmacology and Toxicology, West Virginia University.

5/96 - 8/96: Biological Sciences Laboratory Technician, National Institute for Occupational Safety and Health, Morgantown, WV.

1/96 - 5/96: Undergraduate Research Project, Department of Biology, West Virginia University and National Institute for Occupational Safety and Health, Morgantown, WV.

Honors:

Best Overall Poster Award, 2000 Allegheny-Erie Society of Toxicology Poster Competition.

Second Place, 2000 E. J. Van Liere Memorial Research Convocation, West Virginia University (Oral Presentation of Original Research).

Society of Toxicology Student Travel Award, 2000.

Allegheny-Erie Society of Toxicology Student Travel Award, 1999.

Professional Activities:

Lecturer in Occupational Toxicology, 1999-2000.
Toxicology of Biological Agents.

Lecturer in Nursing Pharmacology, 2000.
Therapy of Diabetes.
Therapy of Gastrointestinal Disorders.

Student Conference Leader in Medical Pharmacology, 1998-2000.
Led small groups of medical students in problem-solving discussions involving various aspects of medical pharmacology and drug toxicity.

Lecturer in HSTA Anatomy Program, 2000.
Health Effects of Smoking.
Health Effects and Biology of Lung Cancer.

Lecture and Laboratory Demonstration entitled "A Demonstration of Chemical Damage to the Lungs" for Health Sciences Center Open House, 1999-2000.
Lectured college students interested in careers in health sciences about the initiation and progression of inflammation, the cells involved, and methods to study the reaction in animal models.
Laboratory demonstration included slide preparation and staining and microscopic identification of cell types.

Professional Memberships:

Society of Toxicology, Student Member

Allegheny-Erie Society of Toxicology, Student Member

Preceptor:

Mark J. Reasor, Ph.D.

Publications:

Taylor M D, Van Dyke K, Bowman L, Miles P R, Hubbs A F, Mason R J, Shannon K, and Reasor M J. A characterization of amiodarone-induced pulmonary toxicity in F344 rats and identification of surfactant protein-D as a potential biomarker for the development of the toxicity. *Toxicol. and Appl. Pharmacol*., 2000. Sep 15; **167(3)**:182-90

Abstracts:

Taylor M D, Antonini J M, Roberts J R, Van Dyke K, Bowman L L, Castranova V, Hubbs A F, Shi X, Leonard S, and Reasor M J. Intratracheal amiodarone administration to F344 rats causes acute damage to airway and parachymal cells: The possible role of free radical generation. Society of Toxicology Annual Meeting, 2001 (in press).

Taylor M D, Roberts J R, Hubbs A F, Reasor M J, and Antonini J M. Application of laser scanning confocal microscopy in the analysis of drug-induced lung fibrosis. American Thoracic Society Annual Meeting, 2001 (in press).

Taylor M D, Van Dyke K, Bowman L, Miles P R, Castranova V, and Reasor M J. Further characterization of a rat model of amiodarone-induced pulmonary toxicity. *Toxicol. Sciences* **54 (1)**: 18, 2000.

Reasor M J, **Taylor M D**, Miles P R, Shannon K, and Mason R J. Surfactant Protein-D as a possible biomarker for amiodarone-induced pulmonary toxicity in a rat model. *Amer. J. Respir. Crit. Care Med.* **159**: A393, 1999.

Taylor M D, Van Dyke K, Hubbs A F, Bowman L, Miles P R, and Reasor M J. Amiodarone-induced pulmonary toxicity in F344 rats. *Toxicol. Sciences* **48 (1-S)**:118, 1998.

Van Dyke K, Birkle D, Konat G, Reasor M, McConnell P, Marquardt L, and **Taylor M D**. A new screening system for anti-Alzheimer's drugs: magnified enhancement of peroxynitrite-dependent luminol chemiluminescence of microglia and macrophages. Abstract submitted to Experimental Biology, 1998.

Van Dyke K, Birkle D, Konat G, Reasor M, McConnell P, Marquardt L, and **Taylor M D**. Enhancement of peroxynitrite-activated luminol chemiluminescence of macrophages using the Stratagene enhancer. Abstract submitted to the American Society of Cell Biology, Bethesda MD, 1998.